THE UNIVERSITY of ADELAIDE

Emissions from the Co-Generation of Biochar and Bioenergy with Agricultural By-Products

By

Lewis Dunnigan

Submitted in fulfilment of the requirements for the degree of Doctor of Philosophy

School of Chemical Engineering

The University of Adelaide

March 2018

Declaration

I certify that this work contains no material which has been accepted for the award of any other degree or diploma in my name, in any university or other tertiary institution and, to the best of my knowledge and belief, contains no material previously published or written by another person, except where due reference has been made in the text. In addition, I certify that no part of this work will, in the future, be used in a submission in my name, for any other degree or diploma in any university or other tertiary institution without the prior approval of the University of Adelaide and where applicable, any partner institution responsible for the joint-award of this degree. I acknowledge that copyright of published works contained within this thesis resides with the copyright holder(s) of those works. I also give permission for the digital version of my thesis to be made available on the web, via the University's digital research repository, the Library Search and also through web search engines, unless permission has been granted by the University to restrict access for a period of time.

Lewis Dunnigan

March 15th 2018

Abstract

The utilization of agricultural by-products for the co-production of biochar and bioenergy offers a viable way to sequester carbon effectively with added agricultural benefits. The operating pyrolysis temperature (or 'volatile production temperature'), however, strongly influences the balance between biochar production (yield and quality) and energy production (composition and higher heating value (HHV) of the volatiles). In this thesis, the term 'raw pyrolysis volatiles' is used to refer to the mixture of pyrogas and bio-oil produced during pyrolysis. The composition (moisture, ash, volatile matter (VM), sulfur, and nitrogen contents) of the biomass can also influence the yield of pollutants. Using a laboratory-scale combined pyrolysis and combustion (pyrolysis-combustion) process, raw pyrolysis volatiles were produced at varying temperatures (400 – 800 °C) from agricultural by-products and combusted at 850 °C. The particulate matter (PM_{10} and $PM_{2.1}$), gaseous (H_2S, SO_2, and NO_x), and PM-bound polycyclic aromatic hydrocarbon (PAH) emissions were evaluated. These pollutants are responsible for severe short and long-term harmful health impacts and are therefore subject to strict environmental legislation.

Utilizing rice husk in the pyrolysis-combustion process, it was found that the highest yields of both PM_{10} and $PM_{2.1}$ occurred at lower volatile production temperatures (400 – 600 °C). This was attributed to the increased contribution of bio-oil to the raw pyrolysis volatiles HHV which resulted in elevated C/H ratios in the volatile mixture. This increased the tendency of the pyrolysis volatiles to soot during combustion. Linear dependence was observed between PM emissions and the bio-oil fraction in the raw pyrolysis volatiles.

Combustion of the raw pyrolysis volatiles produced at elevated volatile production temperatures resulted in significantly increased PM-bound PAH concentrations. This was primarily due to the elevated PAH and oxy-aromatic content of the bio-oil fraction at higher temperatures. Elevated temperatures also resulted in increased average molecular weights of the PM-bound PAHs. Increased PM toxicity was observed at higher volatile production temperatures due to the elevated concentration of 4, 5, and 6 ring PAHs.

It was demonstrated that increased volatilization of the fuel-bound sulfur and nitrogen contents during pyrolysis at elevated volatile production temperatures increased the energy-based yields of SO_2, H_2S, NO, and NO_2. Utilization of grape pruning demonstrated that elevated biomass VM content resulted in increased energy-based yields of PM. The majority of the increase resided in the sub-micron size fraction due to the increased pyrogas fraction in the raw pyrolysis volatiles. The PM emissions were found to be independent of the feedstock ash content due to its retainment in the biochar.

It was also found that utilization of the as received (AR) rice husk resulted in greater energy-based yields of PM_{10} (1.2 times at 400 °C and 1.6 times at 800 °C). The PM-bound PAH concentration was observed to be 2.1 and 2.8 times higher for the AR rice husk at 400 and 800 °C, respectively. Nevertheless, the majority of the PM-bound PAH species generated from the AR rice husk consisted of 2 and 3 ring PAHs (naphthalene, acenapthylene, and acenaphthene) with relatively low toxicity. This resulted in the toxicity of the PM generated from the AR rice husk being lower than the dried rice husk.

This thesis demonstrated that operation of a pyrolysis-combustion process for the optimized generation of either biochar or bioenergy, at lower and elevated volatile production temperatures, respectively, resulted in significant differences in the emissions of harmful pollutants. It is hoped that the outcomes of this work will provide guidance for facilitating effective evidence based policies for agricultural by-product utilization with beneficial environmental outcomes. It is clear, however, that despite the potential for high ash content agricultural by-products to be utilized in pyrolysis-combustion systems, doubts surrounding the current market demand for biochar need to be addressed before the large-scale co-generation of biochar and bioenergy can become a reality.

Acknowledgments

I would like to first and foremost thank both the University of Adelaide and the Chinese Academy of Sciences (Institute of Process Engineering) for their support during my PhD candidature. None of this would have been possible without the financial support offered by the Beacon of Enlightenment scholarship I was awarded. I would especially like to thank my primary supervisor Dr. Philip Kwong for his guidance, patience, and support throughout my studies. His knowledge has proved invaluable to my development as a researcher. I would also like to sincerely thank my co-supervisors Prof. Xiangping Zhang and Prof. Peter Ashman for their crucial feedback and insight that has helped me develop a deeper understanding of everything relating to biomass and emissions research. I also want to thank Prof. Mark Biggs for supporting my initial application and giving me the opportunity to receive a scholarship.

To my colleagues at the University of Adelaide, thank you for making it such an enjoyable experience and pleasant environment to work in. I would like to especially thank Benjamin Morton for his fantastic chemistry knowledge, without which the impact and quality of our work would be much reduced. I would also like to thank Dr. Tony Hall for his outstanding analytical chemistry abilities that have proved much more fruitful than I could have hoped for. Thanks also to Sue Earle for helping me get settled into life in Adelaide twice during both my Masters and my PhD. Also, without the continuous help and support of the workshop staff, and in particular Jason, there is no way that I would have ever finished my studies on time. Thank you for putting up with me coming into the workshop every day over the course of about

two years and spending more time on my apparatus in those early days than just about anything else.

Finally, I would like to send my heartfelt thank you to my family back in Scotland for their continued love and emotional support throughout these four years. To my parents, I have no doubt that without you I wouldn't have gotten this far, and I hope I can repay at least a small fraction of what you have given to me going into the future. To my wonderful fiancée Lulu, I thank you for always being there for me during the ups and downs of PhD life. You have always kept a smile on my face and I could not have done this without you. I know that the effort we have both put in will serve us well going into the future.

Table of Contents

List of Tables

List of Figures

List of Abbreviations and Formulae

The following list displays the abbreviations and formulae used throughout this thesis.

ADT	Air dilution tunnel
AR	As received
BaP	Benzo(a)pyrene
BaP - TEF	Benzo(a)pyrene – toxic equivalency factor
BaP - TEQ	Benzo(a)pyrene – toxic equivalency quotient
BFB	Bubbling fluidized-bed
C	Carbon
CFB	Circulating fluidized-bed
CH_4	Methane
CI	Cascade impactor
CO	Carbon monoxide
CO_2	Carbon dioxide
d.a.f	Dry ash free basis
GC	Gas chromatograph
GC-MS	Gas chromatograph – mass spectrometer
GC-TCD	Gas chromatograph with thermal conductivity detectors
GHG	Greenhouse gas
H	Hydrogen
H_2S	Hydrogen sulfide
HACA	Hydrogen-abstraction C_2H_2-addition
HHV	Higher heating value
i.d.	Internal diameter
LCA	Life cycle assessment

N	Nitrogen
N_2O	Nitrous oxide
NO	Nitrogen oxide
NO_2	Nitrogen dioxide
NO_X	Nitrogen oxides
O	Oxygen
PM	Particulate matter
PAH	Polycyclic aromatic hydrocarbon
RPM	Revolutions per minute
S	Sulfur
SO_2	Sulfur dioxide
SO_X	Sulfur oxides
T_c	Combustion temperature
TGA	Thermogravimetric analysis
T_p	Pyrolysis temperature
TSP	Total suspended particulates
T_v	Volatile production temperature
VM	Volatile matter

List of Research Output

Journal Articles

1. Dunnigan, L., Ashman, P.J., Zhang, X., Kwong, C.W., 2018. Production of Biochar from Rice Husk: Particulate Emissions from the Combustion of Raw Pyrolysis Volatiles. *Journal of Cleaner Production*. 172, 1639–1645. (Chapter 2).
2. Dunnigan, L., Morton, B.J, van Eyk, P.J., Ashman, P., Zhang, X., Hall, P.A., Kwong, C.W. 2017. Polycyclic Aromatic Hydrocarbons on Particulate Matter Emitted during the Co-Generation of Bioenergy and Biochar from Rice Husk. *Bioresource Technology*. 244, 1015–1023. (Chapter 3).
3. Dunnigan, L., Morton, B.J, Ashman, P.J., Zhang, X., Kwong, C.W. Emission Characteristics of a Pyrolysis-Combustion System for the Co-Production of Biochar and Bioenergy from Agricultural Wastes. *Waste Management*. 77, 59-66. (Chapter 4).
4. Dunnigan, L., Morton, B.J, Hall, P.A., Kwong, C.W. Production of Biochar and Bioenergy from Rice Husk: Influence of Feedstock Drying on Particulate Matter and the associated Polycyclic Aromatic Hydrocarbon Emissions. *Atmospheric Environment.* 190, 218-225. (Chapter 5).

Conference Article

5. Dunnigan, L., Ashman, P.J., Zhang, X., Kwong, C.W., 2015. Atmospheric Emissions from the Co-Combustion of Biomass Tars and Synthesis Gas during Biochar and Bioenergy Production. In: Asia Pacific Confederation of Chemical Engineering Congress 2015: APCChE 2015, incorporating CHEMECA 2015. Melbourne: Engineers Australia, 2015: 486-495. ISBN: 9781922107473.

Patent Application

6. Apparatus and Method of Producing Activated Carbon Material (Provisional Patent - 2017904838). Provisional patent submitted on 30th of November, 2017.

Chapter 1: Introduction

1.1. Background

The influence of anthropogenic GHG emissions on climate change is one of the major concerns of our time. One significant contributor to this problem is the increasing concentration of atmospheric CO_2 resulting from the combustion of fossil fuels for energy generation purposes (Lehmann, 2007). It has therefore been suggested that an ambitious programme of mitigation measures are needed in order to reverse our progress towards irreversible climate change (Woolf et al., 2010). This means that technologies that can actively withdraw CO_2 from the atmosphere, and sequester that C safely for extended periods of time, must be included due to the continuing presence of unavoidable GHG emissions from both fossil fuel burning and biomass decomposition (Lehmann, 2007). Indeed, CO_2 reduction should be at the forefront of any long-term mitigation measures as it remains the primary anthropogenic source of GHG, representing 76 % of total GHG emissions ($CO_{2,equivalent}$) in 2010 (IPCC, 2014).

One way to effectively reduce atmospheric CO_2 concentrations is through the growth of plants. Plants remove CO_2 from the atmosphere during photosynthesis and store it in their soil organic matter or tissue (Lehmann, 2007). Combustion of this plant matter (biomass) is C-neutral, and will not result in long-term effective atmospheric CO_2 reduction. Instead, conversion of the readily decomposable C present in the biomass to much more stable forms is an effective means to sequester C (Lehmann, 2007). This can be achieved through the heating of biomass to elevated temperatures (generally from 300 – 800 °C) in the absence of oxygen by a process known as “pyrolysis”. As a result of the pyrolysis reaction the biomass

thermally decomposes to leave a solid carbonaceous product named “biochar” (Fig. 1.1). The biochar is characterized by high C content (> 40 %) and increased durability when compared to the original feedstock. The production of biochar from sustainable biomass sources is generally considered to be a C-negative process (Glaser et al., 2009). It has been estimated that sustainable biochar implementation could offset approximately 130 Pg of CO_2-equivalent emissions over a 100 year time period, and a maximum of 12 % of anthropogenic GHG emissions on an annual basis (Woolf et al., 2010).

Estimates for the length of C sequestration vary, but typically range from hundreds to thousands of years (Lehmann, 2007). The application of biochar to soils has also been shown to provide added-value to biomass wastes by improving agricultural productivity. This is especially true of low-fertility and degraded soils (Woolf et al., 2010). Biochar can improve soil health by reducing the leaching of nutrients into ground water (Hagemann et al., 2017); reducing the soil emissions of N_2O (Cayuela et al., 2013); increasing the cation-exchange capacity of the soil (Jien and Wang, 2013); increasing water holding capacity (Karhu et al., 2011); moderating soil acidity (Obia et al., 2015); and being beneficial to the health of soil microbes (Han et al., 2017). Numerous studies have demonstrated the effectiveness of biochar for increasing plant yields in various soil types (Chan et al., 2007; Major et al., 2010; Yamato et al., 2006).

Biochar can be made through various pyrolysis approaches (Antal Jr and Gronli, 2003). The majority of these methods, however, are relatively simple, and do not result in the co-generation of bioenergy. Often these traditional methods are also inefficient (Sparrevik et al., 2015). Modern pyrolysis processes typically separate the condensable (bio-oil) and non-condensable (pyrogas) products of the pyrolysis

reaction to generate an oil-free gas for power generation (Ning et al., 2013). This approach of separating the fractions, however, reduces the available energy content from combustion of the volatile mixture. This is the due the significant contribution of bio-oil to the HHV of the volatiles at the lower pyrolysis temperatures that favor biochar production (Williams and Nugranad, 2000). It is therefore suggested that co-combustion of the pyrogas and bio-oil fractions of the raw pyrolysis volatiles may be advantageous to the performance of modern pyrolysis processes. In this thesis the mixture of pyrogas and bio-oil is termed the “raw pyrolysis volatiles”.

Co-combustion of the pyrogas and bio-oil results in the production of energy that can be used to power the endothermic pyrolysis reaction and drying requirements of wet biomass. On-site heating requirements can also be reduced (Moon et al., 2011). Higher combustion efficiencies (due to enhanced fuel/air mixing and elevated combustion temperatures) are achievable through modern pyrolysis-combustion processes when compared to conventional biomass disposal methods (including open burning and cook stoves). This may therefore offer the additional advantage of reducing the harmful emissions associated with current disposal practices, which are significant contributors to premature mortality in developing countries (Smith et al., 2000; Reddy and Venkataraman, 2002). Attempts to increase the utilization rates of agricultural by-products have also traditionally been hindered by the low bulk and energy densities of the feedstocks (Chen et al., 2015; Vassilev et al., 2010). This means that future utilization strategies must be able to use the by-products on-site, reducing transportation costs. These benefits suggest that distributed pyrolysis-combustion systems may offer a method for upgrading waste biomass that cannot currently be utilized due to it being currently economically

prohibitive. This approach can be mobile (allowing difficult to access biomass to be accessed) and offers additional sustainability benefits.

It is therefore clear that the large-scale production of biochar and bioenergy by pyrolysis-combustion can address the following major challenges that society currently faces: 1) It can reduce atmospheric CO_2 concentrations to help combat climate change, 2) help improve the productivity and yields of agricultural practices, ensuring enhanced food security in a world with a growing population, 3) increase global bioenergy production to reduce fossil fuel consumption, 4) reduce the emissions associated with conventional methods of biomass disposal, and 5) provide an additional income stream for agricultural producers with abundant biomass wastes. One type of abundant biomass feedstock that currently has little or no value and is therefore suitable for the co-generation of biochar and energy are agricultural by-products.

1.2. Agricultural By-Products: Properties and Availability

Agricultural by-products are attractive feedstocks for increasing the global production of biochar and bioenergy. This is because there is no competition with existing agricultural lands, no potential for deforestation, and no exploitation of existing farming industries. In addition, by producing biochar and energy from current by-products with little or no value, an additional revenue stream will be generated for agricultural producers by creating added-value for these materials. As agricultural by-products represent a potentially abundant source of feedstocks (Huang et al., 2013; Yin et al., 2017), they are extremely attractive for the development of sustainable waste management practices with energy generation.

Agricultural by-products are a diverse class of materials with variable properties and compositions. The wide-range of fuel qualities possessed by these feedstocks is demonstrated in Table 1.1. The ash content of the rice husk (16.1 %) is, for example, greater than most other types of biomass, which typically varies between 0.3 – 8 % (Alper et al., 2015). This results in variable VM contents, with the rice husk (56.1 %) being considerably lower than that of olive husk (73.7 %). In addition, significant variations in feedstock moisture content are observed in Table 1.1, which leads to inconsistencies in the HHV of the feedstocks. The composition of the biomass-bound ash is also significantly different to that of traditional fossil fuels. Relative to coal, agricultural by-products generally have less aluminium, iron, titanium, and S. They also have more oxygen, silica, chlorine, potassium, and calcium (Khan et al., 2009).

The desire to increase the utilization rate of agricultural by-products is being partly driven by the abundance of relatively cheap feedstocks (Roberts et al., 2010). Considering China in 2009 alone, it is estimated that the total yield of straw by-products was 806.9 million tons (Jiang et al., 2012). The three principle by-products were the straws of maize (40.6 %), wheat (24.2 %) and rice (15.7 %) (Table 1.2). The values presented in Table 1.2 indicated the total bioenergy potential from agricultural straw by-products in China was 7.4 EJ in 2009, equivalent to 254 million tonnes of standard coal (Jiang et al., 2012). The potential for agricultural by-products to be used for the co-generation of biochar and bioenergy in other major agricultural economies is also vast. Taking India as an example, it has been estimated that there are approximately 511 million tonnes of by-products available each year. By-products from rice (170 million tonnes), cotton (53 million tonnes), and maize (27 million tonnes) cultivation were the biggest potential sources of feedstocks (Kumar et

al., 2015). This thesis investigates the utilization of both rice husk and grape pruning. These by-products were used due to their vast potential for biochar production, current harmful disposal practices, as well as their significantly different compositions. Further detail on the composition, fuel properties, and availability of these two feedstocks is provided in Section 1.5.1.

Due to the vast potential of agricultural by-products to contribute to global energy production, many developed and developing countries have promoted such practices through instrumented policies and financial incentives, including enhanced feed-in tariffs (Kumar et al., 2015). There is therefore a substantial economic incentive for agricultural producers to utilize these materials efficiently. Significant problems (both environmentally and economically) associated with the conventional methods of agricultural by-product disposal are also accelerating the development of new and innovative utilization practices.

1.3. Conventional Methods of Agricultural By-Product Disposal

For many agricultural by-products, current utilization approaches are inefficient, provide little or no added-value, and are potentially harmful to the local environment. Although practices vary between countries, it is clear that the majority of approaches are not desirable for long-term practices. Fig. 1.2 shows the breakdown in utilization rates for agricultural by-products in China in 2009.

Fig. 1.2 shows that the most common method of agricultural by-product disposal is simply leaving it in the field to either decompose or be openly burned (31 %). Only 19 % of the available by-products were utilized for energy purposes. This trend is also reflective of other major agricultural countries. In India, 97 million tonnes of rice straw is produced every year, and around 23 % of it is disposed of (Ghosh,

2016). The majority of the disposed straw is openly burned. The straw by-products that are utilized are generally for animal feed, resulting in little added-value for agricultural producers. Additional conventional methods for rice paddy waste disposal across many different countries include burying in the soil (Zhang et al., 2015), applying to the top layer of soil as a mulch for soil amelioration (Jiang et al., 2012), and heating purposes in cook stoves (Smith et al., 2000; Kim Oanh et al., 2005). These approaches, however, are generally inefficient, and can result in serious negative side-effects.

1.3.1. Decomposition

Leaving agricultural by-products in the field to decompose is not an effective method of nutrient recycling for soil enhancement. Significant quantities of the N contained in the waste are lost to the atmosphere through volatilization (Woolf et al., 2010). This approach does not allow for effective application timing, which is also important for increased plant yields. CH_4 emissions are also a concern from such practices. It is well established that the anaerobic decomposition of biomass leads to significant CH_4 production, which is a potent GHG (Gunaseelan et al., 1997). Overall, these factors make decomposition an extremely poor choice for increasing the utilization rates of agricultural by-products. For similar reasons, the addition of these raw wastes to fertilizers is also not an approach that will provide significant improvements in crop yields or increased fertilizer value.

1.3.2. Open Burning

One of the most common approaches for agricultural by-product disposal is through open burning. This approach, however, directly results in gas and particle emissions that have been shown to influence the physical and chemical properties of

the atmosphere (Crutzen and Andreae, 1990). This occurs through several different routes (Christian et al., 2003), including: the release/redistribution of C resulting from incomplete combustion (Prather et al., 1994), changes in oxidative capacity (Mason et al., 2001), and changes in atmospheric radiative transfer (Hobbs et al., 1997; Kaufman and Fraser, 1997). Significant emissions of PM, PAHs, and CO have been reported from the open burning of biomass (Christian et al., 2003; Jenkins et al., 1996). The yields of these pollutants during open burning are generally high as they are products of incomplete combustion and this approach is characterized by low combustion efficiencies. As PM_{10} and $PM_{2.5}$ emissions are major contributors towards premature mortality in developing countries, the importance of reducing this practice is clear (Barron and Torero, 2017). In addition, many PAH species are subject to strict emission standards due to their carcinogenic and mutagenic properties (Keith, 2015). The concern resulting from the harmful emissions during the open burning of agricultural by-products has led to the banning of the practice in many different locations. As a result, the percentage of straw by-products burned directly in the fields has decreased dramatically in China (Jiang et al., 2012). Therefore, due to the high yields of harmful pollutants, as well as the lack of an additional revenue stream for by-product producers, open burning cannot be considered a viable utilization approach for agricultural by-products looking into the future.

1.3.3. Cook Stoves

One of the most common approaches for utilizing agricultural by-products is in cook stoves. Biomass fuels (including agricultural by-products) are used extensively in developing countries for heating and cooking requirements (Abdullahi et al., 2013).

Globally, the annual residential consumption of biomass fuels in 2007 was equivalent to 3.7 x 10^{16} J, over 93 % of which occurred in developing countries (Shen et al., 2013a). Due to the low efficiencies of these cook stoves, however, significant emissions of PM (Kim Oanh et al., 2005), PAHs (Shen et al., 2013a), and CO (Smith et al., 2000) have been reported. Conservative estimates indicate that around 1 million people die from chronic obstructive pulmonary disease annually due to indoor exposure to smoke (Hetland et al., 2000). It was also previously reported that PAH exposure caused 1.6 % of lung cancer morbidity in the Chinese population in 2003 (Zhang et al., 2009). Indeed, 63 % of PAH global emissions in 2007 were derived from use of solid fuels in homes, of which China contributed 62 % of the total (Shen et al., 2013c).

It can therefore be seen that the current practices of utilizing agricultural by-products by either open burning or in cook stoves are not viable long-term strategies for reducing the emissions problems associated with conventional methods of by-product disposal. These methods are contributing to localized air pollution issues. They are also not providing significant added-value for agricultural producers. Similarly, leaving the by-products to decompose in the field is not an efficient way to recycle nutrients back into the soil. This approach is also not an effective measure to reduce GHG emissions through carbon sequestration as the anaerobic digestion of the by-products produces significant quantities of CH_4. It can therefore be concluded that is it of significant importance that new, viable, technologies become available for the development of effective resource management practices. To be considered viable, it must be possible for agricultural by-products to be utilized in such a way that significant added-value is generated; while at the same time the emissions of harmful pollutants are minimized. One of the suggested approaches for achieving

these criteria is the direct combustion of agricultural by-products for bioenergy generation.

1.4. Improved Utilization of Agricultural By-Products

1.4.1. Direct Combustion

Agricultural by-products are considered suitable candidates for increasing global energy production through direct combustion processes. As they are both renewable and a C-neutral fuel source (Chao et al., 2008), there have been numerous efforts to incentivise their use for bioenergy purposes through government led initiatives (Moon et al., 2011). A significant amount of research investigating various direct combustion approaches for agricultural by-products has also been published.

Janvijitsakul and Kuprianov (2008) investigated the major gaseous and PAH emissions from rice husk utilization in a fluidized-bed combustor. They reported extremely high combustion efficiencies (all > 99 %), the greatest of which was with an excess air of ≈ 40 %. With the same excess air feed, the heat loss due to unburned C and incomplete combustion were at their lowest (0.5 and 0.1 % respectively). The PM-bound PAH emissions were reported to be approximately 10 µg/kWh, the greatest of which was acenaphthylene (4.1 µg/kWh). They concluded that the total PAHs emissions from biomass combustion were relatively low, but that concern should be given when utilizing fuels with higher moisture and ash contents due to the likelihood of increased PAH emissions.

Chao et al. (2008) investigated the PM and PAH emissions resulting from the co-combustion of coal and rice husk/bamboo in a fluidized bed. They observed that operation between 10 % and 30 % biomass to coal blending ratios was the optimum

for minimizing pollutant emissions per unit energy output. Combustion efficiencies were greater than 90 % for all coal/biomass mixtures, implying that the blending of biomass in coal did not have significant effect on the operating efficiency. It was observed that the PM_{10} and $PM_{2.1}$ concentrations increased by 5 % and 10 % for rice husk between moisture contents of 8 % and 14 % (average). For the same moisture content range there was a 5 % and 15 % increase in PM_{10} and $PM_{2.1}$ concentrations for bamboo. This was due to decreased combustion temperatures owing to additional heat being transferred to the latent heat of vaporization of the water. At 10 % excess air and a rice husk blending ratio of 50 %, the reported emissions of PM_{10}, $PM_{2.1}$, and PM-bound PAHs were approximately 4050 mg/kWh, 430 mg/kWh, and 480 µg/kWh, respectively. They concluded that the issues of slagging, fouling and the formation of clinker need to be addressed for biomass co-combustion.

Sirisomboon and Kuprianov (2017) investigated the co-combustion of sunflower shells and coconut coir dust/moisturized rice husk in a 205 kW fluidized-bed combustor with bottom air injection. They observed that the excess air had the most significant impact on the emissions and combustion performance of the reactor. Combustion efficiencies of around 99 % were achieved. The heat losses due to incomplete combustion and unburned C ranged from 0.5 – 3.0 % and 0.1 – 0.5 % respectively. NO emission reductions of up to 25 % were achieved through the fuel-staged co-firing of sunflower shells with coconut coir dust/moisturized rice husk when compared to the sunflower shells only.

Numerous other studies have investigated the direct combustion of agricultural by-products for energy generation purposes. These include the combustion of wheat straw in a fixed bed combustor (Cepic et al., 2016), combustion

of rice straw in a fluidized bed (Okasha, 2007), and the combustion of torrefied sugarcane bagasse (Valix et al., 2017). The majority of these studies offer methods for increasing the utilization rates of abundant biomass wastes with high combustion efficiencies. This therefore appears to present a viable method to reduce the harmful pollution associated with conventional methods of by-product disposal.

1.4.2. Emission Reduction Potential of Direct Combustion

Due to the high combustion efficiencies offered by direct combustion, effective emissions reduction is readily achievable when compared to conventional disposal methods. The emission factors for various agricultural by-products utilized in direct combustion processes is compared to both cook stoves and open burning in Table 1.3. It is observed in Table 1.3 that the emission factors for direct combustion are generally lower than both cook stoves and open burning. In particular, the reduction in the emissions of products of incomplete combustion during direct combustion (PM, PAHs, and CO) is significant when compared to open burning. As previously mentioned, this is due to the much improved combustion efficiency during the controlled direct combustion. Due to the severe health impacts of these emissions, improving utilization practices by adopting direct combustion technologies for energy production is clearly desirable. Indeed, direct combustion has been called the most mature technology available nowadays for biomass utilization (Nussbaumer, 2003). There are, however, numerous problems that exist with this approach that have led to relatively low utilization rates.

1.4.3. Problems with Direct Combustion of Agricultural By-Products

Despite the environmental and economic advantages associated with utilization of agricultural by-products in direct combustion processes rather than open

burning or cook stoves, several issues relating to fuel quality and availability have hindered wide-scale adoption. The lack of available high-quality biomass fuels has resulted in the need to utilize low-quality feedstocks with variable properties and compositions (see Table 1.1). Many of these qualities are detrimental to the operation of direct combustion processes (Jenkins et al., 1998).

Significant variations in ash content are one of the major problems for increasing agricultural by-product utilization. For example, the significant ash content of rice husk shown in Table 1.1 (16.1 %) can potentially lead to the formation of slags and clinkers on internal heat transfer surfaces (Gilbe et al., 2008). High potassium and chlorine contents, along with high ash content, in other types of biomass are also of major concern (Khan et al., 2009). Chlorine, which is found in high quantities in straws, can facilitate corrosion. Chlorine also facilitates the mobility of many inorganic compounds (especially potassium) and can form potassium chloride which is among the most stable high temperature, gas phase, alkali-containing species (Khan et al., 2009). In addition, silica is abrasive and can react with alkali metals to form alkali silicates that melt at low temperatures to form slag and clinker (Gilbe et al., 2008; Jenkins et al., 1998). It is also of concern that increases in PM emissions associated with high ash content biomass fuels have previously been reported (Gao and Wu, 2011; Johansson et al., 2003; Johansson et al., 2004).

High moisture contents are also problematic for increasing the utilization rates of agricultural by-products. The moisture content of biomass can vary substantially (5 - 70 %) (Khan et al., 2009). Increased moisture contents result in decreased fuel HHV and higher energy requirements due to drying and the latent heat of

vaporization (Demirbas, 2007). The HHV of coal is approximately 40 % greater than that of biomass (Chao et al., 2008). It is therefore required that greater amounts of agricultural by-product are used to achieve the same energy output as coal. High moisture content can also cause start-up issues and reduce the combustion temperature, which negatively affects the quality of combustion (Demirbas, 2005). Ignition issues are also a problem for the direct combustion of biomass with elevated moisture contents (McKendry, 2002). Reduced combustion temperatures are also associated with elevated emissions of PM, PAHs, and CO (Kwong et al., 2007; Chao et al., 2008).

The decentralized nature of agricultural by-product availability also means that decomposition may occur during storage and transportation. LCA studies of potential agricultural by-product utilization approaches have indicated that the transportation distance of the biomass is a significant hurdle to the economic viability of any new approaches (Roberts et al., 2010; Dutta and Raghavan, 2014). Increased transportation requirements also result in additional GHG emissions (Roberts et al., 2010). Many of these location problems are exacerbated by the low bulk density of agricultural by-products. For example, the bulk densities of chopped straw (50 – 120 kg/m^3) and rice husk (100 – 125 kg/m^3) are much lower than brown coal (560 – 600 kg/m^3) and bituminous coals (800 – 900 kg/m^3) (Khan et al., 2009). For these reasons it is appropriate for utilization of agricultural by-products to occur on-site. This is not viable for large-scale direct combustion approaches, as the distributed nature of agricultural by-products does not facilitate exploitation of feed-in tariffs or supplementing large on-site energy demands.

It is therefore concluded that direct combustion is not a viable utilization approach for many agricultural by-products. Significant problems with biomass ash, moisture, low bulk density, and location constraints dramatically increase utilization difficulty. It is appropriate that technology capable of utilising problematic feedstocks and is deployable on-site is favoured for increasing the utilization rate of distributed agricultural by-products. The co-production of biochar and energy using a pyrolysis-combustion process may be considered viable for this purpose due to the inherent separation of fuel-bound ash in the biochar prior to combustion. There is, however, very little information available regarding the emissions from such a process utilizing agricultural by-products. In order to investigate the emissions of common pollutants during pyrolysis-combustion it is important to understand the mechanisms of their formation.

1.4.4. Pollutant Formation

The primary pollutants of concern in this thesis are PM (both PM_{10} and $PM_{2.1}$), PM-bound PAHs, SO_2, and NO_x. These pollutants are responsible for the majority of short and long-term negative health impacts on local populations from conventional methods of disposal (Smith et al., 2000; Reddy and Venkataraman, 2002). The organic constituents of the PM (soot) are believed to form through a HACA mechanism (Lima et al., 2005). During combustion the constituents of the fuel form free radicals that, via cyclization reactions, form the first aromatic rings (Ritchter and Howard, 2000). These ring species then react with other small aromatic compounds (e.g. C_2H_2 – acetylene) to form larger and more stable multi-ring compounds (Lima et al., 2005). The HACA mechanism is slightly endothermic as the abstraction of H leads to an increase in entropy and reduces the overall Gibbs free energy, promoting growth (Wang, 2011). This reaction pathway for soot formation is shown in Fig. 1.3.

Multiple ring polymerization reactions ultimately lead to the formation of large aromatic polymer species. High molecular weight PAHs (~500 - 1000 AMU) function as molecular precursors of soot particles (Lima et al., 2005). Pyrogenic oxidation of the PAH species is generally caused by OH• radicals under fuel-rich conditions. Under fuel-lean conditions O is primarily responsible (Ritchter and Howard, 2000). Organic super-micron emissions are usually formed through incomplete burnout of residual char and tar droplets in the combustion region, forming hollow cenospheres (Linak et al., 2000a).

The inorganic species in the biomass ash tend to promote the formation of sub-micron PM at high combustion temperatures/efficiencies through a mechanism of vaporization, nucleation, coagulation, and condensation (Linak et al., 2000a). At lower combustion temperatures/efficiencies many of the ash constituents will fail to vaporize and the sub-micron emissions will be lower. Because particles tend to "accumulate" in the size range from 0.1 to 1 μm, this range is called the accumulation mode (Wilson and Suh, 1997). This formation route of PM appears to terminate around 1 μm in particle size.

The emissions of SO_2 originate from the fuel-bound S content. Volatilization of fuel-bound S during the initial pyrolysis reaction forms H_2S that is then oxidised to form SO_2 (Shirai et al., 2013; Kramlich et al., 1981). For efficient combustion systems that operate in excess air the emissions of H_2S are generally very low (Shirai et al., 2013). NO_x emissions during direct combustion can result from volatilization of the fuel-bound N. Oxidation of the nitrogenous species produced during volatilization (including hydrogen cyanide and ammonia) in the initial pyrolysis step can lead to NO_x formation (Darvell et al., 2014). Both NO_x and SO_x emissions have been found

to increase with higher fuel N and S contents respectively (Mitchell et al., 2016). NO_x can also be produced through thermal and prompt formation routes during combustion (Löffler et al., 2005).

1.4.5. Alternative Approaches to Direct Combustion

Several alternative utilization approaches exist for agricultural by-products. These technologies are in differing stages of development and are all currently active areas of research. This Section outlines the foundations of these technologies and explains recent progress that has been made towards making them viable options for increasing the utilization rate of agricultural by-products.

Torrefaction is one such technology that is currently under development due to its ability to improve the properties of biomass, including HHV and bulk density, and possesses significant potential for industrial applications (Chen et al., 2015). With this approach, the raw biomass feedstock undergoes thermal pre-treatment in an inert atmosphere (200 – 300 °C) for the purpose of upgrading the fuel (Tran et al., 2013). Due to these operating conditions, torrefaction has been referred to as “mild pyrolysis” (Chen et al., 2015). The purpose of torrefaction is to improve the poor fuel qualities of most biomass feedstocks (see Section 1.2), including its high moisture content, low HHV, hygroscopic nature, and low bulk density. Previous work on the torrefaction of biomass has demonstrated that improvements in feedstock HHV, lower atomic O/C and H/C ratios, lower moisture content, higher hydrophobicity, improved grindability, and more uniform properties can all be achieved (Chen et al., 2015; van der Stelt et al., 2011). The removal of O from the raw biomass causes the fuel to become more coal like, which is demonstrated in the van Krevelen diagram (Fig. 1.4). Torrefaction is, however, limited as it cannot both add value to the

biomass and effectively sequester C. The future of this technology is likely in conjunction with the use of biomass for large-scale centralized bioenergy purposes, including direct combustion. It is therefore unlikely to be utilized for the on-site distributed utilization of agricultural by-products. It also does not offer an approach to increase the uptake of by-products with high ash contents for bioenergy generation.

Gasification is another potential approach for increasing the utilization rates of abundant agricultural by-products for bioenergy purposes. Gasification is the partial oxidation of carbonaceous feedstocks above 800 °C to produce syngas that can be used for applications such as gas turbines, engines, and fuel cells (van der Stelt et al., 2011). Gasification is generally characterised by high thermal efficiencies. The syngas produced is a mixture of CO, H_2, CH_4, and CO_2, as well as light hydrocarbons, such as ethane and propane, and heavier hydrocarbons (tar) that condense at temperatures between 250 and 300 °C (Molino et al., 2016). Undesirable gases, such as H_2S, can also be present in the syngas. The lower heating value of the syngas ranges from 4 to 13 MJ/Nm^3 (Molino et al., 2016). A solid carbonaceous residue containing char and ash is also produced (van der Stelt et al., 2011). Several problems exist, however, that have hitherto hindered the development of gasification technologies for many agricultural by-products. Moisture contents above 30 % makes fuel ignition difficult in gasification processes and has a negative effect on the HHV of syngas (McKendry, 2002). In addition, high fuel ash content (which is common with many biomass feedstocks), can increase gasification difficulty. The oxidation temperature is often above the melting point of the biomass ash, leading to clinkering/slagging problems in the process (McKendry, 2002). Ash contents above 5 % (especially if the ash is high in alkali oxides and salts) may cause clinker problems. This can therefore result in increased process downtime. It

is therefore concluded that, without significant pre-treatment of the by-product feedstocks (such as torrefaction), gasification processes are unlikely to contribute to the on-site utilization of distributed agricultural by-products. Such pre-processing requirements may incur significant economic disadvantages for agricultural by-product utilization.

Hydrothermal carbonization is another potential approach for improving the utilization rates of low quality biomass feedstock. It is characterised by the combined dehydration and decarboxylation of the biomass at elevated temperatures (180 – 220 °C) in a suspension of water under saturated pressure for several hours. This process increases the C content of the feedstock (increasing the HHV) (Funke and Ziegler, 2010). A lignite-like, easy to handle fuel, with improved thermal properties can be created from agricultural by-products. This solid product (hydrochar) has reduced equilibrium moisture content, so it is less likely to deteriorate in storage (Reza et al., 2014). This approach, however, is suitable only for feedstocks with higher moisture contents as drier by-products require large amounts of water. In addition, the detailed reaction mechanisms involved during hydrothermal carbonization are largely unknown and evaluations of the resulting reaction network are not possible in detail yet (Funke and Ziegler, 2010). The lack of understanding of the complicated reaction pathways involved during the production of hydrochar means there has been little demonstration of the concept on a large-scale. It is therefore clear that, although hydrothermal carbonization has significant potential to increase the utilization rates of wet feedstocks going into the future, it is not yet a mature enough technology to be considered viable for distributed agricultural by-products.

1.5. Combined Pyrolysis and Combustion Processes

It is clear that any attempts to increase the uptake of agricultural by-products for the production of more valuable materials will result in the need to utilize problematic feedstocks with significant fuel ash and moisture contents. While conventional disposal methods are inefficient and result in localized air pollution problems (Section 1.3), modern approaches, including direct combustion (Section 1.4.3), torrefaction, gasification, and hydrothermal carbonization (all Section 1.4.5), also suffer from drawbacks that mean they are not currently suitable for improving value-adding efforts.

It has been suggested that a combined pyrolysis and combustion process (pyrolysis-combustion) for the co-generation of biochar and bioenergy is the most suitable approach for increasing the utilization rate of agricultural by-products (Roberts et al., 2010). As mentioned in Section 1.1, this approach involves co-combustion of the liquid (bio-oil) and gaseous (pyrogas) products generated from the initial pyrolysis step and differs from conventional pyrolysis processes that separate the condensable fraction prior to combustion. Separation of the bio-oil fraction is not recommended for self-sustaining pyrolysis-combustion processes as the liquid fraction contributes significantly to the energy content of the raw pyrolysis volatiles (Williams and Nugranad, 2000). In addition, the upgrading of bio-oil in centralized facilities is currently uneconomical due to problems with the bio-oil quality, catalyst instability, and deterioration during storage (Hassan et al., 2016). The heat generated from combustion of the raw pyrolysis volatiles can be used to sustain the endothermic pyrolysis reaction (further details provided in Section 1.6). The energy

flow for a simulated pyrolysis-combustion system for biochar and bioenergy production using late stover is shown in Fig. 1.5 (Roberts et al., 2010).

The solid biochar product is removed prior to combustion of the volatile mixture. This effectively results in an ash free raw pyrolysis volatile mixture as the majority of the ash is retained in the biochar (Claoston et al., 2014). This therefore allows feedstocks with high ash contents to be utilized effectively with reduced fouling/slagging potential. Pyrolysis-combustion is also attractive for feedstocks with elevated moisture contents and it is less likely to suffer from ignition issues due to the volatilization of the fuel-bound moisture in the pyrolysis reaction (Demirbas, 2004b). For these reasons the pyrolysis-combustion process is the focus of this thesis. The potential of this approach to utilize abundant yet problematic agricultural by-products in a manner that helps address many of the major challenges that society currently faces (see Section 1.1) expedites its study in greater depth. This is compounded by the lack of available literature currently dealing with this topic.

1.5.1. Choice of Feedstock

One of the major advantages of the pyrolysis-combustion process is its ability to process feedstocks with wide-ranging fuel qualities. In order to examine the influence of biomass properties and composition on the performance of the pyrolysis-combustion process, two significantly different agricultural by-products were utilized. The first of these is rice husk, which is an abundant agricultural by-product with traditionally limited methods of utilization and distributed availability. Approximately 822 million tonnes produced annually worldwide (Naqvi et al., 2014). Rice husk is characterised by low VM and N content, and high ash and S content (Claoston et al., 2014). This by-product is typically openly burned or applied to the

soil following detachment of the chaff from the grain (Zhang et al., 2015). The second agricultural by-product that is used is grape pruning. Grape pruning is comparable to the majority of biomass compositions, with low ash and S contents, and high VM and N content (Liang et al., 2016; Marshall et al., 2017; Nasser et al., 2014). Grape pruning is typically openly burned, landfilled, or used for composting (Liang et al., 2016).

1.6. Pyrolysis Fundamentals

Pyrolysis is the thermal decomposition of organic matter at elevated temperatures (300 – 800 °C) in the absence of oxygen. The pyrolysis reaction is primarily endothermic. There are three primary products from the pyrolysis reaction: Biochar (solid), bio-oil (liquid), and pyrogas (gas). Depending on the operating conditions, varying amounts of solid, liquid and gas will be produced (Bridgwater, 2004). As previously mentioned, biochar is the solid carbonaceous product which consists mainly of stable C and ash. Bio-oil is a complex mixture of different species, including aliphatic hydrocarbons, PAHs, and oxygen substituted aromatic species (oxy-aromatics) (Hu et al. 2014; Biswas et al. 2017). Pyrogas (often termed 'syngas') is the non-condensable product of the pyrolysis reaction and consists mainly of CH_4, CO, CO_2, and H_2 (Williams and Nugranad, 2000). The reaction mechanisms of biomass pyrolysis can be defined by the following three primary steps (Demirbas, 2004a):

$$Biomass \rightarrow Water + Unreacted\ Residue \quad (1.1)$$

$$Unreacted\ Residue \rightarrow (Volatile + Gases)_1 + (Char)_1 \quad (1.2)$$

$$(Char)_1 \rightarrow (Volatile + Gases)_2 + (Char)_2 \quad (1.3)$$

The initial step of the pyrolysis reaction is the loss of moisture from the biomass feedstock at low temperatures (Eq. 1.1). The secondary step involves significant temperature rises and the start of primary pyrolysis reactions. This leads to the initial release of volatiles $(Volatile + Gases)_1$ and the gradual formation of char $(Char)_1$ (Eq. 1.2). Flow of the hot volatiles towards the cooler residues leads to heat transfer between the two mediums. During the final step (Eq. 1.3), the char begins to decompose slowly and takes on its C rich solid form $(Char)_2$. Secondary charring makes the char less reactive and forms additional volatiles $(Volatile + Gases)_2$. Condensation of volatiles in cooler regions leads to bio-oil production. Further thermal cracking of the bio-oil fraction at higher temperatures leads to higher pyrogas yields (Tsai et al., 2007). Secondary reaction of volatiles at elevated pyrolysis temperatures can also lead to increases in CO, H_2, and CH_4 production rates at the expense of CO_2 (Xu et al., 2009).

1.6.1. Influence of Operating Conditions

The relative yields of primary pyrolysis products are influenced by several different operating conditions. These include the pyrolysis temperature, heating rate, particle size, and reactor atmosphere (Beis et al., 2002). The process conditions can be varied to optimize the yields of biochar, bio-oil, or pyogas. Table 1.4 shows the typical pyrolysis product yields obtained from different operating conditions (split into different modes of pyrolysis).

Fast pyrolysis is characterised by short residence times (2 – 25 s), moderate pyrolysis temperatures (≈ 500 °C), high biomass heating rates, and high product cooling rates. The primary product from fast pyrolysis is the condensable bio-oil fraction. These conditions also inhibit biochar formation (Manya, 2012). As the fast

pyrolysis reaction occurs rapidly, heat transfer, mass transfer, and reaction kinetics play an important role. Further information can be found in Babu (2008), who discusses several different kinetic models for fast pyrolysis. Higher heating rates generally result in greater bio-oil yields, as demonstrated by Gao et al. (2016). The results showed that the maximum bio-oil yield of 76 wt. % (including water) occurred with a final pyrolysis temperature of 575 °C, heating rate of 20 °C/min, and a biomass particle size of 5 mm. The feedstock particle size also played a major role in the heating rate of the biomass and therefore the bio-oil yield. The highest yield was seen with intermediate sized particles. The smallest particles had rapid heat transfer and increased secondary cracking reactions that decreased the yield of bio-oil. Larger particles had slower heating rates, which negatively affected the final yields (Gao et al., 2016).

Fast pyrolysis, however, suffers from several drawbacks that complicate any attempts to utilize agricultural by-products on a large-scale. The primary product of fast pyrolysis (bio-oil) is not currently economically or technically viable as a fuel due to several issues. High oxygen content, low pH resulting from the presence of acids (including acetic acid), and high moisture content render bio-oil inferior to traditional hydrocarbon fuels (Isahak et al., 2012). In addition, the upgrading of bio-oil to a higher quality fuel has issues with catalyst instability, bio-oil deterioration, and general quality issues that render it uneconomical currently (Mortensen et al., 2011).

Slow pyrolysis is the preferred approach for optimizing biochar production. This method is characterized by low pyrolysis temperatures (≈ 400 °C), slower heating rates, and long residence times (> 10 mins) (Russell et al., 2017). Slow pyrolysis also yields reduced fractions of bio-oil in the raw pyrolysis volatiles. This

approach can be considered the conventional approach of pyrolysis as it has been applied for many years for the production of charcoal from wood (Mohan et al. 2006). This approach is also beneficial for the production of biochar with higher contents of stable C (Roberts et al., 2010). This is essential for effective long-term C sequestration in soils with added benefits to agricultural productivity. While lower pyrolysis temperatures generally result in higher biochar yields, elevated pyrolysis temperatures (600 – 800 °C) result in greater C content in the biochar (Williams and Nugranad, 2000). Biochar total ash content also increases with pyrolysis temperature as the majority of the species in the ash are not volatilized between 400 and 800 °C (Claoston et al., 2014).

1.6.2. Reactor Types

1.6.2.1. Screw (Auger) Reactor

Screw reactors are commonly used for the pyrolysis of biomass due to their simplicity and ease of operability (Brown, 2009). These reactors typically consist of a single or twin-screw enclosed in a tube that is rotated at a low RPM to maximize residence times for biochar production (Brassard et al., 2017). The residence time can be easily controlled by the variable RPM. As the biomass is continuously fed into the reactor the screw rotation transports the product along the screw axis until the end of the screw. Heating of the biomass can either be done indirectly, or directly with a heat transfer medium that is fed with the biomass, such as sand (Brown and Brown, 2012). As the raw pyrolysis volatile products evolve they exit the reactor due to pressure differences (Brown, 2009). The biochar will typically drop under gravity at the end of the screw to be collected. These reactors can be mobile, they require little or no carrier gas, and have low energy requirements (Brassard et al., 2017). Screw reactors are also tolerant to biomass feedstocks with high ash contents. The bio-oil

can be condensed out of the raw pyrolysis volatiles to generate a bio-oil-free pyrogas for combustion, or the bio-oil and pyrogas can be co-combusted (Ning et al., 2013).

One problem for screw reactors is the limitations of heat transfer, especially at large-scale (Bahng et al., 2009; Kan et al., 2016). This has resulted in reported heat-transfer problems associated with scaling up screw reactors to industrial scale (Funke et al., 2017). Due to the significant amount of work investigating the pyrolysis of biomass in screw reactors, however, they are considered a mature technology (Babu, 2008; Brown, 2009; Brown and Brown, 2012; Li et al., 2014). An example of a two-stage continuous screw-kiln reactor for the production of pyrogas and biochar from the pyrolysis of waste wood with subsequent catalytic steam reforming of the pyrolysis oils and gases is shown in Fig. 1.6 (Efika et al., 2012).

1.6.2.2. Rotary Kilns

Rotary kilns are cylindrical vessels that transport the biomass by slow rotation about an axis that is slightly inclined to the horizontal. The vessel is rotated slowly, facilitating long residence times for the material travelling from the upper to lower end. Stirring and mixing provides the necessary heat transfer for the pyrolysis reaction. Carrier gas is typically supplied so that it passes counter-current to the biomass, improving reaction rates. The rotary kiln typically prevents agglomeration and ensures a good mixing of the biomass particles because of the rotation of the reactor (Acevedo and Barriocanal, 2015). Limitations of feedstock shape, size and HHV are less of an issue for rotary kilns when compared to other reactor types (Conto et al., 2016). This has made rotary kilns an active research area for the utilization of waste tyres for char production (Fig. 1.7) (Acevedo and Barriocanal, 2015; Antoniou and Zabaniotou, 2015).

Very few studies, however, have been reported for the performance of rotary kiln reactors for the pyrolysis of agricultural by–products. Conto et al. (2016) investigated the performance of a rotary kiln reactor for the pyrolysis of elephant grass. They observed that the C content of the biochar increased and the O/C ratio decreased with rotational speed. Rotary speed did not appear to influence the composition of the ash in the biochar. Other published studies include the pyrolysis of wheat straw (Kern et al., 2012), olive stone (Sanginés et al., 2015), and eupatorium adenophorum spreng/tobacco stem (Meng et al., 2015). The lack of available literature on the use of rotary kilns for this purpose compared to other reactor types, however, means that it cannot be considered a common reactor design for pyrolysis reaction.

1.6.2.3. Fixed-Bed Reactor

Numerous studies have investigated the production of biochar from agricultural by-products in fixed-bed reactors. The traditional method of charcoal production through slow pyrolysis, including earth or metal kilns, is one example of fixed-bed reactor. Here, the biomass is piled into the batch reactor and sealed so that the atmosphere is O-free (Brassard et al., 2017). More recent studies have investigated the use of fixed-bed reactors for the production of biochar from various agricultural by-products. This includes the pyrolysis of pine wood, wheat straw, green waste, and dried algae in fixed-bed reactors by Ronsse et al. (2013). It was noted that the fixed C content in the biochar samples increased with higher temperatures and longer residence times in the pyrolysis process. Other studies have investigated fixed-bed reactors for the production of biochar from brown alga (saccharina japonica) (Choi et al., 2016), dairy manure (Liu and Tsai, 2016), and pine wood (Li et

al., 2014). Fixed-bed reactors are, however, limited by their throughput and have difficulties in scaling-up to produce large quantities of biochar.

1.6.2.4. Fluidized-Bed Reactor

Research into biomass pyrolysis with fluidized-bed reactors has generally been split into BFB and CFB reactors (Brown, 2009). For BFBs, the biomass is first fed into a vertical reactor vessel with a bed of solid material (Fig. 1.8a). Large flows of inert gas are used to fluidize the bed material. Multiple orientations of heating arrangements can be used, including indirect heating from hot combustion products or arrays of tubes inside the reactor (Bridgwater, 2007). The pyrolysis products exit at the top of the reactor with the fluidizing gas. CFB reactors differ from BFBs as they have a separate combustion chamber to re-heat the bed material which is continuously circulated, rather than having the bed material suspended in one reactor (Fig. 1.8b) (Brown, 2009). Fluidized-beds are characterized by excellent heat and mass transfer rates at a small-scale, resulting in high efficiencies (Song et al., 2015).

Numerous problems still exist however. Though fluidized-bed reactors have been demonstrated on a commercial scale, their construction and operation at this scale is often complex. Heat transfer problems and significant energy requirements associated with handling the fluidization gas have also been reported during scaling (Brown, 2009). High inert gas flows are also required to maintain fluidization (Brown and Brown, 2012). Problems with ash agglomeration, especially in agricultural by-products with high ash contents, can also be problematic (Khadilkar et al., 2015). For these reasons, the number of studies reporting the production of biochar using fluidized-bed pyrolysis is still very limited (Yang et al., 2016). Wang et al. (2013) investigated the co-production of bio-oil and biochar from microalgae in a fluidized

bed reactor at 500 °C. The reported yields of bio-oil, biochar, and pyrogas were 53, 31, and 10 wt. %, respectively. Yang et al. (2016) also studied the production of biochar from reed black liquor in a fluidized bed. They found that a reactor temperature of 500 °C and a reaction time of 5.7 min was optimum for producing biochar with maximum adsorption capacities.

Numerous other studies have investigated different reactor types for the pyrolysis of agricultural by-products. These include microwave reactors (Huang et al., 2016), ablative reactors (Bahng et al., 2009), and cone reactors (Verma et al., 2012). The primary focus of this thesis, however, is the co-production of biochar and bioenergy from agricultural by-products in a screw reactor. Due to their tolerance of variable ash and moisture contents (a typical issue with increasing biomass utilization rates), as well as their relative simplicity of design and operation, screw reactors are a mature technology for slow pyrolysis.

1.7. Significance of this Thesis

The co-generation of biochar and bioenergy from agricultural by-products offers an attractive approach for sustainable waste management. The added-value processing of biomass materials that currently have little or no value can potentially contribute to the development of the bio-economy. By co-producing biochar and bioenergy on a large-scale, many of the problems currently faced by society can be addressed in a timely and efficient manner. In particular, pyrolysis-combustion systems offer a method to fully utilize abundant biomass wastes with variable ash and moisture contents. Pyrolysis-combustion processes, despite their obvious potential to increase utilization rates of agricultural by-products, are plagued by uncertainty regarding the influence of operating conditions and feedstock

composition/properties on the emissions from the process. As the conventional methods of disposal are significantly impacting on the health of populations exposed to these emissions, a better understanding of the relationship between key process parameters and pollutant yields for pyrolysis-combustion is needed. Without this insight, effective policy making for agricultural by-product utilization cannot be achieved.

It is well known that the choice of pyrolysis temperature influences both the yield and the quality of the biochar (Claoston et al., 2014). It is also known that the pyrolysis temperature affects the yields, HHV, and composition of the pyrogas and bio-oil (and therefore the raw pyrolysis volatiles) (Williams and Nugranad, 2000). It is therefore clear that the development of pyrolysis-combustion processes will incur a trade-off between effective biochar production and heat/power generation. The extent of this trade-off is currently unclear. It is also expected that the pyrolysis temperature will influence the emissions from the process. This is because the bio-oil/pyrogas ratio, aromatic concentration, S, and N content of the raw pyrolysis volatiles will all vary with pyrolysis temperature (Biswas et al., 2017; Claoston et al., 2014). As a result, it is expected that energy-based yield of the pollutants from the pyrolysis-combustion process will be affected.

The influence of feedstock drying has also not been investigated for the pyrolysis-combustion processes. It is well known that this parameter significantly influences the emissions of PM and PM-bound PAHs during direct combustion (Shen et al., 2013b; Sanchis et al., 2014). The concentration of char-bound PAHs is also of concern, as application of biochar with significant PAH contents will facilitate the existence of carcinogenic contaminants in the soil that are extremely difficult to treat once buried (Dutta et al. 2016). It is also not yet known if the pyrolysis-combustion

process offers a pathway to reduced yields of harmful pollutants during the utilization of agricultural by-products when compared to the conventional methods of disposal, including open burning and cook stoves.

This thesis has therefore focused on developing a better understanding of the influence of process conditions (pyrolysis/volatile production temperature), feedstock properties (moisture, ash, and VM content) and composition (S and N content) on the harmful emissions from the pyrolysis-combustion process. It is only through this endeavour that a viable conclusion can be arrived at regarding the improvement in performance (especially in terms of pollution potential) of pyrolysis-combustion systems over the conventional methods of agricultural by-product utilization. As the co-generation of biochar and bioenergy is an extremely attractive approach to utilizing these abundant materials in a way that addresses many of the world's problems, this work is of crucial importance.

1.8. Aims of this Thesis

In order to achieve the objectives set in this research topic, the following aims were identified for this thesis:

1. Investigate the influence of volatile production temperature (and therefore bio-oil/pyrogas ratios in the raw pyrolysis volatiles) on the energy-based yield of PM and PM-bound PAHs during combustion of the raw pyrolysis volatiles.
2. Understand how the varying degree of volatilization of biomass-bound S and N at various volatile production temperatures influences the energy-based yield of H_2S, SO_2, NO, and NO_2 during combustion of the raw pyrolysis volatiles.

3. Investigate the relationship between pyrolysis temperature and the composition of the biochar (C, H, N, S, and ash) and the concentration of char-bound PAHs.
4. Understand how utilization of agricultural by-products with significantly different ash, VM, S, and N contents influences the energy-based yields of PM, H_2S, SO_2, NO, and NO_2.
5. Investigate the influence of feedstock drying on the PM, PM-bound PAH emissions, and quality of the primary pyrolysis products.

1.9. Outline of Thesis

This thesis is comprised of 6 main Chapters. Chapter 1 provides a detailed outline of the potential for the co-production of biochar and bioenergy to address many of society's current problems. The advantages of utilizing agricultural by-products as feedstocks are described, along with a discussion of the problems associated with conventional methods of disposal. The fundamentals of pyrolysis, as well as the different potential reactor types that can be deployed, are provided in detail. The importance and aims of the thesis are also discussed.

In Chapter 2, the energy-based yields of PM_{10} and $PM_{2.1}$ during the co-generation of biochar and bioenergy from rice husk are presented. Using a lab-scale pyrolysis-combustion facility, various volatile production temperatures (400 – 800 °C) are used to generate raw pyrolysis volatiles with varying bio-oil to pyrogas ratios. The volatiles are then combusted at 850 °C. The aim of this Chapter is to investigate the influence of the varying bio-oil fraction of the volatile mixture on the energy-based yields of PM. The PM emission factor from the pyrolysis-combustion process for rice husk is compared to those from alternative combustion processes with other

high ash content feedstocks to determine the effectiveness of the process for emission mitigation.

Chapter 3 investigates the influence of volatile production temperature (400 – 800 °C) on the emissions of PM-bound PAHs from a lab-scale pyrolysis-combustion process utilizing rice husk. Five different raw pyrolysis volatiles are produced at each temperature and combusted at 850 °C. The concentrations of 15 priority pollutant PAH levels in the resulting PM are evaluated. The influence of pyrolysis temperature on the PAH concentration of the biochar is also investigated. The primary aim of this Chapter is to develop an understanding of how the PAH and oxy-aromatic content of the bio-oil fraction of the raw pyrolysis volatiles (which changes with pyrolysis temperature) influences the PM-bound PAH concentration.

Chapter 4 investigates the influence of feedstock composition (S, N, ash, and VM content) on the yields of harmful PM and gaseous pollutants (SO_2, H_2S, NO_2, NO). A lab-scale continuous pyrolysis-combustion facility utilizing rice husk and grape pruning (which have significantly different compositions) is operated at various volatile production temperatures (400 – 800 °C) and a combustion temperature of 850 °C for the raw pyrolysis volatiles. The first aim of this Chapter is to determine the difference in the yields and HHV of the primary pyrolysis products from the two feedstocks. The influence of feedstock ash and VM content of the energy-based yield of PM and predominance of different PM sizes is also investigated. Finally, the influence of feedstock S and N content, and their respective volatilization rate at each volatile production temperature, on the energy-based yields of NO, NO_2, H_2S, and SO_2 is also discussed.

The aim of Chapter 5 is to investigate the influence of drying of the rice husk (by utilizing both dried and AR) on various process outcomes. This includes the yields of primary pyrolysis products and the HHV of the raw pyrolysis volatiles, the energy-based yields of PM_{10}, $PM_{2.1}$, $PM_{1.1}$, and the concentration of PM-bound PAHs and their toxicity relative to BaP. The lab-scale pyrolysis-combustion process was operated at various volatile production temperatures (400 – 800 °C) and the raw pyrolysis volatiles were combusted at 850 °C.

Chapter 6 presents a summary of the key findings of this thesis and outlines the potential for pyrolysis-combustion processes to contribute towards the global production of biochar and bioenergy. Recommendations for future work are also discussed.

Chapter 2: Production of Biochar from Rice husk: Particulate Emissions from the Combustion of Raw Pyrolysis Volatiles

Lewis Dunnigan[1], Peter J. Ashman[1], Xiangping Zhang[2], Chi Wai Kwong[1*]

[1] School of Chemical Engineering, The University of Adelaide, Adelaide, SA 5005, Australia

[2] Institute of Process Engineering, Chinese Academy of Sciences, Beijing, China

* Author for correspondence (Telephone: +61 8313 0724; Email: philip.kwong@adelaide.edu.au)

This is the revised and corrected version of the paper which appears in:

Journal of Cleaner Production, 172 (2018), 1639 – 1645.

Statement of Authorship

Title of Paper	Production of biochar from rice husk: Particulate emissions from the combustion of raw pyrolysis volatiles
Publication Status	☑ Published ☐ Accepted for Publication ☐ Submitted for Publication ☐ Unpublished and Unsubmitted work written in manuscript style
Publication Details	Journal of Cleaner Production, 172 (2018), 1639 – 1645. DOI: https://doi.org/10.1016/j.jclepro.2016.11.107. At time of final thesis submission: Journal impact factor = 5.651, times cited = 11.

Principal Author

Name of Principal Author (Candidate)	Lewis Dunnigan		
Contribution to the Paper	Construction and development of experimental apparatus. Performance of experiments and interpretation of results. Responsible for the drafting and revision of the paper for publication.		
Overall percentage (%)	70		
Certification:	This paper reports on original research I conducted during the period of my Higher Degree by Research candidature and is not subject to any obligations or contractual agreements with a third party that would constrain its inclusion in this thesis. I am the primary author of this paper.		
Signature		Date	27/02/18

Co-Author Contributions

By signing the Statement of Authorship, each author certifies that:

i. the candidate's stated contribution to the publication is accurate (as detailed above);

ii. permission is granted for the candidate in include the publication in the thesis; and

iii. the sum of all co-author contributions is equal to 100% less the candidate's stated contribution.

Name of Co-Author	Philip Kwong		
Contribution to the Paper	Corresponding author. Provided original idea of the study and financial support through the Catalyst Research Grant from the Government of South Australia. Major contributor to the development of the methodology and critical analysis of experimental results. Significant contribution to the writing and revision of the paper.		
Signature		Date	27/02/18

Name of Co-Author	Peter Ashman		
Contribution to the Paper	Contribution to result interpretation and input for the writing of paper.		
Signature		Date	27/02/18

Name of Co-Author	Xiangping Zhang		
Contribution to the Paper	Contribution to result analysis and input for the writing of paper.		
Signature		Date	27/02/18

Abstract

Increasing energy demands and waste management concerns have motivated agricultural producers to consider the decentralized conversion of agricultural by-products for energy and value-added product (biochar) generation. Due to the variability of fuel properties, direct combustion of agricultural by-products with high ash contents, such as rice husk, may suffer from increased fouling and slagging issues with high PM emissions. Combustion of the raw pyrolysis volatiles (bio-oil and pyrogas mixtures) produced from pyrolysis with the inherent separation of ash in the biochar may potentially mitigate these issues. In this study, PM emissions from the combustion of the raw pyrolysis volatiles derived from the pyrolysis of rice husk were evaluated at laboratory scale by using a combined pyrolysis and combustion facility. Volatile production temperatures ranging from 400 °C to 800 °C were used to generate raw pyrolysis volatiles with differing bio-oil to syngas ratios which were then combusted at 850 °C. It was found that bio-oil dominated the higher heating value of the raw pyrolysis volatiles produced at low pyrolysis temperatures. The combustion of such raw pyrolysis volatiles with high bio-oil content substantially increased the yields of PM_{10} and $PM_{2.1}$. Linear dependence was observed between PM emissions and bio-oil fraction in the raw pyrolysis volatiles. Nevertheless, the pyrolysis-combustion process, with > 96 % of the ash retained in biochar prior to combustion, is more favorable than direct combustion for high ash biomass as far as PM emissions are concerned.

2.1. Introduction

Re-utilization of agricultural by-products as biomass resources has great potential to contribute to the development of the bioeconomy for the co-generation of value added products and bioenergy (Allen et al., 2015). However, limited availability of high quality agricultural by-products for energy applications results in the need to utilize more problematic raw materials with broader variations in fuel properties (Gilbe et al., 2008). Rice husk is an agricultural by-product with low bulk density and high ash content. They are abundant, with approximately 822 million tonnes produced annually worldwide, about 97 % of which is produced in developing countries (Naqvi et al., 2014). Currently most rice husk is underutilized with limited options for recycling (Zhang et al., 2015). However, it can contribute to the bio-economy significantly if options such as decentralized conversion systems are available for agricultural producers/farmers to utilize rice husk as a renewable resource.

Direct combustion is often utilized for biomass to produce heat and power for energy services. However, combustion of biomass with high ash content suffers from several disadvantages when compared to low ash fuels. Firstly, the residual ash content can deposit on internal heat transfer surfaces, leading to the formation of slags and clinkers (Gilbe et al., 2008; Jenkins et al., 1998) which negatively affect heat transfer rates and decrease boiler efficiency. Secondly, the abundant inherent inorganic species in biomass may potentially lead to significant PM emissions (Gao and Wu, 2011; Johansson et al., 2003; Johansson et al., 2004). Direct combustion of agricultural by-products with high silica ash content, such as rice husk, can result in

the release of fibrous PM, including crystalline silica, which can cause major health concerns (Gilbe et al., 2008).

Considering the negative impact of ash on the performance of combustion systems; ash components can instead be separated into the solid biochar prior to combustion through the pyrolysis of biomass at mild temperatures. Biochar, the solid product of biomass pyrolysis, has demonstrated a high potential to offset C emissions by long-term C sequestration with additional agricultural benefits (Williams and Nugranad, 2000). Gas-cleaning systems, such as condensation, are commonly used in centralized pyrolysis operations to separate the bio-oil products from the raw pyrolysis volatiles in order to generate a clean (bio-oil-free) pyrogas for power generation (Ning et al., 2013). However, separation of the bio-oil substantially reduces the effective energy output, as the production of pyrogas is limited at the mild T_p that favour biochar production. Furthermore, the upgrading of bio-oil is currently economically prohibitive, due to issues with bio-oil quality, catalyst instability, and deterioration during storage (Mortensen et al., 2011; Lehto et al., 2014).

This motivated the investigation of the combustion of raw pyrolysis volatiles (bio-oil and pyrogas mixtures, hereafter called pyrolysis volatiles) for the co-generation of value-added product (biochar) and low-emission bioenergy in a combined pyrolysis and combustion (pyrolysis-combustion) process. This potential approach eliminates the handling of the corrosive bio-oil product (Mortensen et al., 2011) and utilizes the significant energy content of the liquid product for power generation rather than being separated out for further upgrading/disposal (Lehto et al., 2014). This approach is attractive for decentralized biochar and bioenergy

generation in agricultural sectors (Mohammadi et al., 2016) as it minimizes the C emissions due to transportation of the low-bulk density agricultural by-product and upgrading processes (Roberts et al., 2010; Bazmi et al., 2015). However, combustion of the pyrolysis volatiles is not entirely “clean”, as bio-oil is a mixture of complex organic compounds, the combustion of which may result in higher emissions when compared to pyrogas only. To the best of our knowledge, previous work investigating the atmospheric emissions, particularly PM, resulting from combustion of the pyrolysis volatiles during the co-production of biochar and bioenergy is not available in the literature.

The aims of this study are to investigate the energy-based yield of PM from the combustion of pyrolysis volatiles with different fractions of bio-oil and pyrogas generated from the pyrolysis of rice husk; and compare the PM emissions from the pyrolysis-combustion process to the direct combustion of other biomass.

2.2. Materials and Methods

2.2.1. Materials Characterization

The rice husk used in this study was provided by Beerbelly Brewing Equipment (Pooraka, South Australia). Once received the rice husk was ground in a rotary mill and then sieved to 420 - 500 mm. It was then dried in an oven at 105 °C for a minimum of 15 h. Biochar samples were obtained from the pyrolysis of rice husk according to the procedure described in Section 2.2.2 and then subjected to proximate and ultimate analysis. Proximate analyses were carried out using a TGA (SETARAM, Labsys™). Approximately 65 mg of sample was used to determine the weight fractions of VM, ash, and fixed C according to ASTM D7582. The moisture content of the rice husk was determined by the oven-drying method following ASTM

D4442. Ultimate analyses of the rice husk and biochar were carried out using a CHNS determinator (PerkinElmer, 2400 Series II CHNS/O). The ultimate analysis for C, H, N, S, and O was carried out following ASTM D5373. The O content was calculated by difference. The HHV of the rice husk and biochar were calculated using the Boie equation (Boie, 1953).

2.2.2. Pyrolysis, Combustion, and Sampling

Fig. 2.1 shows a schematic diagram of the experimental system for the pyrolysis-combustion study. Rice husk, after the pre-processing stage, was loaded into a hopper and continuously fed into the main screw reactor at a feeding rate of 1.3 g/min. The biomass was then transported along the entire length of the screw reactor where it was heated by two sets of electrical heaters and maintained at 400, 500, 600, 700, and 800 °C for the pyrolysis reactions. It should be noted that the term "T_p" is used in this Chapter when considering sampling of the biochar, bio-oil, and pyrogas. The term "T_v" is used when discussing sampling of the PM generated from combustion of the raw pyrolysis volatiles. N_2 at 0.25 l/min was provided through the hopper to remove O from the system. The solid biochar was collected under gravity in a collection vessel at the end of the screw reactor. The yield of biochar is the recovered yield expressed as a percent by weight of dry feed and was estimated using the mass ratio of feedstock and biochar obtained in the collection vessel. An additional 0.1 l/min of N_2 was provided from the collection vessel to avoid stagnation of the combustible volatiles. The raw pyrolysis volatiles were premixed with the filtered air and transported to a burner situated at the bottom of a quartz tube (150 cm height x 4.5 cm i.d.) within a vertical 3-zone tube furnace (Carbolite®, GVC 12/1050). The furnace temperature was maintained at 850 °C for the combustion (T_c). The piping between the outlet of the pyrolysis reactor and the combustion

region was insulated in order to maintain the temperature above 350 °C and prevent condensation of the bio-oil. The HHV of the pyrolysis volatiles was estimated using a mass and energy balance based on the yields of biochar and the HHVs of the rice husk and biochar.

2.2.3. Bio-Oil Sampling

The yield of bio-oil was obtained using a condensation train consisting of eight 50 ml test tubes connected in series and immersed in an ice/water mixture (≈ 0 °C). Piping between the pyrolysis heater and the first test tube was heated to around 350 °C to prevent condensation of bio-oil. The difference in weight of the condensation train before and after the experimental run was taken as the mass of bio-oil.

2.2.4. Pyrogas Sampling

A Teflon gas-sampling bag was used to collect the pyrogas sample for analysis using GC - TCD (Agilent, 490 Micro GC). The first channel of the gas analyser detected H_2, O_2, N_2, CH_4, and CO with a Molecular Seive 5A column, the second channel detected CO_2 with a Poraplot U column, and the third channel detected hydrocarbons (butane - n-heptane) with a Silicon 5CB column. The HHV of the pyrogas was calculated based on the heating values and concentrations of the individual species. The mass of pyrogas produced was calculated as the difference between the mass of the feedstock used and the combined mass of bio-oil and biochar. The HHV of the raw pyrolysis volatiles (HHV_{RPV}) was calculated using an energy balance around the pyrolysis reactor (1 kg of feed basis):

$$HHV_{RPV} = \frac{HHV_{RH} - (y_{biochar} \times HHV_{biochar})}{y_{RPV}} \quad (2.1)$$

where HHV_{RPV}, HHV_{RH}, and $HHV_{biochar}$ are the heating values of the raw pyrolysis volatiles, rice husk, and biochar respectively (MJ/kg), and $y_{biochar}$ and y_{RPV} are the yields of the biochar and raw pyrolysis volatiles respectively.

2.2.5. Flue Gas Sampling

Two samplings ports were positioned on the stainless steel adaptor between the ADT and the top of the quartz pipe situated above the vertical tube furnace. The CO_2 analysis of the flue gas was carried out using a portable nondispersive infrared sensor (CO2meter.com, CM-0017) with a resolution of 0.5 vol %. A portable CO/O_2 analyser (Bacharach, Fyrite® INSIGHT® Plus) was used to analyse the CO level in the flue gas with a resolution of 20 ppmv and O_2 level with a resolution of 0.3 %.

2.2.6. Dilution and PM Sampling

A CI (Copley Scientific, 8-stage Anderson cascade impactor) was used to collect the PM and generate mass-size distributions. The size range of the CI was 0.1 - 10 µm. PM_{10} and $PM_{2.1}$ refer to particulates in the size fractions 0.1 - 10 µm and 0.1 - 2.1 µm that presented in the flue gas, respectively. The CI was situated immediately downstream of an ADT. The ADT was used to supply a mixture of air and flue gas at a dilution ratio of 8 with a fixed volumetric flowrate of 28.3 l/min to the CI. As all of the flue gas was sampled, isokinetic sampling was not required (Zhang and Morawska, 2002). Quartz fiber filter papers were used for all stages except the back-up stage, which used a PTFE filter with a 0.1 µm pore size. The filters were prepared for the collection of PM following an adapted methodology outlined in the USEPA Method 5 (USEPA, 2000) and the State of California Air Resources Board: Method 501 (CARB, 1990). The filter papers were dried and weighed before and after the experiments. The standard error of the mean from a set of three separate 18 min runs was obtained. The mass-based yields of PM_{10} and $PM_{2.1}$ were divided

by the HHV of the pyrolysis volatiles and presented as the energy-based yields in this study.

2.3. Results and Discussion

2.3.1. Feedstock and Biochar Characteristics

The proximate analysis of the rice husk in Table 2.1 shows that they have a high amount of ash (21.5 %). The ash content of rice husk is significantly greater than other types of biomass. Typical ash contents for other agricultural by-products vary between 0.3 and 8.4 % (Alper et al., 2015). This high ash content clearly suggests that fouling and slagging could potentially occur in the direct combustion of rice husk. In addition, it is well known that silica, the main constituent of rice husk ash, is very abrasive and can react with alkalis to form alkali silicates that melt or soften at low temperatures, promoting the formation of slag and clinker (Gilbe et al., 2008; Jenkins et al., 1998). The ultimate analysis indicated that rice husk had a relatively low C content (38.1 %) when compared to other biomass types (Claoston et al., 2014). Biochars produced from other forms of biomass typically have a C content between 60 and 95 % (Antal Jr. and Gronli, 2003; Claoston et al., 2014). The reduced C content of the rice husk derived biochar (42 – 43 %) compared to that derived from other typical agricultural by-products is a direct result of its high ash content.

The proximate analysis results show that around 96 – 99 % of feedstock ash was retained in the biochar (Table 2.1). In most cases, the C content of biochar increases with T_p (Alper et al., 2015). However, this is often not the case for biochar produced from rice husk due to the significant ash content which is not liberated during pyrolysis (Claoston et al., 2014; Jindo et al., 2014). This agrees with (Enders

et al., 2012) who found that greater T_p for low ash biochars increased fixed C, but decreased for biochars with more than 20 % ash. In addition, the H and N contents were lower than other agricultural by-products, while the S content was relatively high (Antal Jr. and Gronli, 2003). S content in the char was reduced due to its volatilisation at higher temperatures.

2.3.2. Pyrolysis Products

Fig. 2.2a shows the effect of T_p on the yields of pyrogas, bio-oil, and biochar. It was found that the yield of pyrogas increased with T_p. The opposite trend was observed for the yields of bio-oil and biochar, which decreased with temperature. This is consistent with other studies of biomass pyrolysis (Williams and Nugranad, 2000; Antal Jr. and Gronli, 2003; Tsai et al., 2007). The maximum yield of bio-oil is typically obtained at a low temperature, above which higher temperatures promote gas production. The reason for this is that higher temperatures promote further cracking of the condensable hydrocarbons which includes aromatic compounds, along with other oxygen containing hydrocarbons and complex PAHs (Naqvi et al., 2014), leading to a greater production rate and yield of gas (Tsai et al., 2007). The increasing gas yield reduced the mass of the remaining char and therefore decreasing yields of biochar with T_p was observed. Fig. 2.2b shows the effect of T_p on the HHV of the pyrolysis volatiles and its contributions from pyrogas and bio-oil. It was found that the energy content of the pyrolysis volatiles increased slightly by about 7 % from 400 °C (14.2 MJ/kg) to 700 °C (15.2 MJ/kg). However, the contribution of bio-oil to the overall HHV of the pyrolysis volatiles reduced substantially from 90 % to 44 % at the T_p of 400 and 800 °C, respectively.

Fig. 2.3 shows that the major constituents of the pyrogas at different T_p were CO, H_2, CO_2, and CH_4. The concentrations of each species at each T_p were

normalized to 50 % N_2 for comparison. It was found that the concentrations of CO and H_2 in the pyrogas increased significantly with T_p, while CO_2 showed the opposite trend. A slight increasing trend was observed for CH_4, with its concentration maintained at around 3 % before 700 °C and then increasing to around 6 % at 800 °C. It has been suggested that the secondary reactions of volatiles at high temperatures generate mostly CO, H_2, and CH_4 rather than CO_2 (Xu et al., 2009; Luo et al., 2004). Aside from the gas species presented in Fig. 2.3, trace amounts of ethane and propane were also detected at each T_p. The HHV of the pyrogas and carrier gas mixture increased from around 2.3 MJ/kg at 400 °C to 5.4 MJ/kg at 800 °C due to the increase in H_2 and CH_4 concentrations.

2.3.3. PM Emissions during the Combustion of Pyrolysis Volatiles

2.3.3.1. Particle Size Distribution

Fig. 2.4a shows the normalized particle mass-size distribution resulting from the combustion of the pyrolysis volatiles at 850 °C. In this study, a relatively low T_c of 850 °C was used as this is a typical temperature found in small-scale combustion systems (Obernberger, 1998; Miles et al., 1996). For each of the combustion experiments, the CO_2 and CO levels of the flue gas at 5 % O_2 were maintained at around 13 % and 400 ppmv, respectively. It was found that the coarse mode (≈ 9 – 10 μm) was the predominant size range of PM generated from the combustion of pyrolysis volatiles. In addition, no distinctive sub-micron peak was observed, suggesting minimal ash vaporization. This result was expected as the T_c of 850 °C was not sufficiently high to vaporize the majority of the ash. Furthermore, the majority of the ash (> 96 %) was retained in the biochar prior to combustion. This result closely resembles the PM mass-size distributions that can be found in fuel-oil combustion (Linak et al., 2000a; Umbria et al., 2004).

2.3.3.2. Energy-Based Yields of PM_{10} and $PM_{2.1}$

Fig. 2.4b shows the energy-based yield of PM_{10} and $PM_{2.1}$ during the combustion of the pyrolysis volatiles at 850 °C. Yields of PM_{10} and $PM_{2.1}$ from the combustion of the pyrolysis volatiles were estimated to be between 2 - 5 and 0.3 - 2 $mg/g_{volatiles}$ respectively. This corresponds to energy-based yields of 154 - 370 mg/MJ for PM_{10} and 21 - 118 mg/MJ for $PM_{2.1}$. The yields of both PM_{10} and $PM_{2.1}$ reduced substantially with the increasing T_V. Between 400 °C and 800 °C there is a 58 % decrease in the yield of PM_{10} and 82 % decrease in $PM_{2.1}$. This demonstrated that the greatest PM emissions occur when the pyrolysis-combustion system is optimized for biochar production. In contrast, when the system is optimized for energy generation (i.e. higher T_V), lower PM yields were observed.

Despite similar combustion conditions being used, there is a strong linear correlation between the energy-based yields of PM and the bio-oil fraction of the pyrolysis volatiles (Fig. 2.5a). It is suggested that the increasing number of C atoms in the fuel molecules would increase the unburned C contents (soot) in premixed flames under similar combustion conditions (Calcote and Manos, 1983; Olson et al., 1985). Therefore, increasing the bio-oil fraction has a similar effect because bio-oil produced from biomass pyrolysis consists of complex compounds including organic acids, carbonyls, phenols, anhydrosugars, and hydrocarbons (Naqvi et al., 2014; Alper et al., 2015). These compounds contain much longer hydrocarbon chain lengths than the pyrogas constituents (CO, CH_4, H_2), which strongly increases the tendency to soot due to greater ability to resist oxidation and survive into the burned gas zone (Calcote and Manos, 1983). As a result, increased yields of PM from pyrolysis volatiles combustion were observed with the increased bio-oil fraction.

2.3.3.3. $PM_{10}/PM_{2.1}$

Even though the total yield of PM_{10} and $PM_{2.1}$ increased with the bio-oil fraction in the pyrolysis volatiles, a decrease in $PM_{10}/PM_{2.1}$ was observed (Fig. 2.5b). This suggested that higher bio-oil fractions in the pyrolysis volatiles favoured $PM_{2.1}$ formation at a greater rate than PM_{10} during combustion. This is counterintuitive; as it would be expected that higher pyrogas fractions in the pyrolysis volatiles would favour sub-micron particulate formation due to more complete C burnout. However, both the sub- and super-micron size range of particulates were included in $PM_{2.1}$ (0.1 - 1 µm and 1 - 2.1 µm) and their formation mechanisms were different (Linak et al., 2000a). Therefore, it is appropriate to examine not only the total $PM_{2.1}$ mass, but also the contribution from the sub and supermicron fractions in $PM_{2.1}$.

Table 2.2 summarises the weight contribution of the smallest and largest particulate size fractions to the overall yield of $PM_{2.1}$ at different bio-oil fractions in the pyrolysis volatiles. It can be seen that increased bio-oil fractions in the pyrolysis volatiles increase the contribution of the largest particulates, while increased pyrogas fractions increase the contribution of the smallest particulates. This suggests that although $PM_{10}/PM_{2.1}$ decreased with the increasing bio-oil fraction, the proportion of $PM_{2.1}$ mass made up of super-micron particulates (1 - 2.1 µm) increased. This agrees with the conclusion of (Linak et al., 2000a), who suggested that total super-micron PM fractions increase when incomplete C burnout is the dominating PM formation mechanism, while sub-micron PM fractions increase when ash vaporization and complete C burnout dominates.

2.3.4. Comparison of PM emissions of Pyrolysis-Combustion with Direct Combustion

A meta-analysis was carried out in order to compare the energy-based yield of PM_{10} when utilizing rice husk in the pyrolysis-combustion process with other biomass types in small-scale combustion devices. Fig. 2.6 indicates that lower PM emissions for a given energy output could be achieved when compared to other small-scale direct combustion devices utilizing high ash content biomass (Gao and Wu, 2011; Nussbaumer et al., 2008; Schmidl et al., 2011; Shen et al., 2012; Smith et al., 2000; Zhang et al., 2000). Fig. 2.6 also indicated that, although the energy-based yield can vary significantly between different combustion systems, the results from each study showed a trend of increasing energy-based yield of PM with the ash content of the biomass feedstock. This agrees with (Johansson et al., 2003; Yani et al., 2015; Khalil et al., 2013), who all arrived at a similar conclusion while investigating the relationship between fuel ash content and PM emissions from raw biomass combustion. The substantial PM emission reduction during pyrolysis-combustion is an important finding. It demonstrates a potential low emission technique that enables the effective utilization of abundant high ash biomass resources, such as rice husk, for simultaneous clean bioenergy and biochar generation.

2.4. Conclusion

An experimental comparison of the PM emissions from the combustion of raw pyrolysis volatiles at 850 °C derived from the pyrolysis of rice husk at different temperatures (400 - 800 °C) was carried out. It was found that combustion of the raw pyrolysis volatiles generated at 400 °C with the highest bio-oil fraction had substantially increased energy-based yields of PM_{10} and $PM_{2.1}$ by 58 % and 82 %

respectively when compared to combustion of the raw pyrolysis volatiles with the lowest bio-oil fraction (800 °C). This implied that the PM emissions were higher if the pyrolysis-combustion process was optimized for biochar production at lower T_v. Despite a high ash content feedstock (21.5 %) being used, the energy-based yields of PM_{10} of 154 - 370 mg/MJ were comparable to or lower than those from the small-scale direct combustion of low ash biomass.

Chapter 3: Polycyclic Aromatic Hydrocarbons on Particulate Matter Emitted during the Co-Generation of Bioenergy and Biochar from Rice Husk

Lewis Dunnigan[1], Benjamin J. Morton[1], Philip J. van Eyk[1], Peter J. Ashman[1], Xiangping Zhang[2], Philip Anthony Hall[3], Chi Wai Kwong[1*]

[1] School of Chemical Engineering, The University of Adelaide, Adelaide, SA 5005, Australia

[2] Institute of Process Engineering, Chinese Academy of Sciences, Beijing, China

[3] School of Physical Sciences, The University of Adelaide, Adelaide, SA 5005, Australia

* Author for correspondence (Telephone: +61 8313 0724; Email: philip.kwong@adelaide.edu.au)

This is the revised and corrected version of the paper which appears in:

Bioresource Technology, 244 (2017), 1015–1023.

Statement of Authorship

Title of Paper	Polycyclic aromatic hydrocarbons on particulate matter emitted during the co-generation of bioenergy and biochar from rice husk
Publication Status	☑ Published ☐ Accepted for Publication ☐ Submitted for Publication ☐ Unpublished and Unsubmitted work written in manuscript style
Publication Details	Bioresource Technology, 244 (2017), 1015–1023. DOI: http://dx.doi.org/10.1016/j.biortech.2017.08.091. At time of final thesis submission: Journal impact factor = 5.807, times cited = 4.

Principal Author

Name of Principal Author (Candidate)	Lewis Dunnigan		
Contribution to the Paper	Construction and development of experimental apparatus. Performance of experiments and interpretation of results. Responsible for the drafting and revision of the paper for publication.		
Overall percentage (%)	60		
Certification:	This paper reports on original research I conducted during the period of my Higher Degree by Research candidature and is not subject to any obligations or contractual agreements with a third party that would constrain its inclusion in this thesis. I am the primary author of this paper.		
Signature		Date	27/02/18

Co-Author Contributions

By signing the Statement of Authorship, each author certifies that:

i. the candidate's stated contribution to the publication is accurate (as detailed above);

ii. permission is granted for the candidate in include the publication in the thesis; and

iii. the sum of all co-author contributions is equal to 100% less the candidate's stated contribution.

Name of Co-Author	Philip Kwong		
Contribution to the Paper	Corresponding author. Provided original idea of the study and financial support through the Catalyst Research Grant from the Government of South Australia. Major contributor to the development of the methodology and critical analysis of experimental results. Significant contribution to the writing and revision of the paper.		
Signature		Date	27/02/18

Name of Co-Author	Benjamin J. Morton		
Contribution to the Paper	Involved with the analysis of the experimental results. Contributed to the writing of the paper.		
Signature		Date	27/02/18

Name of Co-Author	Philip J. van Eyk		
Contribution to the Paper	Contribution to improving the technical content and writing style of the paper.		
Signature		Date	27/02/18

Name of Co-Author	Peter Ashman		
Contribution to the Paper	Contribution to result analysis and input for the writing of paper.		
Signature		Date	27/02/18

Name of Co-Author	Xiangping Zhang		
Contribution to the Paper	Contribution to result analysis and input for the writing of paper.		
Signature		Date	27/02/18

Name of Co-Author	Philip Anthony Hall		
Contribution to the Paper	Performed the GC-MS work for the PAH analysis sections of the paper. Provided quantification work for the PAH experiments.		
Signature		Date	27/02/18

Abstract

The aim of this study was to evaluate the emissions of PAHs bound to the PM during the combustion of raw pyrolysis volatiles (bio-oil and pyrogas mixture) generated from the pyrolysis of rice husk. Five different raw pyrolysis volatiles were produced at varying volatile production temperatures (400–800 °C) and subsequently combusted in a laboratory-scale, continuous pyrolysis-combustion facility at 850 °C. 15 priority pollutant PAH levels in the resulting biochar, bio-oil, and PM were evaluated. Results showed that combustion of the raw pyrolysis volatiles produced at elevated pyrolysis temperatures resulted in greater concentrations of PM-bound PAHs (119 % increase between 400 and 800 °C) due to the increased PAH and oxy-aromatic content of the bio-oil fraction. Significantly increased BaP – equivalent toxicity of the biochar and PM was observed at elevated pyrolysis temperatures.

3.1. Introduction

The utilization of agricultural by-products for the co-generation of bioenergy and value-added products (i.e. biochar) is an attractive approach for sustainable waste management. These materials represent a potentially abundant and renewable source of energy (Huang et al., 2013; Yin et al., 2017). One approach for the co-generation of bioenergy and biochar is to utilize the by-products is a pyrolysis-combustion process. Rice husk is one abundant agricultural by-product with traditionally limited options for recycling due to its significant ash content and distributed availability (Sun et al., 2017). Currently these resources are not only being wasted (Valix et al., 2017), but are also contributing to environmental pollution through their direct combustion and open burning (Sun et al., 2017; Ma et al., 2016). Decentralized pyrolysis-combustion systems are especially advantageous for the utilization of rice husk because ash related fouling/slagging issues are minimized due to the fuel ash being retained with the biochar prior to combustion. The application of rice husk biochar to soil has demonstrated effective nutrient recycling capability (Marshall et al., 2017; Pratiwi and Shinogi, 2016; Dutta et al., 2016), while also sequestering C effectively (Yue et al., 2016). Conventional recycling methods of rice husk, such as open burning or burying in the soil, are inefficient at recycling nutrients and provide little added-value to the by-product. Furthermore, reduced PM emissions have also been reported for pyrolysis-combustion when compared to other small-scale direct combustion processes (Chapter 2). This approach is therefore a possible sustainable pathway for the full utilization of agricultural by-products with high ash contents, such as rice husk.

Pyrolysis-combustion involves co-combustion of the untreated liquid (bio-oil) and gaseous (pyrogas) products from pyrolysis (a mixture termed ‘raw pyrolysis volatiles’). This is especially attractive when the system favours bio-oil production over pyrogas at low pyrolysis temperatures, as it allows full utilization of the heating value from the liquid products (Williams and Nugranad, 2000). This is in contrast to the typical approach of bio-oil production, which involves condensation and separation from the raw pyrolysis volatile mixture prior to combustion in order to be upgraded to a higher quality fuel in a centralized facility (Islam and Ani, 2000). The upgrading of bio-oil is currently economically prohibitive due to issues with bio-oil quality, catalyst instability, and deterioration during storage (Hassan et al., 2016). Despite combustion of raw pyrolysis volatiles with significant bio-oil contents being beneficial for a self-sustaining pyrolysis-combustion process, to date there have been no studies investigating the toxicity of the PM emissions from such a process. One of the most toxic components of PM emissions are PAHs. Many PAHs are known carcinogens and mutagens, and are therefore subject to strict environmental guidelines (NRC, 2002; Keith, 2015). Generally, the PAHs that are considered to be carcinogenic have higher molecular weights (i.e. greater number of aromatic rings), lower vapor pressures, and lower solubility constants (Nisbet and LaGoy, 1992). Estimation of PAH-related toxicity is provided through the application of a BaP –TEF to PAH concentrations and provides a more accurate risk assessment for environmental exposure to PAHs (Jung et al., 2010).

Despite the influence of pyrolysis operating conditions on the PAH content and BaP – TEQ of biochar being well documented (Hale et al., 2012), there is currently no information available on the role of pyrolysis temperature and aromaticity of the raw pyrolysis volatiles on the PAH-related toxicity of the PM

emissions. While PAHs are generally formed in fuel-rich regions of hydrocarbon combustion reactions (Richter and Howard, 2000), the origin of PM-bound PAHs from the pyrolysis-combustion process is complicated by the fact that the bio-oil can itself possess significant amounts of both PAHs and oxygen substituted aromatic species (oxy-aromatics) (Hu et al., 2014; Biswas et al., 2017). The pyrolysis temperature plays a major role in pyrolysis reactions, with increasing PAH production typically found at higher temperatures (Ledesma et al., 2002; McGrath et al., 2003). As such, the raw pyrolysis volatiles that are combusted for the purpose of bioenergy generation in the pyrolysis-combustion process can possess a wide-range of PAH concentrations depending on the pyrolysis temperature.

The influence of “fuel” (in this case the raw pyrolysis volatiles) PAH content on the PM-bound PAH concentration has typically been limited to studies for gasoline and diesel combustion (Westerholm et al., 1988; Atal et al., 1997; Pedersen et al., 1980). Some of these studies have shown that increased aromatic and PAH content in the fuel can result in increased PM-bound and gas-phase PAH emissions (Atal et al., 1997; Pedersen et al., 1980), while others have suggested little or no correlation (Westerholm et al., 1988). The aromatic constituents of the raw pyrolysis volatiles can undergo transformation during the combustion process via HACA reactions or resist oxidation and survive through to the flue products (Richter and Howard, 2000). In addition, the influence of the pyrolysis temperature on the PAH concentration of the biochar is also of concern, as the application of biochar to the soil may facilitate the persistence of PAHs in the environment (Quilliam et al., 2013; Lyu et al., 2016; Nisbet and LaGoy, 1992). The presence of oxy-aromatics in the bio-oil also requires consideration, as they are known to cause damage to cell tissue upon exposure (Dellinger et al., 2000).

The objectives of this study are to determine the influence of 1) pyrolysis temperature on the concentration and composition of biochar-bound PAHs, 2) pyrolysis temperature on the concentration and composition of bio-oil PAHs and oxy-aromatics, and 3) bio-oil aromatic content on the PM-bound PAH concentrations and associated BaP – TEQ.

3.2. Materials and Methods

3.2.1. Pyrolysis-Combustion System

The rice husk used in this study was provided by Beerbelly Brewing Equipment (Pooraka, South Australia). Once received the rice husk was first oven-dried at 105 °C for a minimum of 15 h. It was then ground in a rotary mill and sieved to 420 – 500 µm. The proximate and ultimate analysis of the rice husk and biochar are shown in Table 2.1.

A schematic diagram of the pyrolysis-combustion process is shown in Fig. 2.1. N_2 carrier gas was supplied at 0.25 L/min through the hopper and 0.1 L/min above the char pot to purge the system. The prepared rice husk was fed into the main screw at a feeding rate of 1.3 g/min and heated to temperatures of 400, 500, 600, 700, and 800 °C by two electrical heaters, pyrolyzing the rice husk in the approximately 1 m long heating section with a residence time of 16 min. The term "T_p" is used in this paper when considering sampling of the biochar and bio-oil. The term "T_v" is used when discussing sampling of the PM generated from combustion of the raw pyrolysis volatiles. A premixed flame was generated through the mixing of HEPA filtered air and the raw pyrolysis volatiles inside a combustion furnace. The burner was situated at the bottom of a quartz tube (1.5 m height × 45 mm I.D.) within a vertical 3-zone tube furnace (Carbolite®, GVC 12/1050). The furnace temperature

was maintained at 850 °C for the combustion (T_c) as this is a typical temperature found in small-scale combustion systems (Miles et al., 1996).

3.2.2. Pyrolysis Product Analysis

A collection vessel at the end of the screw reactor was used to collect the biochar that had passed through the main screw. No accumulation of the pyrolysis products was found inside the screw reactor. The recovered yield of biochar was calculated using the mass ratio of biochar in the collection pot and the mass of feed (on a dry basis). The bio-oil fraction of the raw pyrolysis volatiles was collected by connecting a heated pipe (≈ 350 °C to prevent condensation of bio-oil at the burner outlet) to a condensation train consisting of eight 50 ml test tubes immersed in an ice/water mixture (≈ 0 °C) and connected in series with insulated piping. The difference in weight of the condensation train before and after the experimental run was taken as the mass of bio-oil. The bio-oil samples were stored in 15 ml sealed glass test-tubes in a refrigerator at 3 °C before further analysis. The yields (Fig. 2.2a) and HHV (Fig. 2.2b) of the primary pyrolysis products resulting from pyrolysis of rice husk in the continuous pyrolysis-combustion reactor were discussed in Chapter 2.

3.2.3. Flue Gas and PM Sampling

A CI (Copley Scientific, 8-stage Anderson cascade impactor) made of stainless steel with a size range of 0.1 – 10 µm was used to collect the PM generated from combustion of the raw pyrolysis volatiles. An ADT was used to dilute the flue gas with HEPA filtered ambient air (dilution ratio ≈ 8) in order to provide a fixed volumetric flowrate of 28.3 L/min to the CI. Quartz fibre filter papers were used for all stages except the back-up stage, which used a PTFE filter with a 0.1 µm pore size. The filters were prepared for collection of the PM following an adapted

methodology outlined in the USEPA Method 5 (USEPA, 2000) and the State of California Air Resources Board: Method 501 (CARB, 1990). Continuous flue gas monitoring was carried out by drawing the flue gas into two separate gas analysers. The CO_2 analysis of the flue gas was carried out using a portable non-dispersive infrared sensor (CO2meter.com, CM-0017) with a resolution of 0.5 vol %. A portable CO/O_2 analyser (Bacharach, Fyrite® INSIGHT® Plus) was used to analyse the CO level in the flue gas with a resolution of 20 ppmv and the O_2 level with a resolution of 0.3 %. For each of the combustion experiments, the CO_2 and CO levels of the flue gas at 5 % O_2 were maintained at around 13 % and 400 ppmv, respectively. The dried biochar and PM samples were stored in air-tight containers after collection.

3.2.4. PAH Analysis of the Biochar, Bio-Oil, and PM

PAH analysis of the solid biochar and PM samples from the pyrolysis-combustion process was carried out using a GC – MS (Perkin Elmer Clarus 680 & iQT). PM smaller than 2.1 µm was not analysed as the particulates collected in the CI were embedded in the filter paper, making separation before analysis unfeasible. The collected particulates therefore fall within the $PM_{2.1\text{-}10}$ size range. All samples were examined for the 16 PAHs listed in Table 3.1. 15 of these PAHs are identified in the USEPA 16 priority PAHs list of known concerns to human health (Keith, 2015).

Approximately 1 mg of PM or 10 mg of biochar was weighed into a thermally cleaned 4 mm ID injection liner on a balance accurate to 6 decimal points (A&D, BM-22). 10 ng of anthracene-d10 internal standard dissolved in dichloromethane was added and the liner was inserted into the injection port of the GC – MS. Samples were thermally desorbed from 40 °C to 300 °C in the injection port with helium carrier gas. A 30 m, 0.25 mm ID Perkin Elmer Elite 5 MS capillary column was utilized for

the separation of analytes with a constant flow rate of 2 mL/min at 50 °C held for 1 min and then ramped to 300 °C at 8 °C/min and held for 7 min. Compounds were detected using time-of-flight (TOF) mode over a range of 45 to 400 AMU. Quantification of the PAHs was conducted using eCipher 3 data processing software against a calibration curve generated by adding known quantities of QMX PAH mix diluted in dichloromethane onto the injection liner following the same thermal desorption methodology as the PM and biochar.

Bio-oil was investigated by extracting 1 mL of representative oil in 1 mL of dichloromethane. Analysis was conducted on a GC – MS system (Agilent, 5977 B) by direct injection of 1 µL of extract. Separation was conducted using a 30 m, 0.25 mm ID HP-5 MS capillary column with helium carrier gas at a constant flow rate of 1 mL/min at 50 °C held for 1 min and then ramped to 300 °C at 8 °C/min and held for 7 min. Compounds were detected using scanning mode over a range of 45 to 600 AMU. Semi-quantification was conducted against a calibration curve generated by injecting know quantities of QMX PAH Mix diluted in dichloromethane. Oxy-aromatic components were calculated against the naphthalene reference.

The BaP – TEQ was calculated using the concentrations of individual PAH species and their respective TEF presented in Table 3.1, following the procedure outlined in Jung et al. (2010). Uncertainties for the PAH concentrations of the biochar, bio-oil, and PM were calculated as the standard error of the mean for a triplicate set of runs. The relative errors for the energy-based yield of PAHs were assumed to propagate from the errors of the PM-bound PAH concentration and energy-based yield of $PM_{2.1\text{-}10}$. The energy-based yield of PAHs was calculated by

multiplying the PM-bound PAH concentration ($\mu g_{PAH}/g_{PM}$) by the energy-based yield of PM ($g_{PM}/_{MJ}$) derived from the HHV_{RPV}.

3.3. Results and Discussion

3.3.1. Biochar PAH Concentrations and BaP-TEQ

Table 3.2 shows the concentration of each of the individual biochar-bound PAH species at each T_p. It is apparent that increasing the T_p resulted in an increase in the total biochar PAH concentrations. An increase from 1.0 $\mu g_{PAH}/g_{biochar}$ at 400 °C to 11.3 $\mu g_{PAH}/g_{biochar}$ at 800 °C was observed. The increase in the biochar PAH content has been explained as a complex pyrosynthetic formation route, the rate of which increases at elevated T_p (Buss et al., 2016). The PAH concentration of the rice husk biochar (observed in this study) are comparable to the biochars derived from other biomass sources (Dutta et al., 2016; Hale et al., 2012). Total biochar-bound PAH concentrations (Σ16 USEPA PAHs) ranging from negligible (Singh et al., 2010) to 65 µg/g (Quilliam et al., 2013) have been reported. Slow pyrolysis biochars, however, tend to range between 0.1 and 5 µg/g (Dutta et al., 2016; Hale et al., 2012). Given that there are a wide range of factors (such as temperature, residence time, and feedstock type) that can influence both the rate of PAH formation and devolitization, there are large variations in the reported results. For each of the biochars produced between 400 and 800 °C, the most predominant PAH species is naphthalene, with the concentration generally increasing with temperature. The naphthalene concentration of the 800 °C biochar (3.7 $\mu g_{PAH}/g_{biochar}$) is approximately 9 times higher than that of the 400 °C biochar (0.4 $\mu g_{PAH}/g_{biochar}$). For all the biochar, the total PAH contents are dominated by 2 – 3 ring species. In particular, acenaphthylene, phenanthrene, and anthracene are all abundant in each, which

agrees well with previous studies investigating the PAH content of biochar produced by slow pyrolysis (Dutta et al., 2016; Lyu et al., 2016).

Results also indicated that only the 400 and 500 °C rice husk derived biochar are below the 6 µg/g limit set by the USEPA for the maximum PAH concentration for soil application (NRC, 2002). Furthermore, significantly higher concentrations of BaP and dibenz(a,h)anthracene were found in the 600 and 800 °C biochar, which resulted in a BaP – TEQ of 0.70 and 0.37 $\mu g_{PAH}/g_{biochar}$ respectively. Although the 700 °C biochar has a total PAH concentration similar to that of the 600 °C biochar, the predominant PAH species are those with low molecular weights, such as naphthalene (3.6 $\mu g_{PAH}/g_{biochar}$) and acenaphthylene (1.2 $\mu g_{PAH}/g_{biochar}$). As a result, the 700 °C biochar possesses a BaP – TEQ of only 0.01 $\mu g_{PAH}/g_{biochar}$, which is significantly lower than the 600 °C biochar. The application of biochar to the soil with significant BaP – TEQ values is of obvious concern, as it may facilitate the existence of carcinogenic contaminants that are difficult to treat once buried (Dutta et al., 2016). Using the concentration of biochar-bound PAHs presented in previous studies, the BaP – TEQ values of biochar produced from a wide range of agricultural by-products were calculated. The reported BaP – TEQ's ranged from 0.001 to 0.99 µg/g (Freddo et al., 2012; Dutta et al., 2016), while the BaP – TEQ of rice husk derived biochar was calculated as 0.85 µg/g (Quilliam et al., 2013), which agrees with the results presented in this study.

3.3.2. Bio-Oil PAH Concentrations

Table 3.3 shows the influence of T_p on the bio-oil PAH concentrations. As with the biochar, increasing T_p resulted in increased PAH concentrations in the bio-oil (1 $\mu g_{PAH}/mL_{bio\text{-}oil}$ at 400 °C and 1113 $\mu g_{PAH}/mL_{bio\text{-}oil}$ at 800 °C). Increasing T_p also

resulted in greater concentrations of heavier 5 – 6 ring PAHs in the bio-oil at the expense of the lighter 2 – 3 ring PAHs that dominate at lower temperatures. The same trend has also been observed for bio-oil produced from the pyrolysis of rice husk (Williams and Nugranad, 2000) and other biomass (Hu et al., 2014). For the bio-oils produced at 400 and 500 °C, the most predominant PAH species are low molecular weight PAHs such as naphthalene, acenaphthylene, and acenaphthene. At 700 °C there is a significant increase in the total PAH concentration, which is mainly caused by an increase in the concentration of naphthalene and acenaphthylene. Heavier PAHs such as benzo(b)fluoranthene and BaP are also present at this temperature. It is in the 800 °C bio-oil, however, that the highest concentration of medium and high molecular weight PAHs can be found. Significant increases in the amount of 4 ring PAHs such as fluoranthene and pyrene, as well as all 5 – 6 ring PAHs are observed, leading to the high concentrations of benzo(b)fluoranthene, BaP, and dibenz(a,h)anthracene in the 800 °C bio-oil. The mechanism for the increase in both the total concentrations of PAHs, as well as the increase in average molecular weight, at higher T_p has been proposed to be a Diels-Alder reaction mechanism followed by dehydrogenation (Cunliffe and Williams, 1988; Morf et al., 2002). Increased fragmentation of the lignocellulosic feedstock yields hydrocarbon radicals which may capture hydrogen producing alkanes and/or proceed via free radical reaction to form alpha-olefins (Domínguez et al., 2005). In addition, it has also been suggested that secondary reactions of hydrocarbons at elevated T_p can lead to increased aromatic production (Cyprès, 1987). It appears that the increased devolatization of the rice husk observed at greater T_p results in a steeper increase in the PAH content of the bio-oil at 700 and 800 °C than that in the biochar.

Table 3.4 shows the concentration of the most predominant aromatic compounds present in each of the bio-oils. The most abundant compounds observed in each of the bio-oils are oxygenated aromatics, such as phenols and cresols. Phenol concentration is observed to increase significantly with T_p (384 and 1249 $\mu g/mL_{bio\text{-}oil}$ at 400 and 800 °C respectively). It is also observed that a higher proportion of the total bio-oil aromatic concentration is provided by oxygenated species, rather than PAHs, at lower T_p. For example, bio-oil PAHs account for 0.04 % of total aromaticity by mass at 400 °C, while bio-oil PAHs account for 46 % of total aromaticity by mass at 800 °C. The O content of the aromatics is derived from the highly oxygenated structures present in the cellulose, hemicellulose, and lignin of the rice husks (Williams and Nugranad, 2000).

3.3.3. PM-Bound PAH Emissions

Fig. 3.1a shows the total PM-bound PAH concentrations ($\mu g_{PAH}/g_{PM}$) and the energy-based yield of PM-bound PAHs (μg_{PAH}/MJ) generated from combustion of the raw pyrolysis volatiles at 850 °C. It was observed that the PAH concentration of the PM was 119 % higher when the 800 °C raw pyrolysis volatiles were combusted (882 $\mu g_{PAH}/g_{PM}$), compared to the 400 °C volatiles (403 $\mu g_{PAH}/g_{PM}$). The energy-based yields of PAHs were observed to be the highest when the volatiles produced at 500 and 600 °C were combusted, despite the total PM-bound PAH concentration being higher when 700 and 800 °C temperatures were used. This discrepancy is due to the decrease in the energy-based yield of PM ($g_{PM2.1\text{-}10}$/MJ) resulting from combustion of the raw pyrolysis volatiles produced at elevated T_v (Chapter 2). Fig. 3.1b shows the contribution of 2 – 3 ring, 4 ring, and 5 – 6 ring PAHs to the total PM-bound PAH concentration. It is observed that combustion of the raw pyrolysis volatiles produced

at lower T_V generate PM with higher contributions of smaller (2 – 3 ring) PAHs, while higher temperatures generate PM with higher contributions of heavier (5 – 6 ring) PAHs. No clear trend was observed between the T_V and the contribution of 4 ring PAHs to the total PM-bound PAH concentration. The increase in average molecular weight of the PM-bound PAHs with higher T_V originate from increases in PM−bound benzo(b)fluoranthene, BaP, indeno(1,2,3-cd)pyrene, and benzo(g,h,i)perylene concentrations.

The increasing concentration of heavier 5 – 6 ring PAHs on the PM when higher T_V were used suggested that the parent PAHs in the bio-oil play a fundamental role in determining the PAH content of the PM. A comparison of Table 3.3 and Fig. 3.1b shows that the total PM-bound PAH concentration increased when the total bio-oil PAH concentration was higher for elevated T_V. Combustion of the raw pyrolysis volatiles with greater contributions of 5 – 6 ring PAHs in the bio-oil fraction resulted in PM with higher concentrations of 5 – 6 ring PAHs. The same relationship was observed when the bio-oil contained greater amounts of 2 – 3 ring PAHs. No such relationship was observed for the 4 ring PAH species. The significant increase in 5 – 6 ring PAHs bound to the PM at 700 and 800 °C suggests that some of the 4 ring PAHs may be undergoing ring-addition reactions. The role of the abundant oxy-aromatic species within the bio-oil in this additional multi-ringed PAH formation is unclear, but the presence of 5 – 6 ring PAHs on the PM (that were not present in the bio-oil at low T_p) suggests that one of the possible routes for this additional ring formation is through a HACA mechanism. It is believed that some oxy-aromatics may be undergoing carbonyl group losses in the high temperature combustion region followed by ring polymerization reactions via recognised HACA addition products (Richter and Howard, 2000) to form higher order aromatics. Although combustion

conditions, such as T_c, excess air ratio, and burner design, play a significant role in PAH emissions (Lima et al., 2005), a similar combustion setting was employed in this study so their effects were considered minimal.

Fig. 3.2 presents the BaP – TEQ of the PM ($\mu g_{PAH}/g_{PM}$) and the BaP – TEQ energy-based yield (μg_{PAH}/MJ) resulting from combustion of the raw pyrolysis volatiles. Increased PM toxicity was observed when higher T_v were used, which was due to greater contribution of 5 – 6 ring PAHs to the total PM-bound PAH concentration. Between T_v of 400 – 800 °C the BaP – TEQ of the PM increased from 19.1 to 149.1 $\mu g_{PAH}/g_{PM}$. Despite Fig. 3.1a demonstrating that the energy-based yield of PM-bound PAHs was highest at 500 and 600 °C, it is observed in Fig. 3.2 that the BaP – TEQ energy-based yield was highest at 700 and 800 °C due to greater weighting being placed on higher order PAHs. It is therefore concluded that operation of the pyrolysis-combustion process at lower T_p for the optimization of biochar yields results in lower potential toxicity of the PM. The PM-bound PAH concentrations reported here are comparable to previously reported values for solid and liquid fuel combustion studies, which range from 19 to 6260 µg/g (Mastral et al., 1996; Singh and Prakash, 2007).

3.3.4. PAH Formation and Survival

Fig. 3.3 shows the relationship between the PAH mass ratio (PM/bio-oil) and T_v. The PAH mass ratio was calculated by dividing the mass of PAHs on the PM by the mass of PAHs in the bio-oil at each temperature. Mass ratios > 1 suggest that additional PAHs are being formed in the combustion region; mass ratios ≈ 1 suggest that the majority of PAHs contained in the bio-oil end up on the PM; while mass ratios < 1 suggests that only a small number of bio-oil PAHs ends up on the PM. The

results indicate a significant difference between these ratios when bio-oil PAH concentration is low (< 700 °C), compared to when the bio-oil PAH concentration is high (≥ 700 °C). For combustion of the raw pyrolysis volatiles produced at low temperatures, the PAH mass ratio suggests that additional PAHs were formed during combustion (PAH mass ratio > 1). As a result, the PAH content of the PM appears to originate from both the slight inherent aromaticity of the bio-oil and additionally formed PAHs. Previous studies have observed that, for fuels with low PAH contents, the majority of emitted PAHs are formed in the combustion region (Westerholm et al., 1988). In contrast, T_V of 700 and 800 °C appear to result in only a small fraction of bio-oil PAHs ending up on the PM surface. As the PAH content of the bio-oil is higher at these elevated temperatures, the concentration of PM-bound PAHs is much greater despite a reduction in the number of bio-oil PAHs ending up on the PM surface. This suggests that there is a limit to gas-phase PAH (originating from the bio-oil) adsorption onto the surface of the PM, the mechanism for which has been previously discussed (Lima et al., 2005).

It is therefore suggested that there are two possible fates for the remainder of the bio-oil PAHs present in the raw pyrolysis volatiles: 1) they remain in the gas-phase given the limited availability of surface area on the PM for adsorption/condensation to occur, or 2) they undergo destruction through direct burnout in the combustion region due to the fuel-lean conditions (Lima et al., 2005). This study does not, however, include the mass of gas-phase PAHs found in the flue gas, which can in some cases significantly contribute to the total amount of PAHs present in the combustion products (Westerholm et al., 1988). Further study is needed to determine the ultimate fate of the bio-oil PAHs that are not involved in adsorption/condensation reactions on the surface of the PM. In addition, it is also

recommended that any further study of the PM and biochar toxicity resulting from the utilization of agricultural by-products, such as rice husk, in the pyrolysis-combustion process also examine the dioxin and furan concentration of the products and emissions. These compounds can pose significant health risks upon exposure, meaning that any conclusion regarding the environmental implications of adopting this process for by-product utilization should consider these pollutants.

3.4. Conclusion

The pyrolysis-combustion process provides a pathway for adding value to high ash content agricultural by-products through the co-production of bioenergy and biochar, which is an effective soil enhancer. Using rice husk, it was observed that the BaP – equivalent toxicity of the PM and biochar was greater when the process was operated at T_V. Between 400 and 800 °C, the BaP – TEQ of the PM increased from 19.1 to 149.1 $\mu g_{PAH}/g_{PM}$ respectively. The majority of PM-bound PAHs appeared to originate from the parent bio-oil PAHs and oxy-aromatics due to the fuel-lean conditions; which did not favour significant additional PAH formation.

Chapter 4: Emission Characteristics of a Pyrolysis-Combustion System for the Co-Production of Biochar and Bioenergy from Agricultural By-Products

Lewis Dunnigan[1], Benjamin J. Morton[1], Peter J. Ashman[1], Xiangping Zhang[2], Chi Wai Kwong[1*]

[1] School of Chemical Engineering, The University of Adelaide, Adelaide, SA 5005, Australia

[2] Institute of Process Engineering, Chinese Academy of Sciences, Beijing, China

* Author for correspondence (Telephone: +61 8313 0724; Email: philip.kwong@adelaide.edu.au)

This is the revised and corrected version of the paper which appears in:

Waste Management, 77 (2018), 59-66.

Statement of Authorship

Title of Paper	Emission characteristics of a pyrolysis-combustion system for the co-production of biochar and bioenergy from agricultural wastes.
Publication Status	☑ Published ☐ Accepted for Publication ☐ Submitted for Publication ☐ Unpublished and Unsubmitted work written in manuscript style
Publication Details	Waste Management 77, 59-66. DOI: https://doi.org/10.1016/j.wasman.2018.05.004. At time of final thesis submission: Journal impact factor = 4.723, times cited = 0.

Principal Author

Name of Principal Author (Candidate)	Lewis Dunnigan		
Contribution to the Paper	Construction and development of experimental apparatus. Performance of experiments and interpretation of results. Responsible for the drafting and revision of the paper for publication.		
Overall percentage (%)	70		
Certification:	This paper reports on original research I conducted during the period of my Higher Degree by Research candidature and is not subject to any obligations or contractual agreements with a third party that would constrain its inclusion in this thesis. I am the primary author of this paper.		
Signature		Date	27/02/18

Co-Author Contributions

By signing the Statement of Authorship, each author certifies that:

i. the candidate's stated contribution to the publication is accurate (as detailed above);

ii. permission is granted for the candidate in include the publication in the thesis; and

iii. the sum of all co-author contributions is equal to 100% less the candidate's stated contribution.

Name of Co-Author	Philip Kwong		
Contribution to the Paper	Corresponding author. Provide original idea of the study and financial support through the Catalyst Research Grant from the Government of South Australia. Major contributor to the development of the methodology and critical analysis of experimental results. Significant contribution to the writing and revision of the paper.		
Signature		Date	27/02/18

Name of Co-Author	Benjamin J. Morton		
Contribution to the Paper	Contribution to analysis of the results, discussion of significance, and input for writing of the paper.		
Signature		Date	27/02/18

Name of Co-Author	Peter Ashman		
Contribution to the Paper	Contribution to result analysis and input for the writing of paper.		
Signature		Date	27/02/18

Name of Co-Author	Xiangping Zhang		
Contribution to the Paper	Contribution to result discussion and provided input for the writing of paper.		
Signature		Date	27/02/18

Abstract

The co-production of biochar and bioenergy using pyrolysis-combustion processes can potentially minimize the emission problems associated with conventional methods of agricultural by-product disposal. This approach also provides significant added-value potential through biochar application to soil. Despite these advantages, variations in biomass composition, including sulfur, nitrogen, ash, and VM content, may significantly influence both the biochar quality and the emissions of harmful PM and gaseous pollutants (SO_2, H_2S, NO_2, NO). Using a laboratory-scale continuous pyrolysis-combustion facility, the influence of biomass composition (rice husk and grape pruning) and volatile production (pyrolysis) temperature (400 – 800 °C) on the biochar properties and emissions during combustion of the raw pyrolysis volatiles were evaluated. Utilization of grape pruning resulted in higher energy-based yields of PM_{10} than the rice husk, the majority of which consisted of the $PM_{1.1}$ fraction due to the elevated pyrogas content of the volatiles. The PM emissions were found to be independent of the feedstock ash content due to its retainment in the biochar. Greater volatilization of biomass sulfur and nitrogen during pyrolysis at higher temperatures resulted in higher yields of sulfurous and nitrogenous gaseous pollutants. The energy-based yields of NO and NO_2 were found to increase by 16 % and 50 % for rice husk and 21 % and 189 % for grape pruning respectively between 400 and 800 °C. The same trend was also observed for the emissions of H_2S and SO_2 for both feedstocks.

4.1. Introduction

Agricultural by-products generated within the horticulture industry present numerous challenging and financially burdensome disposal problems for food producers. At present, many of these by-products have little or no value and do not provide an additional revenue stream for producers. Rice husk is one such abundant by-product, of which approximately 822 million tonnes are produced annually worldwide (Naqvi et al., 2014). Grape pruning, a common woody waste from the growing of grape vines, is also an agricultural by-product with few options for recycling. Current utilization rates for both feedstocks are low, with rice husk typically openly burned or buried following detachment of the chaff from the grain after cultivation (Zhang et al., 2015). Grape pruning is typically disposed of by burning or landfilling, or on very few occasions used for composting (Liang et al., 2016). These conventional methods of disposal are not only providing little added-value to the by-product, but they are in many cases also resulting in significant emissions of harmful PM and gaseous pollutants (SO_2, H_2S, NO_2, NO) when openly burned (Hays et al., 2005). This is of significant concern, as PM_{10} and $PM_{2.5}$ emissions are currently one of the primary causes of premature mortality in developing countries (Barron et al., 2017), while the negative health consequences of exposure to harmful gaseous pollutants is well documented (Zhang and Smith, 2007). One potential option for providing both added-value to these agricultural by-products and a method for reducing the harmful emissions associated with disposal is a pyrolysis-combustion process for the co-generation of biochar and bioenergy.

Biochar, the solid carbonaceous product of pyrolysis, can provide value adding potential to the agricultural by-products given its ability to offset C emissions by long-term C sequestration with additional agricultural benefits (Taherymoosavi et

al., 2017). The co-generation of bioenergy through utilization of the heat liberated from combustion of the raw pyrolysis volatiles can also potentially reduce on-site energy costs. Alternative approaches for the generation of bioenergy from agricultural by-products, such as direct combustion and gasification (Xin et al., 2017), have often been hampered by the wide-variability in the fuel qualities possessed by such feedstocks, including fuel ash contents (Gilbe et al., 2008). Pyrolysis-combustion processes have previously been shown to be tolerant of wide-ranging feedstock ash contents, as the majority of the biomass-bound ash is retained in the solid pyrolysis product (biochar) prior to combustion (Claoston et al., 2014; Hung et al., 2017). The diversity of agricultural by-products also implies that attempts to increase utilization rates will result in broad variations in biomass properties, such as S and N content. The volatilization and subsequent oxidation of these species has been shown to strongly influence the emissions of gaseous pollutants (including SO_2, H_2S, NO_2, NO) during direct combustion (Moron and Rybak, 2015; Reddy and Venkataraman, 2002). Variations in the VM content of feedstocks are also of concern, as this affects not only the HHV for energy generation, but may also promote the formation of sub-micron PM (Mitchell et al., 2016). Fine particle emissions are considered a significant health concern as they cannot be cleared readily from the lung once inhaled (Salvi, 2007). Therefore, despite it being well documented that fuel S, N, ash, and VM content strongly influences the yields of both gaseous and PM emissions during direct combustion, there is currently no information available regarding their influence on the emissions from the pyrolysis-combustion process.

In order to examine the influence of biomass composition on the emissions associated with by-product utilization through the pyrolysis-combustion process, two

abundant agricultural by-products with significantly different compositions (grape pruning and rice husk) were used in this study. Grape pruning is considered more representative of the majority of biomass types, with low ash and S contents, as well as a high VM and N content (Liang et al., 2016; Marshall et al., 2017; Nasser et al., 2014). Rice husk is abundant, but less typical of the majority of biomass, as it has high ash and S content, along with low VM and N content (Claoston et al., 2014). Conventionally, the condensable (bio-oil) and non-condensable (pyrogas) fractions are separated from the raw (untreated) pyrolysis volatiles generated from biomass pyrolysis (Alper et al., 2010). However, it has been suggested that separation is not the most suitable approach for the distributed utilization of agricultural by-products as bio-oil contributes significantly to the heating value of the raw pyrolysis volatiles, especially at lower volatile production temperatures (< 500 °C) (Chapter 2). Therefore, co-combustion of the bio-oil and pyrogas (i.e. combustion of raw pyrolysis volatiles) is a viable approach for distributed generation as it avoids the need for separation and energy intensive bio-oil upgrading processes (Mortensen et al., 2011). The composition of the raw pyrolysis volatiles are not only dependent on the feedstock used, but are also influenced by the volatile production temperature. These factors can therefore influence the emissions from the process associated with bioenergy generation. High volatile production temperatures can lead to an increase in volatilization of feedstock S and N (Claoston et al., 2014), as well as variations in the ratio of pyrogas and bio-oil in the raw pyrolysis volatiles (Chapter 2). To date there have been no studies investigating the role of volatile production temperature on the gaseous emissions from a pyrolysis-combustion process utilizing agricultural by-products.

Therefore, the objectives of the study are to determine 1) the yields and HHV of the primary pyrolysis products from the grape pruning and compare them to those from the rice husk, 2) the influence of feedstock ash and VM content on the energy-based yields of PM, and 3) the influence of biomass S and N content, and volatile production temperature, on the energy-based yields of NO, NO_2, H_2S, and SO_2.

4.2. Materials and Methods

4.2.1. Material Characterizations

The grape pruning used in this study was grown in Urrbrae, South Australia, while the rice husk used was supplied by Beerbelly Brewing Equipment (Pooraka, South Australia). Both feedstocks were first ground in a rotary mill and then sieved to 420 – 500 µm. Drying was done in an oven at 105 °C for a minimum of 15 hours, following ASTM D4442. The ultimate analysis of the grape pruning and biochar (produced following the method outlined in Section 4.2.2) was carried out using an Elemental Analyser (PerkinElmer, 2400 Series II CHNS/O) following ASTM D5373, with the O content calculated by difference. The proximate analysis of the samples was carried out using a TGA (METTLER TOLEDO, TGA/DSC 2 STARe System) following ASTM D7582 with modifications. Approximately 65 mg of sample was loaded into the TGA and heated to 800 °C at 30 °C/min under N_2. The sample was then held until a constant weight was achieved, at which point the atmosphere was switched to O_2 to determine the ash content. The HHV of the feedstock and biochar were calculated using the Boie equation (Boie, 1953). The characterization results of the grape pruning were compared to those previously presented for rice husk in Chapter 2.

4.2.2. Lab-Scale Pyrolysis-Combustion Process

A schematic diagram of the experimental pyrolysis-combustion system is shown in Fig. 4.1. The dried and ground biomass samples were first loaded into a hopper and fed into the main screw at a rate of 1.3 g/min. The main screw reactor (length ≈ 1 m with residence time of 16 min) was heated externally with two electrical heaters to 400, 500, 600, 700, or 800 °C. These temperatures are referred to as "T_p" when discussing the properties of the biochar and bio-oil, and "T_v" when discussing the PM and gaseous emissions generated from combustion of the raw pyrolysis volatiles. The solid biochar was collected from a char collection pot at the exit of the main screw reactor. The yield of biochar was calculated using the mass ratio of biochar collected and the mass of feed (on a dry basis). N_2 carrier gas was supplied at two different gas inlets to purge the system. The first of these was located on the top of the hopper (0.25 l/min) and the second was above the char collection pot (0.1 l/min). The raw pyrolysis volatiles generated during the pyrolysis reaction were directed into a burner where they were then mixed with the HEPA filtered combustion air. The raw pyrolysis volatiles produced between 400 and 800 °C were combusted at 850 °C. The heat required for auto-ignition of the volatile/air mixture was provided by a vertical 3-zone tube furnace (Carbolite®, GVC 12/1050). This combustion temperature (T_c = 850 °C) was fixed through the combustion experiments and was chosen as a typical temperature found in small-scale combustion systems (Obernberger, 1998). The flue gas generated from the combustion reaction was contained within a quartz tube (1.5 m height x 45 mm I.D.) where it was diverted into an ADT situated above the combustion furnace and mixed with HEPA filtered air.

4.2.3. Pyrogas and Bio-Oil Sampling

The pyrogas (non-condensable) fraction of the raw pyrolysis volatiles was sampled by attaching a Teflon gas sampling bag to the burner outlet via a sampling pipe. Once the bag was full, the pyrogas was then passed through a coalescing filter before analysing in a GC - TCD (Agilent, 490 Micro GC). The first channel of the GC separated H_2, N_2, CH_4, and CO with a Molecular Sieve 5A column. The second channel separated CO_2 with a Poraplot U column. The HHV of the pyrogas was calculated as a mass-weighted average based on the concentration of the individual species. The bio-oil (condensable) portion of the raw pyrolysis volatiles was collected using a condensation train consisting of eight 50 ml test tubes immersed in an ice/water mixture (≈ 0 °C) that were connected in series via insulated piping. The connection between the burner outlet and the condensation train was heated (≈ 350 °C) using rope heaters to avoid bio-oil condensation. The mass of bio-oil was taken as the difference in weight of the condensation train before and after the experimental run. There was negligible accumulation of char/bio-oil on any of the interior surfaces of the pyrolysis reactor or feeding systems. The composition, yields and HHV energy balance calculation for the primary pyrolysis products resulting from rice husk pyrolysis in the continuous pyrolysis-combustion process have been previously presented in Chapter 2.

4.2.4. Particulate and Gaseous Pollutant Sampling

Sampling of the flue gas was achieved by extracting a portion from a gas sampling port situated at the entrance of the ADT into two separate flue gas analysers. The CO_2 content of the flue gas was measured using a portable NDIR sensor (CO2meter.com, CM-0017) with a resolution of 0.5 vol %. A portable CO/O_2 analyser (Bacharach, Fyrite® INSIGHT® Plus) was used to measure the CO

concentration in the flue gas with a resolution of 20 ppmv and O_2 level with a resolution of 0.3 %. The flue gas composition was maintained at an O_2 concentration of around 3.5 % during PM and gaseous pollutant sampling.

The concentrations of gaseous pollutants, including H_2S, SO_2, NO, and NO_2 were measured using a portable multi-component gas analyser with electrochemical sensors (RAE Systems, MultiRAE). The resolution for the detections are 0.1 ppm for H_2S, SO_2, and NO_2, and 0.5 ppm for NO with a higher detection limit of 100 ppm for H_2S, 20 ppm for SO_2, 250 ppm for NO and 20 ppm for NO_2. The analyser was connected to another gas sampling port located at the outlet of the ADT. A dilution ratio of 3 was used for analysis of the gaseous pollutants in order to ensure it did not exceed the higher detection limits of the instrument. The dilution ratio was determined using the CO_2 concentrations at the inlet and outlet of the ADT. The percentage of feedstock S/N volatilization was calculated using a mass balance and expressed as the ratio of S/N in the raw pyrolysis volatiles over the S/N that remained in the biochar. At 100 % volatilization, all the S/N from the feedstock was present in the raw pyrolysis volatiles with no retention in the biochar. The standard errors in the energy-based yield of gaseous pollutants were calculated from the mean result of three separate 18 minute experiments.

The gaseous and PM sampling experiments were conducted separately. A CI (Copley Scientific, 8-stage Anderson cascade impactor) made with stainless steel was used for PM sampling and connected to the outlet of the ADT operating at a dilution ratio of 8. This dilution ratio was chosen to ensure a fixed volumetric flowrate of 28.3 l/min of diluted flue gas was supplied to the CI. Quartz fibre filters were used from stage 1 to 8 while a PTFE filter (0.1 µm pore size) was used in the back-up stage. The sampling stages in the CI provided a PM collection size range of 0.1 - 10

μm. Each filter was dried and weighed before and after PM sampling following an adapted methodology outlined in the USEPA Method 5 (USEPA, 2000) and the State of California Air Resources Board: Method 501 (CARB, 1990). The energy-based yields of PM_{10}, $PM_{2.1}$, and $PM_{1.1}$ generated from combustion of the raw pyrolysis volatiles produced were calculated by dividing the mass-based yield of PM by the HHV of the raw pyrolysis volatiles. The standard errors in the energy-based yield of PM were calculated from the mean result of three separate 18 minute experiments. The results for the grape pruning were compared to those for the rice husk presented in Chapter 2 which were determined using the same sampling procedure.

4.3. Results and Discussion

4.3.1. Feedstock and Biochar Characteristics

Table 4.1 shows the proximate and ultimate analysis of the rice husk, grape pruning, and biochar produced at T_p between 400 and 800 °C. It is clear that there are significant compositional differences between the two feedstocks. Firstly, the ash content of the rice husk (22 %) is much greater than that of the grape pruning (7 %). The ash content of the rice husk is greater than most other types of biomass, which typically varies between 0.3 – 8 % (Alper et al., 2010). As the main constituent of rice husk ash is silica (Ng et al., 2015), which is very abrasive and can react with alkalis contained within the ash to form alkali silicates that melt or soften at low temperatures, this may promote the formation of slag and clinker in small-scale combustion devices (Gilbe et al., 2008; Jenkins et al., 1998). Both the VM and the C content of the rice husk are significantly lower than the grape pruning due to the high ash content. The C content of the grape pruning (49 %) is representative of the

majority of biomass types; while the rice husk (38 %) is at the lower end (Claoston et al., 2014).

It was observed that the properties of biochar are strongly influenced by their respective raw feedstock compositions. The effect of T_p on the C content of the biochar was more pronounced for the grape pruning than the rice husk. The C content of the biochar derived from the grape pruning increased from 69 % at 400 °C to 81 % at 800 °C due to the higher level of carbonization at elevated temperatures. In contrast, the C content in rice husk biochar decreased slightly over the same T_p range due to the increased ash content of the biochar (Claoston et al., 2014; Jindo et al., 2014). Grape pruning possesses a relatively low S content (0.3 %) and high N content (1 %). In contrast, rice husk possesses higher S content (0.5 %) and low N content (0.3 %). Agricultural by-products typically possess N contents ranging between 0.1 – 0.7 % and S contents between 0.01 – 0.3 % (Vassilev et al., 2010). For both feedstocks, increasing T_p resulted in greater volatilization of their H and S contents. This resulted in a decrease in the concentration of these species in the biochar between 400 and 800 °C. For the rice husk biochar, the concentration of H decreased from 2.2 to 1.2 % and S decreased from 0.4 to 0 % between 400 and 800 °C. For the grape pruning biochar, the concentration of H decreased from 4.6 to 1.2 % and S decreased from 0.2 to 0.03 % between 400 and 800 °C.

4.3.2. Influence of Pyrolysis Temperature on the Distribution of the Pyrolysis Products

Fig. 4.2 shows the yields of each pyrolysis product (biochar, bio-oil, and pyrogas) collected between 400 and 800 °C. It is observed that, for both the rice husk and grape pruning, increasing T_p resulted in decreased yields of bio-oil and

biochar, along with increased yields of pyrogas. The maximum yields of bio-oil are obtained at reduced temperatures (≤ 500 °C) due to the promotion of further thermal cracking of the condensable hydrocarbons at elevated temperatures. This also resulted in increased yields of pyrogas at higher T_p (Tsai et al., 2007). Fig. 4.2 also suggested that the yield of pyrogas resulting from pyrolysis of the grape pruning is significantly greater than that from the rice husk. Between 400 and 800 °C, the yield of pyrogas increased from 39 to 64 % for the grape pruning, and 19 to 46 % for the rice husk. This is due to the greater VM content of the pruning, originating from its enhanced lignin content (Nasser et al., 2014) which promotes pyrogas formation with temperatures greater than 600 °C at the expense of biochar (Yang et al., 2007), along with its reduced ash content. The HHV of the raw pyrolysis volatiles (bio-oil and pyrogas mixture) of grape pruning (17.4 – 18.9 MJ/kg) was also found to be higher than that from rice husk (14.2 – 15.1 MJ/kg).

Table 4.2 shows the composition (normalized to 50 % N_2 for comparison) of the pyrogas fraction of the raw pyrolysis volatiles produced between 400 and 800 °C. The pyrogas constituents at each temperature were observed to be primarily CH_4, H_2, CO_2, and CO. It was found that the concentrations of CO and H_2 increased significantly with temperature while CO_2 exhibited the opposite trend. CH_4 concentrations were observed to increase with temperature for both feedstocks, although this trend was more significant in the case of grape pruning. This is likely due to secondary reactions of volatiles at elevated temperatures which promote CO, H_2, and CH_4 formation at a greater rate with the release of CO_2 from carboxyls at relatively low temperatures (Xu et al., 2009). The differences in pyrogas composition between the two feedstocks primarily originated from the greater lignin content of the grape pruning. It is well established that decomposition of lignin at elevated

temperatures yields primarily H_2 and CH_4 (Yang et al., 2007), with the increase in the concentration of these two species particularly evident at the highest T_v of 700 and 800 °C. As a result of the increased CH_4 and H_2 content, the HHV of the pyrogas produced from grape pruning is significantly greater at these elevated temperatures. Between 400 and 800 °C, the HHV of the pyrogas and carrier gas mixture increased from 2.3 MJ/kg at 400 °C to 5.4 MJ/kg at 800 °C and 1.8 MJ/kg to 6.8 MJ/kg for the rice husk and grape pruning respectively.

4.3.3. Influence of Feedstock Ash and VM on the Energy-Based Yields of PM

Fig. 4.3 shows the energy-based yields of PM_{10}, $PM_{2.1}$, and $PM_{1.1}$ resulting from combustion of the raw pyrolysis volatiles generated from the pyrolysis of grape pruning and rice husk. It is observed that the PM emissions from the pyrolysis-combustion of grape pruning are higher than that of rice husk. Between T_v of 400 and 700 °C, the increase in the energy-based yield of PM_{10} for the grape pruning over the rice husk was found to range from 6 to 24 %, while at 800 °C the yield was found to be greater for the rice husk. The increase in the energy-based yields of $PM_{2.1}$ and $PM_{1.1}$ for the grape pruning over the rice husk between 400 and 800 °C were found to be 4 – 75 % and 12 – 75 % respectively. These results suggested that the increase in the PM emissions from the pyrolysis-combustion process for the grape pruning were a result of variations in the raw pyrolysis volatiles composition, which is mainly influenced by T_v (Fig. 4.2, Table 4.2) and feedstock VM content (Table 4.1). Previous studies have shown that increased fuel-VM content is linked to increasing yields of $PM_{2.5}$ for direct combustion (Li et al., 2016; Mitchell et al., 2016). For pyrolysis-combustion, the raw pyrolysis volatiles produced from the grape pruning had greater fractions of pyrogas than the rice husk (Fig. 4.2) due to the higher VM content of the feedstock. This resulted in an increased contribution of

$PM_{1.1}$ to the energy-based yield of PM_{10}. For the grape pruning, 16 – 60 % of the PM_{10} yield is contributed by the $PM_{1.1}$ fraction, while for rice husk only 11 – 23 % of the PM_{10} yield is contributed by the $PM_{1.1}$ fraction. The increase in the energy-based yield of $PM_{1.1}$ was the primary reason for the greater PM_{10} emissions for the grape pruning.

Fig. 4.3 also suggested that the contribution of the super-micron PM size fraction to the energy-based yield of PM was greater for the rice husk for every T_v except 400 °C. The $PM_{10}/PM_{1.1}$ ratio for the rice husk ranged from 4.4 to 9.3 between 400 and 800 °C. In contrast, over the same temperature range this ratio for the grape pruning ranged from 2.5 to 4.2. The predominance of sub-micron PM generated from the grape pruning, and the contrasting super-micron PM generated from the rice husk, indicate different formation pathways. It is well established that the mechanism for PM formation resulting from the organic constituents of pyrogas contributes primarily to the sub-micron particulate fraction (Li et al., 2016; Linak et al., 2000b). PM formation from these non-condensable species is believed to primarily occur through initial PAH inception by cyclization reactions via radical intermediates (Richter and Howard, 2000). These PAHs are then expected to undergo further polymerization reactions through a HACA mechanism, ultimately leading to sub-micron soot formation (Richter and Howard, 2000). In contrast, super-micron particulates are generally formed through incomplete burnout of bio-oil and entrained char particles, resulting in low-density char cenospheres (Linak et al., 2000b). It was also observed that the PM emissions for pyrolysis-combustion were independent of the feedstock ash content. This is because the majority of the feedstock ash is retained in the biochar. A mass balance around the pyrolysis reactor showed that 95 - 99 % of rice husk ash and 97 – 100 % of grape pruning ash was retained in the

biochar. Further details for the relationship between T_v and the energy-based yield of PM are discussed in Chapter 2.

4.3.4. Influence of Biomass-Bound Sulfur Volatilization on H_2S and SO_2 Energy-Based Yields

Figs. 4.4a and b show the energy-based yields of SO_2 and H_2S respectively for the pyrolysis-combustion of rice husk and grape pruning with differing amounts of feedstock S volatilization. Greater volatilization of biomass-bound S was observed at higher T_v for both feedstocks. In the case of rice husk, the fraction of feedstock S volatilized increased from 65 % to 100 % between T_v of 400 °C and 800 °C. This corresponded to a flowrate of S in the volatiles of 0.004 g/min at 400 °C and 0.0062 g/min at 800 °C, based on a mass balance calculation. Figs. 4.4a and b demonstrated that combustion of the raw pyrolysis volatiles produced at elevated T_v with enhanced S contents led to increased energy-based yields of SO_2 and H_2S. The SO_2 yield was found to increase from 6 to 57 mg/MJ during combustion of the pyrolysis volatiles produced at 400 °C and 800 °C, respectively for rice husk (Fig. 4.4a). In the case of grape pruning, the SO_2 yield was found to increase from 5 to 17 mg/MJ during combustion of the pyrolysis volatiles produced at 400 °C and 800 °C, respectively. The H_2S yield was observed to increase from 1 to 11 mg/MJ for the rice husk between 400 and 800 °C (Fig. 4.4b). Over the same temperature range the H_2S yield was observed to increase substantially from 0.4 to 4 mg/MJ for the grape pruning. The S emissions were higher for the rice husk when compared to the grape pruning due to the increased feedstock S content (Table 4.1). This relationship between fuel S content and the emissions of sulfurous pollutants has previously been investigated (Kwong et al., 2007; Moron and Rybak, 2015; Reddy and Venkataraman, 2002). It is believed that the volatilization of biomass-bound S during

the pyrolysis process primarily results in the formation of H_2S in the pyrolysis gas (Shirai et al., 2013). The oxidation of this species in the combustion region contributes to the formation of SO_2 (Kramlich et al., 1981).

The yields of sulfurous pollutants observed for the rice husk and grape pruning in this study are at the lower-end of previously reported emission factors for the direct combustion of biomass fuels with similar S contents (Fournel et al., 2015; Jenkins, 1991; Moron and Rybak, 2015). Results suggested that the operation of the pyrolysis-combustion process at lower T_v for the purpose of biochar generation is a viable means to control the emissions of harmful sulfurous pollutants associated with agricultural by-product disposal.

4.3.5. Influence of Biomass-Bound Nitrogen Volatilization on NO_x Energy-Based Yields

Figs. 4.5a and b show the energy-based yields of NO and NO_2 respectively for the pyrolysis-combustion of rice husk and grape pruning with differing amounts of feedstock N volatilization. For both feedstocks, it can be seen that increasing volatilization of biomass-bound N occurred at elevated T_v. In the case of grape pruning, the amount of feedstock N volatilized increased from 45 % to 68 % between T_v of 400 °C and 800 °C. This corresponded to a flowrate of N in the volatiles of 0.0049 g/min at 400 °C and 0.0073 g/min at 800 °C, based on a mass balance calculation. The resulting increase in the N content of the raw pyrolysis volatiles resulted in greater energy-based yields of NO and NO_2. For the rice husk, the NO yield increased from 100 to 117 mg/MJ between T_v of 400 and 800 °C (Fig. 4.5a). For the grape pruning, the NO yield increased from 155 to 188 mg/MJ over the same temperature range. The NO_2 yield increased from 4 to 7 mg/MJ for the rice husk and 10 to 29 mg/MJ for the grape pruning between T_v of 400 and 800 °C (Fig. 4.5b).

Similar observations have previously been made regarding the influence of fuel-bound N content on NO_x emissions from biomass direct combustion (Mitchell et al., 2016). The formation of NO_x from combustion of the volatiles is expected to originate from oxidation reactions of N containing species such as ammonia and hydrogen cyanide liberated from the feedstocks during pyrolysis (Darvell et al., 2014). Given the low-temperature T_c used in this study (850 °C); it is believed that thermal NO_x did not contribute significantly to the NO_x emissions.

The energy-based yields of NO_x observed in this study are at the higher-end of those previously reported for the direct combustion of biomass with similar N contents (Bhattacharya et al., 2002; Kwong et al., 2007; Mitchell et al., 2016). It has previously been reported that combustion of bio-oil results in greater NO_x emissions than the combustion of conventional fuels such as diesel (Martin and Boateng, 2014). This was due to increased contribution of both prompt NO_x and fuel-bound N. With these two formation routes, fuel NO_x has been reported to be the dominant formation mechanism during bio-oil combustion (Tzanetakis et al., 2010). The elevated NO_x yields observed in this study at higher T_v may be attributed to the well-mixed flame that minimized fuel rich regions in the combustion zone (Munir et al., 2011). In addition, the abundance of O containing species in the raw pyrolysis volatiles (such as oxy-aromatic compounds), which originate from the highly oxygenated structures present in the cellulose, hemicellulose, and lignin, may facilitate the availability of oxidizing species (Singh et al., 2016). Despite the significant NO_x emissions reported both in this study and in the previously mentioned studies, the yields of NO_x during bio-oil combustion can be controlled by using a conventional staged combustion strategy typically employed for other fuels containing N (Tzanetakis et al., 2010). Further study, however, is needed to examine

the predominant formation routes for NO_x in pyrolysis-combustion processes, as the T_v may influence the availability of different NO_x precursors in the raw pyrolysis volatiles.

4.4. Conclusion

This study demonstrated that feedstock composition and T_v influenced the PM and gaseous emissions from the pyrolysis-combustion of agricultural by-products. Grape pruning had high VM (65 %) and low ash (7 %) content when compared to the rice husk. The pyrolysis-combustion of grape pruning resulted in higher PM_{10} energy-based yields than the rice husk between T_v of 400 and 700 °C. The greater pyrogas content of the grape pruning volatiles resulted in enhanced contributions of the $PM_{1.1}$ fraction to the PM_{10} yield. The energy-based yields of PM from the combustion of the raw pyrolysis volatiles were found to be independent of the feedstock ash content. Gaseous emission results suggested that the increased biomass-bound S content from rice husk resulted in greater energy-based yields of H_2S and SO_2. The higher N content of the grape pruning also resulted in greater energy-based yields of NO and NO_2. The feedstock S and N volatilization increased with T_v and therefore the combustion of high temperature volatiles resulted in elevated emissions of S and N containing gases. Gaseous emissions were minimised when the pyrolysis-combustion system was optimized for biochar production at low T_v.

Chapter 5: Production of Biochar and Bioenergy from Rice Husk: Influence of Feedstock Drying on Particulate Matter and the associated Polycyclic Aromatic Hydrocarbon Emissions.

Lewis Dunnigan[1], Benjamin J. Morton[1], Philip Anthony Hall[2], Chi Wai Kwong[1*]

[1] School of Chemical Engineering, The University of Adelaide, Adelaide, SA 5005, Australia

[2] School of Physical Sciences, The University of Adelaide, Adelaide, SA 5005, Australia

* Author for correspondence (Telephone: +61 8313 0724; Email: philip.kwong@adelaide.edu.au)

This is the revised and corrected version of the paper which appears in:

Atmospheric Environment, 190 (2018), 218-225.

Statement of Authorship

Title of Paper	Production of biochar and bioenergy from rice husk: Influence of feedstock drying on particulate matter and the associatec polycyclic aromatic hydrocarbon emissions.
Publication Status	☑ Published ☐ Accepted for Publication ☐ Submitted for Publication ☐ Unpublished and Unsubmitted work written in manuscript style
Publication Details	Atmospheric Environment 190, 218-225. DOI: https://doi.org/10.1016/j.atmosenv.2018.07.028. At time of final thesis submission: Journal impact factor = 3.708, times cited = 0.

Principal Author

Name of Principal Author (Candidate)	Lewis Dunnigan		
Contribution to the Paper	Construction and development of experimental apparatus. Performance of experiments and interpretation of results. Responsible for the drafting and revision of the paper for publication.		
Overall percentage (%)	70		
Certification:	This paper reports on original research I conducted during the period of my Higher Degree by Research candidature and is not subject to any obligations or contractual agreements with a third party that would constrain its inclusion in this thesis. I am the primary author of this paper.		
Signature		Date	27/02/18

Co-Author Contributions

By signing the Statement of Authorship, each author certifies that:

i. the candidate's stated contribution to the publication is accurate (as detailed above);

ii. permission is granted for the candidate in include the publication in the thesis; and

iii. the sum of all co-author contributions is equal to 100% less the candidate's stated contribution.

Name of Co-Author	Philip Kwong		
Contribution to the Paper	Corresponding author. Provide original idea of the study and financial support through the Catalyst Research Grant from the Government of South Australia. Major contributor to the development of the methodology and critical analysis of experimental results. Significant contribution to the writing and revision of the paper.		
Signature		Date	27/02/18

Name of Co-Author	Benjamin J. Morton
Contribution to the Paper	Contribution to analysis of the results, discussion of significance, and input for writing of the paper.

Signature		Date	27/02/18

Name of Co-Author	Philip Anthony Hall		
Contribution to the Paper	Performed the GC-MS work for the PAH analysis sections of the paper. Provided quantification work for the PAH experiments.		
Signature		Date	27/02/18

Abstract

This study investigates the effect of feedstock drying on the emissions of PAHs associated with the PM produced during the co-generation of biochar and bioenergy. Raw pyrolysis volatile mixtures were generated from the pyrolysis of rice husk at 400, 500, 600, 700, and 800 °C using a laboratory-scale continuous pyrolysis-combustion system and combusted at 850 °C. PM samples from the combustion were collected and analysed for 15 priority PAH species with a GC/MS. It was found that the utilization of the AR rice husk resulted in significantly greater energy-based yields of PM_{10} (1.2 times at 400 °C and 1.6 times at 800 °C) than the dried rice husk. The majority of the increase was of the $PM_{2.1\text{-}10}$ size fraction. The PM-bound PAH concentration was found to be 2.1 and 2.8 times higher for the AR rice husk at 400 and 800 °C, respectively. This resulted in a significant increase in the energy-based yield of PAHs over the entire volatile production temperature range for the AR rice husk. Nevertheless, the majority of the PM-bound PAH species generated from the AR rice husk consisted of 2 and 3 ring PAHs (naphthalene, acenapthylene, and acenaphthene) with relatively low toxicity. The concentration of 4, 5, and 6 ring PAHs was generally lower than that generated from the dried rice husk. This resulted in the BaP-equivalent toxicity of the PM generated from the AR rice husk being lower than the dried counterpart.

5.1. Introduction

The co-production of biochar and bioenergy from agricultural by-products offers a potential approach for developing sustainable land-management practices with additional economic benefits (Roberts et al., 2010). The uptake of these feedstocks, however, often requires on-site utilization due to issues relating to the low-bulk density and decomposition during storage of wet biomass. The reduced throughputs of distributed systems suggests that it is often necessary to minimise the energy intensive drying processes in order to be economically viable. As such, this will result in the need to utilize feedstocks with AR moisture contents (Olave et al., 2017). One potential approach for the distributed co-production of biochar and bioenergy from agricultural by-products is through a combined pyrolysis and combustion process (pyrolysis-combustion) (Roberts et al., 2010).

Pyrolysis-combustion involves combustion of the raw pyrolysis volatiles produced during the initial low temperature pyrolysis step of the process. The co-product of the pyrolysis reaction (biochar) is separated prior to combustion. These volatiles are a mixture of condensable (bio-oil) and non-condensable (pyrogas) fractions. The range of pyrolysis temperatures that typically favour biochar production (< 500 °C) also favour bio-oil formation over pyrogas. Recent study has suggested that it is beneficial to co-combust the two fractions for energy generation purposes (Williams and Nugranad, 2000). The pyrolysis-combustion processes are especially advantageous for feedstocks with variable moisture contents, as the feedstock is dried in the pyrolysis process which volatilizes the fuel-bound moisture into vapor form prior to fuel combustion (Demirbas, 2004a). Therefore, the moisture

variations in the AR feedstocks are less likely to induce the ignition and flame stability issues associated with direct combustion (McKendry, 2002).

Nevertheless, the utilization of agricultural by-products without prior drying may, however, present additional challenges for the pyrolysis-combustion system. The presence of moisture in the biomass results in decreased feedstock HHV and higher energy requirements for drying (Demirbas, 2007). The yield and composition of the bio-oil fraction of the volatiles has also previously been shown to be influenced by feedstock moisture (He et al., 2009; Wang et al., 2008). Bio-oil produced from AR biomass feedstocks is generally characterised by elevated water content and decreased HHV. The physical properties of the bio-oil are also affected by the presence of moisture, with increased density and decreased viscosity reported with elevated feedstock moisture content (He et al., 2009; Wang et al., 2008). The chemical composition of the bio-oil is also strongly influenced by the moisture content of the feedstock. Bio-oil with higher average molecular weights was found from feedstocks with reduced moisture contents (Demirbas, 2004b; He et al., 2009). In addition, elevated concentrations of acidic species (low pH) in the bio-oil produced from biomass with lower moisture contents have also been demonstrated (He et al., 2009). As a result, the physiochemical changes of the bio-oil resulting from the presence of moisture in the feedstock can strongly influence its fuel properties. This includes variations in both the required residence time for combustion and ignition delay (Shihadeh and Hochgreb, 2002). As such, it is plausible that the performance and the emission characteristics from the combustion of the raw pyrolysis volatiles produced from the AR feedstock may differ from the dried feedstock. Increased fuel moisture has previously been demonstrated to result in elevated yields of PM during direct combustion (Sanchis et al., 2014; Shen et al., 2013). It has also been

demonstrated that the PAH content associated with the emitted PM is greater without pre-drying of biomass fuels during direct combustion (Shen et al., 2013). Both these hazardous pollutant species are generally formed through incomplete combustion of the fuel (Nielsen et al., 2017; Zhang et al., 2018), the formation rate of which can be increased by the presence of moisture (Shen et al., 2013). In addition, elevated PM toxicity generated from the open burning of rice paddy wastes has been observed without prior drying of the biomass (Sanchis et al., 2014).

Despite the potential for pyrolysis-combustion processes to contribute to the global production of biochar and bioenergy, the emission characteristics of hazardous pollutants resulting from utilization of agricultural by-products with and without drying has not yet been established. This is of significant concern, as the potential for increased PM and PM-bound PAH emissions must be examined to allow for effective and sustainable land and waste management practices to be developed. There is currently no available information relating to the potential change in PM toxicity without prior drying. Assessment of PAH-related toxicity of the PM can be estimated through the application of a BaP - TEF to PAH concentrations (Jung et al., 2010). In order to investigate the influence of feedstock drying on the characteristics of the PM emissions, rice husk was chosen as a representative agricultural by-product. Rice husk is a widely available by-product that has traditionally presented challenges when attempting to increase utilization rates due to its poor fuel qualities and wide-spread availability (Fernandes et al., 2016).

The objectives of this study are therefore to determine the influence of rice husk drying on 1) the yields of primary pyrolysis products and raw pyrolysis volatiles HHV, 2) the energy-based yields of PM resulting from combustion of the raw

pyrolysis volatiles, and 3) the energy-based yields of PM-bound PAHs and their associated toxicity.

5.2. Materials and Methods

5.2.1. Feedstock Proximate and Ultimate Analysis

The agricultural by-product used in this study was rice husk, which was provided by Beerbelly Brewing Equipment (Pooraka, South Australia). In order to examine the influence of rice husk drying both the AR and dried rice husk was used in the study. Drying was achieved following the oven-drying method (D4442), which was carried out at 105 °C for a minimum of 15 hours. Both the AR and dried rice husk were then ground in a rotary mill and sieved to 420 – 500 µm. The proximate and ultimate analysis of the rice husk used in this study was previously presented in Chapter 2. The moisture content of the AR rice husk was found to be 9.2 %.

5.2.2. Lab-Scale Pyrolysis-Combustion Process

A schematic diagram of the pyrolysis-combustion process is shown in Fig. 2.1. Briefly, N_2 carrier gas was first supplied at 0.25 l/min through the hopper. The rice husk was fed at 1.3 g/min from the hopper into the main screw reactor where the T_p was maintained at 400, 500, 600, 700, or 800 °C by two cylindrical electrical heaters. The residence time for the pyrolysis reaction was approximately 16 min. After pyrolysis the solid biochar was collected in a char pot by gravity at the end of the main screw reactor. The recovered yield of biochar was calculated using the mass ratio of biochar collected and the mass of feed. N_2 was also supplied above the char pot (0.1 l/min) in order to prevent stagnation of the combustible volatiles. The raw pyrolysis volatiles were then directed into a burner situated inside an enclosed quartz tube (1.5 m height x 45 mm I.D.) within a vertical 3-zone tube

furnace (Carbolite®, GVC 12/1050). Auto-ignition of the volatile/air mixture was achieved by maintaining the furnace at 850 °C and supplying HEPA filtered air into the mixing chamber of the burner. The T_c of 850 °C was used as it represents the typical combustion temperature found in small-scale combustion systems (Miles et al., 1996; Obernberger, 1998).

5.2.3. Sampling of the Raw Pyrolysis Volatiles

The pyrogas fraction of the raw pyrolysis volatiles was collected by attaching a Teflon sampling bag directly to the burner outlet. Once full, the gaseous sample was drawn through a GC - TCD (Agilent, 490 Micro GC). The first channel of the GC was used to detect H_2, N_2, CH_4, and CO with a Molecular Sieve 5A column and the second channel to detect CO_2 with a Poraplot U column. The HHV of the pyrogas was calculated as a mass-weighted average. The mass of pyrogas produced was calculated by subtracting the combined mass of bio-oil and biochar from the mass of rice husk fed. It should be noted that there was negligible accumulation of any material along the length of the main pyrolysis screw reactor.

The bio-oil fraction of the raw pyrolysis volatiles was collected in a condensation train consisting of eight 50 ml test tubes connected by insulated piping and immersed in an ice/water mixture (≈ 0 °C). The condensation apparatus was connected to the burner outlet through a heated pipe (≈ 350 °C) to prevent condensation prior to the sampling tubes. After sampling was complete the collected bio-oil was weighed in order to determine the yield. The HHV of the raw pyrolysis volatiles was calculated using an energy balance around the pyrolysis reactor with the yields of each of the products and the HHV values of the biochar and pyrogas. The yields and HHV of the primary pyrolysis products from the dried rice husk have previously been reported in Chapter 2.

5.2.4. Sampling of the PM

The PM generated from combustion at 850 °C of the raw pyrolysis volatiles produced between 400 and 800 °C was collected after diluting the flue gas in an ADT with HEPA filtered air (dilution ratio ≈ 8). This dilution ratio allowed the specific volumetric flowrate of 28.3 l/min to be maintained and supplied to the stainless steel CI (Copley Scientific, 8-stage Anderson cascade impactor) for the collection of the particles with size fractions of 9 – 10 µm, 5.8 – 9 µm, 4.7 – 5.8 µm, 3.3 – 4.7 µm, 2.1 – 3.3 µm, 1.1 – 2.1 µm, 0.65 – 1.1 µm, 0.43 – 0.65 µm, 0.1 – 0.43 µm. The back-up stage of the CI used a PTFE filter with a 0.1 µm pore size, while all other stages used quartz fiber filter papers. The mass-based yields of $PM_{0.1\text{-}10}$, $PM_{0.1\text{-}2.1}$, and $PM_{0.1\text{-}1.1}$ were obtained by summing the yields of PM collected in all the stages smaller than 10 µm, 2.1 µm, and 1.1 µm respectively. Ultrafine particles were considered to represent a negligible portion of the mass of $PM_{1.1}$ collected in the CI. The back-up stage of the CI used a PTFE filter with a 0.1 µm pore size, while all other stages used quartz fiber filter papers. The mass-based yields of $PM_{0.1\text{-}10}$, $PM_{0.1\text{-}2.1}$, and $PM_{0.1\text{-}1.1}$ were obtained by summing the yields of PM collected in all the stages smaller than 10 µm, 2.1 µm, and 1.1 µm respectively. All filters were prepared following an adapted methodology outlined in the USEPA Method 5 (USEPA, 2000) and the State of California Air Resources Board: Method 501 (CARB, 1990). Constant excess combustion air was maintained by continuous flue gas monitoring. The CO_2 analysis of the flue gas was carried out using a portable non-dispersive infrared analyser (CO2meter.com, CM-0017) with a resolution of 0.5 vol %. A portable CO/O_2 analyser (Bacharach, Fyrite® INSIGHT® Plus) was used to analyse the CO level in the flue gas with a resolution of 20 ppmv and O_2 level with a resolution of 0.3 %. For each of the combustion experiments, the O_2 and CO_2 levels

were maintained at 3.5 % and 13 %, respectively. The energy-based yield of PM was calculated by dividing the mass-based yield ($mg_{PM}/g_{volatiles}$) by the HHV of the volatiles ($MJ/g_{volatiles}$). The error for the energy-based yield was calculated as the standard error of the mean for a triplicate set of runs. For each experiment the PM sampling time was 18 minutes.

5.2.5. PAH Analysis of the PM

PAH analysis of the PM collected in the CI was achieved using a GC-MS (Perkin Elmer Clarus 680 & iQT). PM smaller than 2.1 µm was not analysed as it was embedded in the filter paper and could not therefore be removed. The PM-bound PAHs analysed therefore fall within the $PM_{2.1-10}$ size range. The 16 PAHs examined in this study have been described in detail in Chapter 3. 15 of these PAHs are identified in the list of USEPA 16 priority PAHs list of known concerns to human health (Nisbet and LaGoy, 1992).

Approximately 1 mg of PM was weighed on a balance accurate to 6 decimal points (A&D, BM-22) and placed into a thermally cleaned 4 mm ID injection liner. Anthracene-d_{10} internal standard (10 ng) (Sigma-Aldrich) was dissolved in DCM and added to the sample. This was then placed with the injection liner into the injection port of the GC-MS. Thermal desorption of the samples from 40 °C to 300 °C was then carried out in the injection port with He carrier gas. A capillary column (Perkin Elmer Elite, 5MS) (30 m x 0.25 mm ID) separated the analytes with a constant flow rate of 2 ml/min at 50 °C. This temperature was held for 1 min and then ramped at 8 °C/min to 300 °C for 7 mins. Time-of-flight (TOF) mode was used to detect the compounds over a range of 45 to 400 atomic mass units (AMU). eCipher 3 data processing software was used for quantification. A calibration curve was generated

by adding known quantities of PAH standard (Sigma-Aldrich, QTM PAH Mix) diluted in DCM and following the same thermal desorption methodology that was used for the PM. The BaP – TEQ of the PM was calculated using the concentrations of individual PAH species and their respective TEF (Jung et al., 2010). Uncertainties for the PM-bound PAH concentration were calculated as the standard error of the mean for a triplicate set of runs. The energy-based yields of PM-bound PAHs were assumed to propagate from the errors in the PM-bound PAH concentration and the energy-based yield of PM. The PM-bound PAH concentration of the dried rice husk was presented in Chapter 3.

5.3. Results and Discussion

5.3.1. Influence of Feedstock Drying on Pyrolysis Products

Table 5.1 compares the yields of pyrolysis products and HHV of the raw pyrolysis volatiles from both the AR and dried rice husk at each pyrolysis temperature. For both cases it was observed that the yield of biochar and bio-oil decreased at elevated pyrolysis temperatures. The yield of pyrogas exhibited the opposite trend due to the increased devolatilization and thermal cracking of rice husk at higher pyrolysis temperatures. This resulted in the formation of condensable products (which contain both oxygenated species and more complex PAHs) at the expense of biochar (Naqvi et al., 2014). At higher pyrolysis temperatures these condensable hydrocarbons are believed to undergo further cracking to form the constituents of the pyrogas (such as CO, CH_4, and H_2) (Tsai et al., 2007). As a result, the yield of pyrogas generated at increasing pyrolysis temperatures increased from 20 to 46 % and from 19 to 46 % for the AR and dried rice husk, respectively. The yield of bio-oil was observed to decrease from 41 to 25 % and 37 to 16 % for the

AR and dried rice husk respectively over the same temperature range. The yield of bio-oil collected from the AR rice husk was higher than the dried rice husk over the entire pyrolysis temperature range. This was due to the increased moisture content of the AR rice husk, which was volatilized during the pyrolysis reaction and then condensed during bio-oil sampling. It was also observed that the increased moisture content of the AR rice husk strongly influenced the HHV of the raw pyrolysis volatiles. In the case of AR rice husk, the HHV of the raw pyrolysis volatiles ranged from 12.1 to 13.2 MJ/kg at increasing pyrolysis temperatures. The HHV of the dried rice husk volatiles ranged from 14.2 to 15.1 MJ/kg over the same pyrolysis temperature range. The decrease in the HHV was due to the dilution of the raw pyrolysis volatiles with moisture.

5.3.2. Influence of Feedstock Drying on the Energy-Based Yields of PM

Fig. 5.1 shows the energy-based yield of PM in different size fractions from combustion (T_c = 850 °C) of the raw pyrolysis volatiles produced from the a) dried and b) AR rice husk at various volatile production temperatures (T_v = 400 – 800 °C). The total energy-based yield of $PM_{0.1\text{-}10}$ was greater for the AR rice husk at every volatile production temperature. At T_v = 400 - 800 °C the energy-based yields of $PM_{0.1\text{-}10}$ were in the 243 – 456 mg/MJ and 154 – 370 mg/MJ ranges for the AR and dried rice husk, respectively. From Fig. 5.1, it was also observed that utilization of the AR rice husk resulted in significantly higher energy-based yields of PM of the $PM_{2.1\text{-}10}$ size fraction than the dried rice husk. For each volatile production temperature, the yields of PM in the $PM_{9\text{-}10}$, $PM_{5.8\text{-}9}$, and $PM_{4.7\text{-}5.8}$ size fractions were much higher for the AR rice husk. At lower volatile production temperatures (T_v = 400, 500, and 600 °C), there were also elevated yields in the $PM_{1.1\text{-}2.1}$ size fraction.

At 700 and 800 °C, however, the energy-based yield in this size fraction was higher for the dried rice husk. In addition, it was also observed that the energy-based yields of sub-micron particulates ($PM_{0.1\text{-}1.1}$) were higher for the dried rice husk at every volatile production temperature. However, the difference in the energy-based yield of the sub-micron particulates between the dried and AR rice husk was less pronounced at elevated temperatures.

Table 5.2 summarised the percentage contribution of various PM size fractions ($PM_{0.1\text{-}10}$, $PM_{0.1\text{-}2.1}$ and $PM_{0.1\text{-}1.1}$) to the total PM emissions at different volatile production temperatures. It is clear that the majority of the increased energy-based yield of PM for the AR rice husk was contributed by the super-micron $PM_{2.1\text{-}10}$ fraction, rather than the $PM_{0.1\text{-}2.1}$ or $PM_{0.1\text{-}1.1}$ fraction. For the dried rice husk, the $PM_{2.1\text{-}10}$ fraction contributed in the 68 – 86 % range of the total energy-based yield of $PM_{0.1\text{-}10}$ over the entire volatile production temperature range, while for the AR rice husk this figure increased to 73 – 94 %. For the dried rice husk, 14 – 32 % and 11 – 23 % of the energy-based yield of $PM_{0.1\text{-}10}$ was contributed by $PM_{0.1\text{-}2.1}$ and $PM_{0.1\text{-}1.1}$, respectively. The contribution of $PM_{0.1\text{-}2.1}$ and $PM_{0.1\text{-}1.1}$ reduced to 6 – 27 % and 5 – 8 % respectively for the AR rice husk. It can therefore be concluded that the utilization of the rice husk with pre-drying favors sub-micron PM formation. It is believed that increased fuel moisture content results in a significant amount of the heat that is developed during combustion being transferred to the latent heat of vaporization of moisture (Chao et al., 2008; Shen et al., 2013). This results in decreased combustion temperatures with increased unburnt carbon fractions in the PM. This agrees with the conclusion of Linak et al. (2000) who suggested that total super-micron PM fractions increase when incomplete carbon burnout is the dominating PM formation

mechanism, while sub-micron PM fractions increase when ash vaporization and complete carbon burnout dominate.

Nevertheless, the HHV of the raw pyrolysis volatiles generated from the AR rice husk was only from 13 to 15 % lower than the dried rice husk, yet the increase in energy-based yield of $PM_{0.1\text{-}10}$ was 23 – 85 %. It is clearly suggested that the increase in PM yields from the AR feedstock is due to the detrimental role of the increased moisture content in the combustion region. From Fig. 5.2, it was observed that the energy-based yield of another product of incomplete combustion, CO, increased for the AR rice husk. The energy-based yield of CO was observed to have a strong linear correlation with the energy-based yield of $PM_{0.1\text{-}10}$ for both the AR and dried material. This agrees with Bignal et al. (2008), who observed a similar relationship between CO and other products of incomplete combustion. The increase in PM yields from the AR feedstock over the dried feedstock is comparable to that reported in previous studies that investigated the effect of feedstock moisture content on PM emissions during the direct combustion of solid biomass fuels (Chao et al., 2008; Chen et al., 2010; Shen et al., 2013).

5.3.3. Influence of Feedstock Drying on PM-Bound PAH Concentrations

Tables 5.3 and 5.4 present the concentration PM-bound PAH species resulting from combustion (T_c = 850 °C) of the raw pyrolysis volatiles produced from the dried and AR rice husk, respectively, at various volatile production temperatures (T_v = 400 – 800 °C). It was observed that the increased moisture content of the AR feedstock resulted in increased PM-bound PAH concentrations in the collected PM size range (2.1 – 10 µm). The range of PM-bound PAH concentrations reported during AR rice husk utilization was 1139 – 1853 µg/g. For the dried rice husk, this

was reduced to 403 – 882 µg/g. This was due to the presence of moisture in the combustion region, which decreased the flame temperature for the vaporization of moisture (Chao et al., 2008). Moisture content has previously been reported to have a positive effect on the yields of PAHs during direct combustion, since PAHs are products of incomplete combustion (Conde et al., 2005). The reduction in flame temperature associated with the presence of moisture, and the resulting decrease in carbon burnout, is expected to increase the presence of the radical precursors involved in the formation of additional PAHs in the combustion region (Richter and Howard, 2000). These precursors are expected to lead to additional formation following the established hydrogen-abstraction C_2H_2-addition (HACA) mechanism that has been reported to be the main pyrogenic route for PAH formation during combustion reactions (Richter and Howard, 2000). For both moisture contents there were significant increases in the concentration of heavy PAH species (5 and 6 ring) such as benzo(k)fluoranthene, indeno(1,2,3-cd)pyrene, benzo(g,h,i)perylene, and dibenz(a,h)anthracene at 700 and 800 °C. The increase in the total PM-bound PAH concentration with increasing volatile production temperatures, for both the AR and dried rice husk, was due to the higher PAH concentration of the bio-oil fraction of the raw pyrolysis volatiles. The influence of bio-oil PAH content on the PM-bound PAH concentration during pyrolysis-combustion has been discussed in Chapter 3.

5.3.4. Influence of Feedstock Drying on PM-Bound PAH Energy-Based Yields

Fig. 5.3 shows the percentage change in the energy-based yield of individual PM-bound PAH species between the AR and dried rice husk. It is clear that the presence of moisture in the feedstock resulted in a significant increase in the energy-based yield of PM-bound PAHs. The majority of the increase in energy-based yields

of individual PM-bound PAHs for the AR rice husk was of 2, 3, and 4 ring PAHs (including naphthalene, acenaphthylene, acenaphthene, and fluorene). At elevated volatile production temperatures there were also significantly higher concentrations of pyrene, fluoranthene, and phenanthrene compared to the dried rice husk. It was also observed in Fig. 5.3 that the energy-based yield of heavy 5 and 6 ring PAHs was generally higher for the dried rice husk. In particular, the concentrations of benzo(g,h,i)perylene and dibenz(a,h)anthracene were typically higher after drying of the feedstock. Between 400 and 800 °C the energy-based yield of dibenz(a,h)anthracene on the PM generated from the dried rice husk was 57 – 96 % higher than when the AR rice husk was utilized. At 400 °C there was a significant increase in the energy-based yield of benzo(b)fluoranthene without prior drying of the rice husk.

Fig. 5.4 compares the ratios of the PM-bound PAH energy-based yields and PAH BaP – TEQ during combustion (T_c = 850 °C) of the raw pyrolysis volatiles produced from the dried and AR rice husk at various volatile production temperatures (T_v = 400 – 800 °C). These results indicated that utilization of the AR rice husk in the pyrolysis-combustion process for the co-generation of biochar and bioenergy resulted in significantly greater energy-based yields of PM-bound PAHs than the dried rice husk (Dried-AR ratio < 1). The energy-based yields of PM-bound PAHs for the AR rice husk were from 2.2 to 3.8 times greater than when the dried rice husk was utilized, despite the total concentration of PM-bound PAHs being from 1.4 to 2.8 times higher (Tables 5.3 and 5.4). The significant increase in the energy-based yield of PM-bound PAHs for the AR rice husk is due to the elevated energy-based yields of $PM_{2.1\text{-}10}$. The increase in the PM-bound PAH concentration at elevated volatile production temperatures, for both moisture contents, is offset by the

reduction in the energy-based yield of PM ($mg_{PM2.1-10}$/MJ) resulting from combustion of the raw pyrolysis volatiles. As a result, the highest energy-based yield of PM-bound PAHs occurred at 500 and 600 °C for the dried rice husk and 400 and 800 °C for the AR husk.

It is also observed in Fig. 5.4 that utilization of the dried rice husk resulted in increased PM BaP-TEQ yield ratios (dried-AR) for the majority of volatile production temperatures (with the exception of 400 °C). Although the total PM-bound PAH concentration was higher when the AR rice husk is used, the greater contribution of 5 and 6 ring PAHs during utilization of the dried rice husk resulted in greater BaP – TEQ values for the PM at these temperatures. In particular, the concentration of dibenzo(a,h)anthracene, indeno(1,2,3-cd)pyrene, and benzo(a)pyrene were all significantly greater for the PM resulting from utilization of the dried rice husk. Each of these species have significant BaP – TEF's (Jung et al., 2010), which resulted in greater BaP – TEQ's for the PM generated for the dried rice husk. The majority of the total PM-bound PAH concentration for the AR rice husk was contributed by 2, 3, and 4 ring PAHs such as naphthalene, acenaphthylene, acenaphthene, and pyrene. All of these species have low BaP – TEF's, which contributed to the reduced BaP – TEQ of the PM resulting from utilization of the AR rice husk. At 400 °C the contribution of 4 and 5 ring PAHs to the total PM-bound PAH concentration are similar for the AR and dried rice husk, resulting in similar BaP – TEQ's. The greatest increase in the relative toxicity of the PM generated from the dried and AR rice husk was observed at 600 °C. At this temperature, 5 and 6 ring PAHs contributed to 35.5 % and 3.3 % of the total PM-bound PAH concentration for the dried and AR rice husk, respectively, which were greater proportions than at any other temperature. This corresponded to a 298 % increase in the BaP – TEQ of the PM generated

during the use of dried rice husk in the pyrolysis-combustion system at T_v = 600 °C, in comparison to the AR rice husk.

This study established the influence of feedstock moisture level and volatile production temperature on the PM and associated PAH emissions from the coarse mode particles (2.1 – 10 µm) during biochar and bioenergy generation using a pyrolysis-combustion system. Previous fuel combustion studies investigating the size distribution of particle-bound PAHs have observed both comparable concentrations on the fine and coarse mode particles (Shen et al., 2014; Tsai et al., 2015), while another study observed increased PAH emissions from fine mode particles (Shen et al., 1994). Therefore, further work is required to understand the PAH emission characteristics and the toxicity levels from the individual particle size ranges, especially the contributions from the fine mode particles for future biomass utilization practices using pyrolysis-combustion.

5.4. Conclusion

The influence of feedstock drying on the PM and PM-bound PAH emissions during the co-generation of biochar and bioenergy from rice husk using pyrolysis-combustion was investigated. It was observed that utilization of the AR rice husk resulted in greater energy-based yields of PM_{10} than the dried rice husk. The elevated yield of $PM_{2.1\text{-}10}$ was the major contributor to the increase in the overall PM_{10}. This increase in PM emissions for the AR rice husk was due to a decrease in combustion temperature for the vaporization of additional moisture content. It was also observed that higher total PM-bound PAH concentrations were associated with the AR rice husk due to the decreased carbon burnout. The energy-based yields of PM-bound PAHs for the AR rice husk from 2.2 to 3.8 times greater than the dried

rice husk over the volatile production temperatures (T_v = 400 - 800 °C). Nevertheless, the BaP – TEQ of the PM generated from the dried rice husk was higher than the PM generated from the AR husk. This was due to increased concentrations of toxic PAH species, such as dibenzo(a,h)anthracene, indeno(1,2,3-cd)pyrene, and benzo(a)pyrene.

Chapter 6: Contributions and Recommendations

This Chapter summarises the key contributions and recommendations of this thesis for the development of pyrolysis-combustion systems for global biochar and bioenergy production.

6.1. Research Findings

6.1.1. Justification for Research

The work presented in this thesis investigated the potential for a pyrolysis-combustion process to co-generate biochar and bioenergy from agricultural by-products. Agricultural by-products are abundant materials produced in several major industries (including horticulture and viticulture). Despite their abundance, and the vast potential for them to be utilized in ways that generate substantial additional revenue streams for producers, increasing their uptake rate has hitherto been fraught with difficulties. This issue has also been compounded by the severe emissions problems associated with conventional methods of by-product disposal (including open burning and cook stoves). Effective utilization of agricultural by-products has traditionally been hampered by significant variations in fuel moisture and ash contents, which can decrease the available heat and increase the energy requirements of the process. Issues related to the difficulty of accessing the feedstock and high transportation costs (due to low bulk density) have also been problematic.

The advantages of the pyrolysis-combustion process for problematic biomass feedstocks are clear. Firstly, the initial low-temperature pyrolysis step (400 – 800 °C) retains the majority of the fuel-bound ash content in the biochar. This effectively

separates the ash from the raw pyrolysis volatiles prior to combustion, minimising potential fouling/slagging issues. Direct combustion of biomass with high alkali metal contents (including potassium and sodium) is particularly difficult due to their reduced volatilization temperatures, which can in some cases lead to numerous problems. This includes reduced heat transfer performance, disturbance of flows, physical damage to process parts, and corrosion and erosion of internal surfaces (Fatehi et al., 2017). In addition, the high silica content of the primary feedstock used in this thesis, rice husk, may potentially lead to the emissions of crystalline silica during combustion, which can cause major health impacts (Gilbe et al., 2008). Secondly, the in-situ drying of AR feedstocks during the pyrolysis reaction means that costly and energy-intensive drying processes can be avoided. This may help minimize the capital requirements of the process and facilitate the utilization of agricultural by-products on-site rather in centralized facilities. These factors help reduce the costs associated with transportation and improve the economic viability of by-product utilization.

Despite the advantages of the pyrolysis-combustion process for such value-adding purposes, there had previously been no studies investigating the influence of operating conditions (including T_v, fuel ash, moisture, VM content, and elemental composition) on the emissions from the process. Given the negative impacts of the emissions from conventional agricultural by-product disposal methods (Smith et al., 2000), the importance of examining the environmental impact of the process resulting from variable emission characteristics (which depend on operating conditions), was evident.

6.1.2. Influence of Bio-Oil Content of Pyrolysis Volatiles on PM Emissions

By utilizing rice husk in a lab-scale pyrolysis-combustion facility, it was observed that the bio-oil fraction of the raw pyrolysis volatiles (which varied with T_v) strongly influenced the PM emissions from the process. Lower temperatures resulted in elevated bio-oil fractions in the raw pyrolysis volatiles which increased the tendency to soot during combustion (Chapter 2). This was due to the increase in the strength of the intermolecular bonding compared to the constituents of the pyrogas, which increased the unburned C content of the combustion products. Between T_v of 400 and 800 °C the energy-based yield of PM_{10} and $PM_{2.1}$ increased by 58 % and 82 % respectively. It was also observed that the coarse mode dominated the PM mass-size distribution, with no distinctive sub-micron peak observed. This demonstrated that incomplete burnout of the bio-oil fraction of the volatiles was the predominant route for PM formation, while there was minimal ash vaporization due to its retainment in the biochar prior to combustion.

6.1.3. PM and Char-Bound PAH Concentrations at Differing Volatile Production Temperatures

It was also observed that operation of the pyrolysis-combustion process at elevated T_v resulted in increased PM and char-bound PAH concentrations (Chapter 3). While the increase in the biochar PAH content was likely due to a complex pyrosynthetic formation route that was favored at higher temperatures, the higher PM-bound PAH concentration was due to the elevated PAH content of the bio-oil. The results demonstrated that the PAHs and oxy-aromatics present in the bio-oil in higher quantities at elevated T_v contributed to the presence of additional PAHs on the PM surface. It was suggested that the PAHs present in the bio-oil that were not

oxidized underwent adsorption/condensation reactions on the surface of the PM in the cooler regions of the flue gas. It was also demonstrated that the BaP – equivalent toxicity of the PM and biochar was greater when the process was operated at higher T_v. This was due to elevated concentrations of heavier 4, 5, and 6 ring PAHs on the biochar and PM at these temperatures.

6.1.4. Influence of Biomass Ash and VM content on the PM Emissions

The influence of agricultural by-product properties (ash and VM content) and composition (S and N) on the emissions from the pyrolysis-combustion process was also investigated (Chapter 4). This was achieved by comparing the PM and gaseous pollutant emissions from two feedstocks with substantially different fuel characteristics. Rice husk is considered less typical of the majority of biomass types, with high ash and low VM contents. Grape pruning, in contrast, is considered more typical, with low ash and high VM contents. It was found that the elevated VM content of the grape pruning resulted in elevated energy-based yields of PM_{10} over the majority of T_v. This increase primarily originated from the greater pyrogas content of the raw pyrolysis volatiles (due to the higher VM content), which favored the formation of sub-micron ($PM_{1.1}$) emissions. It was also observed that the energy-based yields of PM did not increase for the higher ash content feedstock, in contrast to direct combustion (Johansson et al., 2004).

6.1.5. Influence of Feedstock Sulfur/Nitrogen Content and Volatile Production Temperature on Gaseous Emissions

Utilization of the rice husk and grape pruning also allowed for an effective comparison of the influence of biomass S and N content on the emissions of H_2S, SO_2, NO, and NO_2 from the pyrolysis-combustion process (Chapter 4). The results

demonstrated that the higher S content of the rice husk resulted in elevated energy-based yields of H_2S and SO_2. The higher N content of the grape pruning resulted in elevated energy-based yields of NO and NO_2. The choice of T_v also strongly influenced the emissions of gaseous pollutants. Higher T_v were found to result in greater volatilization of biomass-bound S and N. This resulted in elevated S and N contents in the raw pyrolysis volatiles, which lead to increased yields of H_2S, SO_2, NO, and NO_2 for both feedstocks.

6.1.6. PM and PM-bound PAH Emissions during Utilization of Dried and AR Feedstocks

The economic challenges inflicted by expensive and energy-intensive drying equipment during the distributed utilization of agricultural by-products suggests that it may be required to utilize AR feedstocks. The influence of drying on the PM and PM-bound PAH emissions was investigated by utilizing both dried and AR rice husk (Chapter 5). Elevated energy-based yields of PM_{10} were associated with utilization of the AR husk. The majority of the increase in the PM yield was due to higher yields of $PM_{2.1\text{-}10}$. This was caused by the additional energy requirements for vaporization of the water, which decreased the C burnout due to lower combustion temperatures. The greater degree of incomplete combustion for the AR rice husk also resulted in significantly elevated yields of PM-bound PAHs. However, the predominant PAH species bound to the PM resulting from the AR rice husk were lighter 2 and 3 ring PAHs, while for the dried husk there was greater contributions from heavier 5 and 6 ring PAHs. This resulted in elevated BaP – TEQ's for the PM generated from the dried rice husk compared to the AR husk.

6.1.7. Emissions Associated with Optimized Biochar and Bioenergy Production

One of the key findings presented in this thesis is the relationship between the emissions of harmful pollutants (PM, PAHs, and gaseous pollutants) and the choice of T_V. This operating temperature, however, also significantly influences the balance between biochar and bioenergy production. It was previously observed in Fig. 2.2a and b that the pyrolysis-combustion process was optimized for biochar production at lower temperatures (400 °C), while energy production was optimized at higher temperatures (800 °C). Table 6.1 presents a summary of these key findings and outlines the benefits/drawbacks associated with operation of the pyrolysis-combustion process for either optimized biochar or bioenergy production.

6.2. Implications of the Research Findings

6.2.1. Emission Reduction Potential

To be considered a viable alternative to conventional disposal methods (including open burning and cook stoves); the yield of harmful emissions from the pyrolysis-combustion must be less. The detrimental role of these conventional processes on the health of local populations demonstrates the need for effective comparisons to be made in order to develop beneficial and sustainable land management practices (Barron and Torero, 2017). However, the lack of available literature providing the emission factors for PM_{10}, $PM_{2.5}$, PM-bound PAHs, SO_2, and NO_x from rice husk utilization in open burning and cook stoves enhances the difficulty of making such comparisons.

In order to discuss the emissions reduction potential of the pyrolysis-combustion process, the results presented in this thesis were compared to those in

Table 1.3. Christian et al. (2003) presented a $PM_{2.5}$ emission factor of 4200 mg/kg for rice straw (which has similar fuel properties and composition to rice husk) utilization during open burning. This was significantly higher than the $PM_{2.1}$ emissions reported in this study for the dried (201 – 931 mg/kg) and AR rice husk (157 – 899 mg/kg). TSP emission factors of 5000 mg/kg (Kim Oanh et al., 2005) and 1187 mg/MJ (Smith et al., 2000) for rice husk and rice straw utilization in cook stoves respectively have also been reported. It is difficult to compare PM_{10} and TSP emissions, however, demonstrating the problematic nature of ascertaining the PM emission reduction potential of the pyrolysis-combustion process. The PM emissions reported here were also generally much more favourable than those reported for open burning for a variety of biomass wastes. Akagi et al. (2011) compiled PM emission factors for the simulated burning of a variety of crop wastes. It was reported that the PM_{10} emission factors for the open burning of tropical forest and pasture were 18500 and 28900 mg/kg respectively. The results from this study compare favourably, with PM_{10} emission factors of 1500 – 2900 mg/kg and 2300 – 3400 mg/kg for the dried and AR rice husk respectively.

The PAH emission factors presented in this thesis are less than the majority of those reported for both cook stoves and open burning. The values calculated here range from 0.80 – 1.20 mg/kg of feed and 0.10 – 0.14 mg/MJ for the dried rice husk, and 2.31 – 3.92 mg/kg of feed and 0.32 – 0.42 mg/MJ for the AR rice husk. Values reported for cook stoves include 43 mg/kg for rice straw (Shen et al., 2011), 1.64 mg/kg for rice straw (Zhang et al., 2011), and 140 mg/kg for rice husk (Kim Oanh et al., 2005). The results presented in the latter study also included gas-phase PAHs, which may partly explain the significantly greater PAH emissions reported. The PAH emissions from the pyrolysis-combustion process were also lower than those from

the open burning of rice residues. Jenkins et al. (1996) reported a PAH emission factor of 26.1 mg/kg for the open burning of rice straw. The elevated PAH emissions during the utilization of rice straw and husks is to be expected, as PAHs are generally formed as products of incomplete combustion, the rate of which is expected to be greater for the cook stoves and open burning due to the inefficient fuel-air mixing observed for these devices.

The NO_x emission factors for the pyrolysis-combustion process also compare favourably to those from open burning and cook stoves. The results presented in this thesis ranged from 823 – 1162 mg/kg and 105 – 124 mg/MJ. By comparison, it is observed in Table 1.3 that the emission factors for NO_x during the utilization of rice straw in a cook stove was 3430 mg/kg (Cao et al., 2008). It can also be seen that the NO_x emission factors from the utilization of various wood types (94 – 131 mg/MJ) in cook stoves are similar to the pyrolysis-combustion process, despite the N content being higher than for rice husk (Mitchell et al., 2016). The NO_x emissions presented in this thesis are also significantly lower than those from open burning. Christian et al. (2003) presented an emission factor of 3110 mg/kg for the burning of rice straw, which is greater than those presented in this study. This reduction in NO_x yields for the pyrolysis-combustion process is due to the retention of a significant amount of fuel-bound N within the biochar. As a result, only 20 – 53 % of the N content of the rice husk was volatilized during the initial pyrolysis step, resulting in reduced N content within the pyrolysis volatiles (Chapter 4).

The SO_x emission factors presented in this thesis (49.5 – 536 mg/kg and 6.31 – 56.8 mg/MJ) demonstrated the influence of the T_v on the emissions reduction potential of the pyrolysis-combustion process. Operation at reduced temperatures for

optimized biochar production resulted in a lower SO_x emission factor compared to cook stoves (180 mg/kg), while operation for optimized energy production at higher temperatures resulted in a higher emission factor. This was also the case when compared to the SO_x emission factors from open burning of various biomass wastes (400 – 480 mg/kg). It was therefore concluded that, due to the greater degree of volatilization of fuel-bound S at higher T_V (Chapter 4), the pyrolysis-combustion process does not offer a viable alternative for reducing SO_x emissions from agricultural by-product utilization when optimized for bioenergy generation.

6.2.2. Carbon Sequestration Potential

The production of biochar from agricultural by-products is considered a C-negative process (Roberts et al., 2010). As such, it is considered a viable means to reduce atmospheric CO_2 emissions while at the same time providing added-value to current wastes through soil enhancement. It has been suggested that the majority of the C content of biochar produced via slow pyrolysis (as is done in this thesis) is highly stable, with a mean residence time of 1000 years or longer at 10 °C mean annual temperature (Roberts et al., 2010). Chemical analysis of the composition of slow pyrolysis biochar demonstrated that approximately 80 % of the C content is considered stable, while the remaining 20 % is labile (Baldock and Smernik, 2002; Lehmann et al., 2009). Labile C refers to C that is released into the atmosphere as biogenic CO_2 within the first few years of applying it to the soil (Roberts et al., 2010). Using the results presented in this thesis (Chapter 2), an estimate of the stable and labile C addition to the soil following application of the biochar produced from 1 kg of rice husk in the lab-scale pyrolysis-combustion facility when operated for either

optimized biochar (T_p = 400 °C) or bioenergy (T_p = 800 °C) production is shown in Fig. 6.1.

It was observed in Fig. 6.1 that the greatest mass of C added to the soil occurred when the process was operated for optimized biochar production. At this reduced temperature both the yield and C content of the biochar was higher. The difference in the mass of stable C sequestered between the two operating temperatures was significant (36 % greater when optimized for biochar production). This corresponded to 575 g and 422 g of CO_2 equivalent reductions when optimized for biochar and bioenergy production, respectively, for 1 kg of rice husk utilization. It was therefore concluded that, for the purposes of C sequestration and improving soil organic content, operation of the pyrolysis-combustion process for biochar production at lower T_p is beneficial. The potential for C sequestration through the co-generation of biochar and bioenergy is also clearly vast. Using the global availability of rice husk (822 million tonnes) (Naqvi et al., 2014), this corresponds to 4.73 x 10^8 and 3.47 x 10^8 tonnes of CO_2 sequestration potential for the pyrolysis-combustion process when optimized for biochar and bioenergy production respectively. This calculation does not, however, consider the CO_2 emissions from either the flue gas or from other sources during the biomass life-cycle.

6.3. Recommendations

6.3.1. The Benefits of Pyrolysis-Combustion Systems: Looking into the Future

Agricultural by-products have traditionally been considered wastes that require disposal by laborious, inefficient, and often harmful methods. The harm imposed by utilization in open burning practices (Section 1.3.2) and cook stoves (Section 1.3.3) have previously been discussed. One of the other common methods

of utilization, by mulching in the soil (31.3 % of by-products in Fig. 1.2), also suffers from numerous drawbacks that raise questions over its suitability for future land-management practices. The co-generation of biochar and bioenergy in a pyrolysis-combustion process, however, potentially offers an economically viable method for utilizing abundant yet distributed by-products. There is a strong possibility that the increased energy-efficiency (through recycling of the heat generated from the co-combustion of the pyrogas and bio-oil fractions) and low capital costs associated will provide a viable means to increase the global production rate of biochar (Roberts et al., 2010). If this is the case, the impact on global GHG emission mitigation may be substantial (Gaunt and Lehmann, 2008; Lehmann, 2007).

There is a significant amount of literature which indicates that biochar application to the soil has an effect on the volatilization (in the form of N_2O) of N present therein (Cayuela et al., 2014; Wang et al., 2013). While the production of N_2O from other water soluble nitrogenous species (i.e. NO_3^-, NO_2^-, NH_4^+) via biotic decomposition is relatively well understood (Bremner, 1997), studies into the effect of biochar on these systems has yielded a multitude of differing conclusions as to whether the addition of biochar to soils increases or decreases N_2O production. Although it appears that heterocyclic nitrogenous compounds contained within the biochar are a factor in the formation of N_2O (i.e. through abiotic decomposition of cyclic heterogenous species) (Cayuela et al., 2014), there are significant difficulties in studying the effect of N_2O production from biochar amended soils due to biotic decomposition resulting from a multitude of factors effecting microbial populations (surface area, pH, liming ability, catalytic metal content, different pyrolysis conditions, different feedstocks, etc.). It is believed that the determining factors dictating the effect of biochar on soil N_2O are the C/N ratio and biochar application rate. Cayuela

et al. (2014) provided one of the more comprehensive meta-analyses on the effect of biochar on soil N_2O emissions in recent years. An average reduction of 54 % was attained by the addition of biochar to soil which, given that the GWP of N_2O is 310 times that of CO_2, outlines the potential for GHG mitigation through large-scale biochar application.

The utilization of rice by-products as a feedstock for the pyrolysis-combustion process also prevents it from being left in the field to decompose which, due to the anaerobic conditions rice is grown under, leads to significant CH_4 emissions from the biotic decomposition of labile C contained within the feedstock. Leaving the unwanted parts of the rice plant in the field, and the application of rice by-products back to the fields is a long utilized agricultural practice that continues to this day (Jiang et al, 2012). In fact, the utilization of rice husk/straw as an organic fertilizer in rice fields accounts of 14.8 % of rice residue disposal (Fig. 1.2). The use of waste rice product as a fertilizer, however, yields a significant increase in CH_4 emissions, with in situ studies indicating an increase of two to nine times depending on application rate (Sass et al., 1990; Yagi and Minami, 1989; Wang et al., 1992). In addition, inadequate fuel-air mixing observed in both open burning and cook stoves typically leads to significant emissions of CH_4 (Zhang and Chen, 2010; Wang et al., 2009). Given that CH_4 is a potent GHG (21 times that of CO_2), reducing its emissions on a large-scale will have a significantly positive effect on mitigating anthropogenic climate change.

Combined pyrolysis-combustion processes may also provide additional income streams for agricultural producers (i.e. revenue from biochar and bioenergy generation). This is of fundamental importance for future biochar production

strategies, as it cannot be considered viable otherwise. This is primarily due to the simplicity of conventional methods of disposal, which despite providing little added-value for producers, remains prevalent in many countries. A LCA of combined pyrolysis-combustion systems by Roberts et al. (2010) demonstrated that economic viability of the process is largely dependent on the costs of feedstock production, pyrolysis, and the value of C offsets. By examining biochar production from various biomass wastes, they demonstrated that a minimum $CO_{2,}$eq price for C offsets to facilitate breakeven would be \$ 40/$te_{CO2,eq}$ for late stover, \$ 62/$te_{CO2,eq}$ for switchgrass, and \$ 2/$te_{CO2,eq}$ for yard waste. Late stover was identified as having moderate potential for economic viability (+\$ 35/te_{feed}), while biochar production from switchgrass was generally not considered profitable. The significant potential for by-product stream feedstocks to contribute towards global biochar production in an economically viable manner was highlighted, especially when there are disposal costs associated with the materials. They concluded by remarking that some other biomass by-product resources that may be promising for biochar production are livestock manures, although challenges may arise due to high feedstock moisture content.

It is therefore the author's opinion that the wide-scale adoption of pyrolysis-combustion systems for the co-generation of biochar and bioenergy from agricultural by-products can be characterised by three primary outcomes: 1) Reduced emissions of harmful pollutants (especially PM, PAHs, and NO_x) compared to conventional disposal methods, 2) The mitigation of global GHG emissions through the sequestering of C and avoidance of soil/feedstock N_2O and CH_4 emissions, and 3) The creation of additional revenue streams for agricultural producers from both biochar and bioenergy production.

6.3.2. Future Challenges for Agricultural By-Product Utilization

It is clear from the available literature that a great deal of work has been carried out to develop novel utilization methods for biomass feedstocks. Examples include fixed-bed combustion (Mantananont and Patumsawad, 2016), co-combustion of coal and biomass in a pulverized fuel combustor (Chao et al., 2008), downdraft gasifiers for biomass gasification (Susastriawan et al., 2017), and fluidized-bed combustion (Khan et al., 2009). This desire to increase the utilization rate of biomass for bioenergy generation purposes (which is primarily being driven by the C-neutral nature of the fuel), has also seen the development of a 9.8 MW demonstration facility for rice husk combustion in Thailand (Chungsangunsit et al., 2004). This abundance of research is to be expected, however, as the diverse nature of agricultural by-product properties and compositions will ultimately require a diverse range of applicable technologies to effectively utilize a broad range of feedstocks.

It should be noted that, although pyrolysis-combustion processes may be the most suitable approach for high ash content feedstocks (such as rice husk), it is clear that the future of low ash content by-product utilization will involve, to some degree, direct combustion for energy-generation purposes. Governmental desire to meet international GHG emission reduction targets is seeing direct combustion processes directly incentivised. Taking China as an example, extremely generous economic incentives (via feed-in tariffs) have been introduced in an effort to encourage increased investment in biomass-based power generation. Initial government led tariffs (2005) were 0.25 RMB/kWh ($ 0.04 USD/kWh) for the fifteen years of a facilities life-span. In July 2010, the National Development and Reform Commission (NDRC) proposed the “Notice on Improving the Pricing Policy for

Biomass Power Prices" (Yan et al., 2016). This notice provided a unified price of 0.75 RMB/kWh ($ 0.11 USD/kWh) for biomass power projects. China's renewable energy goals have stated that 2012 levels of biomass power capacity (8 GW) should increase to 30 GW by 2020 (Yan et al., 2016). This substantial economic incentive indicates that the generation of energy from agricultural by-products will continue to grow as its viability increases. This will ultimately lead to an increase in the utilization rate of certain agricultural by-products in direct combustion processes.

This drive to utilize agricultural by-products for bioenergy generation purposes will not, however, result in a significant reduction in the availability of low-quality feedstocks with broad fuel ash and moisture contents that are troublesome for direct combustion (see Section 1.4.3). These by-products are eminently suitable for the co-generation of biochar and bioenergy in pyrolysis-combustion processes. Alternative pyrolysis technologies, such as bio-oil production, can also potentially be used for these low-quality biomass feedstocks. In fact, bio-oil production with fast pyrolysis is 30 % more favourable for energy generation than slow pyrolysis for biochar production (Gaunt and Lehmann, 2008). There are, however, numerous technical challenges that have hindered the production of bio-oil on a large-scale hitherto. These include low pH, high oxygen content, deterioration during storage, and expensive/unstable catalyst requirements for upgrading to higher quality fuel (Mortensen et al., 2011; Lehto et al., 2014). It is therefore apparent that pyrolysis-combustion processes are a prime candidate for increasing the utilization rate of high ash content agricultural by-products going into the future.

The co-generation of biochar and bioenergy is not, however, without its challenges. The LCA conducted by Roberts et al. (2010) that analysed the economic

viability of pyrolysis-combustion systems assigned a monetary value per te of $CO_{2,}$eq emission reduction. This is not yet a reality for many parts of the world, which reduces the potential income for pyrolysis-combustion processes in these locations. In addition, many producers who adopt pyrolysis-combustion techniques for utilization of their by-product streams will be reliant on selling the biochar they produce, rather than utilizing it on-site for soil enhancement/C sequestration purposes. However, the depth of the market demand for biochar is currently unclear, and concerns over consistency in quality have hindered its uptake on a larger scale. Many potential customers are also currently unsure of the benefits of biochar adoption, and are therefore hesitant to purchase it and apply it to their soil. This is being partly caused by inconsistencies in the outcomes of biochar trial studies, with Spokas et al. (2012) reporting that 50 % of publications demonstrated a short-term positive effect of biochar addition, 30 % showed negligible improvements, and 20 % reported negative impacts on yields. These barriers to market entry need to be overcome before biochar can be treated as a commodity and traded freely in the marketplace. This is clearly not an insurmountable problem and can be addressed by a coordinated and unified approach between biochar researchers and the wider agricultural community.

It can therefore be concluded that, for the case of high ash content agricultural by-products, pyrolysis-combustion systems for the co-generation of biochar and bioenergy is the most attractive option for value-adding purposes. Doubts surrounding the market demand for biochar still currently exist, however, and these need to be addressed before the large-scale production of biochar can become a reality. In the case of high quality by-products, it appears that direct combustion processes for bioenergy production are generally more favourable. This is primarily a

result of substantial economic incentives being put in place by governments in order to help meet GHG reduction targets through increasing the rate of biomass-derived power generation.

6.3.3. Future Work

Despite the potential for pyrolysis-combustion systems to substantially contribute to global biochar and bioenergy production, there is still much work that is required to develop a more complete picture of the advantages/disadvantages associated with this approach.

There are currently no available LCA studies that have investigated the environmental and energetic impact of adoption of the pyrolysis-combustion process using published experimental results. Effective pollution mitigation strategies require an analysis of the potential life-cycle impacts using existing experimental data (Roberts et al. 2010). Not only should there be a reduction in the yields of harmful pollutants (including PM, PAHs, SO_x, and NO_x), but the net GHG emissions from the utilization of agricultural by-products should also be less than those from conventional disposal methods (including mulching) in order to be considered a viable long-term strategy for sustainable agricultural practices. The main outcomes of this work would be to balance between the “positive” adoption outcomes (excess power output, recycling of macro agro-nutrients back into the soil, C sequestration, and GHG mitigation) against the “negative” outcomes (PM and gaseous emissions, biochar and PM-bound PAH release).

In addition, any future LCA should consider the techno-economic feasibility of large-scale pyrolysis-combustion processes for agricultural by-product utilization. This should include an analysis of the costs and potential for value-adding with large

throughputs, as such work has not been undertaken previously. As a significant portion of the feedstock energy content is retained in the biochar, pyrolysis-combustion may not be the most attractive approach for future utilization strategies that primarily focus on energy production from agricultural by-products with low ash and moisture contents. It is therefore appropriate that future LCA studies investigate the most appropriate utilization strategy for different agricultural by-products.

It is also recommended that further analysis of the composition of the PM be carried out in order to get a better understanding of the toxicity of the emissions. In particular, the concentration of polychlorinated dibenzodioxins and furans is of great interest given their potential to cause significant harm. This is of greater concern when utilizing biomass feedstocks with higher chlorine contents, such as switchgrass (Bjorkman and Stromberg, 1997). Due to the expected low concentration of these species on the PM, such an analysis will only be possible in larger-scale pyrolysis-combustion systems that are capable of producing greater quantities of PM. The use of specialist fractionation equipment with solvent extraction and analysis using high resolution magnetic sector MS will also be required. It is also of interest to investigate the degree of crystallinity in the PM collected in the CI as a function of temperature. This will allow the relevant environmental authorities and potential manufacturers to understand the risks involved and choose the appropriate PM emission control device.

It is also of great interest to develop a deeper understanding of the formation routes of the SO_x, NO_x, and VOC emissions from the pyrolysis-combustion process. This will involve a detailed analysis of the constituents of the raw pyrolysis volatiles that are combusted for the purposes of energy generation. By doing so it will be possible to understand what the precursors to the formation of these harmful

pollutants are, and the conditions that favor their production will be clearer. This will provide a pathway for agricultural producers to operate their process in such a way that minimizes the formation of these species in the pyrolysis-combustion process. The role of the abundant oxy-aromatics present in the raw pyrolysis volatiles in the formation of both PM and PM-bound PAHs is also unclear. The oxygen containing groups present in these aromatic compounds makes them more susceptible to polymerization reactions through the HACA mechanism than the PAHs present in the volatiles, although the extent of this pathway in PM and multiple ring PAH formation during combustion of the pyrolysis volatiles is not currently well understood. In addition, the fate of the remainder of the PAHs present in the bio-oil fraction of the raw pyrolysis volatiles that is combusted for bioenergy generation purposes is of great interest, as the results presented in Chapter 3 outline that a significant portion do not end up on the PM surface and remain in the gas-phase.

It is also suggested that further investigation into the utilization of alternative agricultural by-product feedstocks is carried out. By building up a database of emission factors for the pyrolysis-combustion process, as has been done for cook stoves (Smith et al., 2000), a more complete understanding of the relationship between feedstock properties and composition on the environmental outcomes for the co-generation of biochar and bioenergy will be formed. This information, combined with further research into the quality and impact of the biochar produced from each feedstock on soil performance, will allow for effective decision making in future policies for sustainable land-management practices.

References

Abdullahi, K.L., Delgado-Saborit, J.M., Harrison, R.M., 2013. Emissions and Indoor Concentrations of Particulate Matter and its Specific Chemical Components from Cooking: A Review. Atmos. Environ. 71, 260-294.

Acevedo, B., Barriocanal, C., 2015. The Influence of the Pyrolysis Conditions in a Rotary Oven on the Characteristics of the Products. Fuel. Process. Technol. 131, 109-116.

Akagi, S.K., Yokelson, R.J., Wiedinmyer, C., Alvarado, M.J., Reid, J.S., Karl, T., Crounse, J.D., Wennberg, P.O., 2011. Emission Factors for Open and Domestic Biomass Burning for use in Atmospheric Models. Atmos. Chem. Phys. 11, 4039–4072.

Alper, K., Tekin, K., Karagöz, S., 2015. Pyrolysis of Agricultural Residues for Bio-Oil Production. Clean Technol. Envir. 17 (1), 211-223.

Antal Jr, M.J., Gronli, M., 2003. The Art, Science, and Technology of Charcoal Production. Ind. Eng. Chem. Res. 42 (8), 1619-1640.

Antoniou, N., Zabaniotou, A., 2015. Experimental Proof of Concept for a Sustainable End of Life Tyres Pyrolysis with Energy and Porous Materials Production. J. Clean. Prod. 101, 323-336.

Atal, A., Levendis, Y. A., Carlson, J., Vouros, P., 1997. On the Survivability and Pyrosynthesis of PAHs during Combustion of Pulverized Coal and Tire Crumb. Combust. Flame. 110 (4), 462-478.

Babu, B.V., 2008. Biomass Pyrolysis: A State-of-the-Art Review. Biofuel. Bioprod. Bior. 2, 393-414.

Bahng, M.K., Mukarakate, C., Robichaud, D.J., Nimlos, M.R., 2009. Current Technologies for Analysis of Biomass Thermochemical Processing: A Review. Anal. Chim. Acta. 651 (2), 117-138.

Baldock, J.A., Smernik, R.J., 2002. Chemical Composition and Bioavailability of Thermally Altered Pinus resinosa (Red pine) Wood. Org. Geochem. 33 (9), 1093–1109.

Barron, M., Torero, M., 2017. Household Electrification and Indoor Air Pollution. J. Environ. Econ. Manag. 86, 81-92.

Bazmi, A.A., Zahedi, G., Hashim, H., 2015. Design of Decentralized Biopower Generation and Distribution System for Developing Countries. J. Clean Prod. 86, 209-220.

Beis, S.H., Onay, O., Kockar, O.M., 2002. Fixed-Bed Pyrolysis of Safflower Seed: Influence of Pyrolysis Parameters on Product Yields and Compositions. Renew. Energ. 26, 21–32.

Bhattacharya, S.C., Albina, D.O., Abdul Salam, P., 2002. Emission Factors of Wood and Charcoal-Fired Cookstoves. Biomass. Bioenerg. 23 (6), 453-469.

Bignal, K.L., Langridge, S., Zhou, J.L., 2008. Release of Polycyclic Aromatic Hydrocarbons, Carbon Monoxide and Particulate Matter from Biomass Combustion in a Wood-Fired Boiler under Varying Boiler Conditions. Atmos. Environ. 42 (39), 8863-8871.

Biswas, B., Pandey, N., Bisht, Y., Singh, R., Kumar, J., Bhaskar, T., 2017. Pyrolysis of Agricultural Biomass Residues: Comparative Study of Corn Cob, Wheat Straw, Rice Straw and Rice Husk. Bioresour. Technol. 237, 57-63.

Bjorkman, E., Stromberg, B., 1997. Release of Chlorine from Biomass at Pyrolysis and Gasification Conditions. Energ. Fuel. 11, 1026-1032

Boie, W., 1953. Fuel Technology Calculations. Energietechnik. 3, 309-316.

Brassard, P., Godbout, S., Raghavan, V., 2017. Pyrolysis in Auger Reactors for Biochar and Bio-Oil Production: A Review. Biosyst. Eng. 161, 80-92.

Bremner, J.M., 1997. Sources of Nitrous Oxide in Soils. Nutr. Cycl. Agroecosys. 49 (1-3), 7-16.

Bridgwater, A.V., 2004. Biomass Fast Pyrolysis. Therm. Sci. 8 (2), 21-49.

Bridgwater, A.V., 2007. The Production of Biofuels and Renewable Chemicals by Fast Pyrolysis of Biomass. Int. J. Global Energ. 27 (2), 160-203.

Brown, J.N., 2009. Development of a Lab-Scale Auger Reactor for Biomass Fast Pyrolysis and Process Optimization using Response Surface Methodology. M.S. thesis, Iowa State University, Ames, IA.

Brown, J.N., Brown, R.C., 2012. Process Optimization of an Auger Pyrolyzer with Heat Carrier using Response Surface Methodology. Bioresour. Technol. 103 (1), 405-414.

Buss, W., Graham, M. C., MacKinnon, G., Masek, O., 2016. Strategies for Producing Biochars with Minimum PAH Contamination. J. Anal. Appl. Pyrolysis. 119, 24-30.

Calcote, H.F., Manos, D.M., 1983. Effect of Molecular Structure on Incipient Soot Formation, Combust. Flame. 49, 289-304.

Cao, G., Zhang, X., Gong, S., Zheng, F., 2008. Investigation on Emission Factors of Particulate Matter and Gaseous Pollutants from Crop Residue Burning. J. Environ. Sci. 20, 50–55.

CARB, Method 50. 1990. Determination of Size Distribution of Particulate Matter from Stationary Sources. State of California Air Resources Board.

Cataluña, R., Kuamoto, P.M., Petzhold, C.L., Caramao, E.B., Machado, M.E., da Silva, R., 2013. Using Bio-oil Produced by Biomass Pyrolysis as Diesel Fuel. Energ. Fuel. 27 (11), 6831–6838.

Cayuela, M.L., Sánchez-Monedero, M.A., Roig, A., Hanley, K., Enders, A., Lehmann, J., 2013. Biochar and Denitrification in Soils: When, How Much and Why Does Biochar Reduce N_2O Emissions? Scientific Reports 3, Article number: 1732.

Cepic, Z., Smaragdakis, B.N., Miljkovic, B., Radovanovic, L., Djuric, S., 2016. Combustion Characteristics of Wheat Straw in a Fixed Bed. Energ. Source. Part A. 38 (7), 1007-1013.

Chan. K.Y., Van Zwieten, L., Meszaros, I., Downie, A., Joseph, S., 2007. Agronomic Values of Green Waste Biochar as a Soil Amendment. Aust. J. Soil. Res. 45, 629.

Chao, C.Y.H., Kwong, P.C.W., Wang, J.H., Cheung, C.W., Kendall, G., 2008. Co-Firing Coal with Rice Husk and Bamboo and the Impact on Particulate Matters and Associated Polycyclic Aromatic Hydrocarbon Emissions. Bioresour. Technol. 99 (1), 83-93.

Chen, W.H., Peng, J., Bi, X.T., 2015. A State-of-the-Art Review of Biomass Torrefaction, Densification and Applications. Renew. Sust. Energ. Rev. 44, 847-866.

Chen, L., Verburg, P., Shackeelford, A., Zhu, D., Susfalk, R., Chow, J., 2010. Moisture Effects on Carbon and Nitrogen Emission from Burning of Wild Land Biomass. Atmos. Chem. Phys. 10 (14), 6617–-6625.

Choi, J.H., Kim, S.S., Suh, D.J., Jang, E.J., Min, K.I., Woo, H.C., 2016. Characterization of the Bio-Oil and Bio-Char Produced by Fixed Bed Pyrolysis of the Brown Alga Saccharina Japonica. Korean. J. Chem. Eng. 33 (9), 2691–2698.

Christian, T.J., Kleiss, B., Yokelson, R.J., Holzinger, R., Crutzen, P.J., Hao, W.M., Saharjo, B.H., Ward, D.E., 2003. Comprehensive Laboratory Measurements of Biomass-Burning Emissions: 1. Emissions from Indonesian, African, and other Fuels. J. Geophys. Res-Atmos. 108 (23), DOI: 10.1029/2003JD003704

Chungsangunsit, T., Gheewala, S.H., Patumsawad, S., 2005. Environmental Assessment of Electricity Production from Rice Husk: A Case Study in Thailand. Int. Energy Journal. 6 (1). Part 3. 47-55.

Claoston, N., Samsuri, A.W., Ahmad Husni, M.H., Mohd Amran M.S., 2014. Effects of Pyrolysis Temperature on the Physicochemical Properties of Empty Fruit Bunch and Rice Husk Biochars. Waste. Manag. Res. 32 (4), 331-339.

Conde, F.J., Ayala, J.H., Afonso, A.M., Gonzalez, V., 2005. Emissions of Polycyclic Aromatic Hydrocarbons from Combustion of Agricultural and Sylvicultural Debris. Atmos. Environ. 39, 6654-6663.

Conto, D.D., Silvestre, W.P., Baldasso, C., Godinho, M., 2016. Performance of Rotary Kiln Reactor for the Elephant Grass Pyrolysis. Bioresour. Technol. 218, 153.

Crutzen, P.J., Andreae, M.O., 1990. Biomass Burning in the Tropics: Impact on Atmospheric Chemistry and Biogeochemical Cycles. Science. 250, 1669–1678.

Cunliffe, A. M., Williams, P. T., 1988. Composition of Oils Derived from the Batch Pyrolysis of Tyres. J. Anal. Appl. Pyrolysis. 44, 131–152.

Cyprès, R. 1987. Aromatic Hydrocarbons Formation during Coal Pyrolysis. Fuel. Process. Technol. 15, 1–15.

Darvell, L.I., Ma, L., Jones, J.M., Pourkashanian, M., Williams, A., 2014. Some Aspects of Modelling NOx Formation Arising from the Combustion of 100% Wood in a Pulverized Fuel Furnace. Combust. Sci. Technol. 186, 672–683.

Dellinger, B., Pryor, W. A., Cueto, B., Squadrito, G. L., Deutsch, W. A., 2000. The Role of Combustion-Generated Radicals in the Toxicity of $PM_{2.5}$. Proc. Combust. Inst. 28, 2675–2681.

Demirbas, A., 2004a. Effects of Temperature and Particle Size on Bio-Char Yield from Pyrolysis of Agricultural Residues. J. Anal. Appl. Pyrol. 72, 243–248.

Demirbas, A., 2004b. Effect of Initial Moisture Content on the Yields of Oily Products from Pyrolysis of Biomass. J. Anal. Appl. Pyrolysis. 71, 803-815.

Demirbas, A., 2005. Fuel and Combustion Properties of Bio-Wastes. Energ. Sources. 27 (5), 451–462.

Demirbas, A., 2007. Effects of Moisture and Hydrogen Content on the Heating Value of Fuels. Energ. Source. Part. A. 29 (7), 649–655.

Domínguez, A., Menéndez, J. A., Inguanzo, M., Pis, J. J., 2005. Investigations into the Characteristics of Oils Produced from Microwave Pyrolysis of Sewage Sludge. Fuel. Process. Technol. 86 (9), 1007-1020.

Dutta, T., Kwon, E., Bhattacharya, S. S., Jeon, B. H., Deep, A., Uchimya, M., Kim, K. H., 2016. Polycyclic Aromatic Hydrocarbons and Volatile Organic Compounds in Biochar and Biochar-Amended Soil: A Review. GCB Bioenergy. DOI: 10.1111/gcbb.12363.

Efika, C.E., Wu, C., Williams, P.T., 2012. Syngas Production from Pyrolysis–Catalytic Steam Reforming of Waste Biomass in a Continuous Screw Kiln Reactor. J. Anal. Appl. Pyrol. 95, 87-94.

Enders, A., Hanley, K., Whitman, T., Joseph, S., Lehmann, J., 2012. Characterization of Biochars to Evaluate Recalcitrance and Agronomic Performance. Bioresour. Technol. 114, 644-653.

Fahlstedt, I., Lindman, E., Lindberg, T., Anderson, J., 1997. Co-Firing of Biomass and Coal in a Pressurized Fluidised Bed Combined Cycle. Results of Pilot Plant Studies. In: Proceedings of the 14th International Conference on Fluidized Bed Combustion in Vancouver, Canada. 1, 295–299.

Fatehi, H., Li, Z.S., Bai, X.S., Aldén, M., 2017. Modeling of Alkali Metal Release during Biomass Pyrolysis. P. Combust. Inst. 36 (2), 2243-2251.

Fernandes, I.J., Calheiro, D., Kieling, A.G., Moraes, C.A.M., Rocha, T.L.A.C., Brehm, F.A., Modolo, R.C.E., 2016. Characterization of Rice Husk Ash Produced using Different Biomass Combustion Techniques for Energy. Fuel. 165, 351-359.

Fournel, S., Marcos, B., Godbout, S., Heitz, M., 2015. Predicting Gaseous Emissions from Small-Scale Combustion of Agricultural Biomass Fuels. Bioresour. Technol. 179, 165–172.

Freddo, A., Cai, C., Reid, B. J., 2012. Environmental Contextualisation of Potential Toxic Elements and Polycyclic Aromatic Hydrocarbons in Biochar. Environ. Pollut. 171, 18–24.

Funke, A., Henrich, E., Dahmen, N., Sauer, J., 2017. Dimensional Analysis of Auger-Type Fast Pyrolysis Reactors. Energ. Technol. 5 (1), 119-129.

Funke, A., Ziegler, F., 2010. Hydrothermal Carbonization of Biomass: A Summary and Discussion of Chemical Mechanisms for Process Engineering. Biofuel. Bioprod. Bior. 4, 160-177.

Gao, X., Wu, H., 2011. Biochar as a Fuel: 4. Emission Behavior and Characteristics of PM1 and PM10 from the Combustion of Pulverized Biochar in a Drop-Tube Furnace. Energ. Fuel. 25 (6), 2702-2710.

Gao, Y., Yang, Y., Qin, Z., Sun, Y., 2016. Factors Affecting the Yield of Bio-Oil from the Pyrolysis of Coconut Shell. Springerplus. 5, 333.

Gaunt, J.L., Lehmann, J., 2008. Energy Balance and Emissions Associated with Biochar Sequestration and Pyrolysis Bioenergy Production. Environ. Sci. Technol. 42, 4152–4158.

Ghosh, S.K., 2016. Biomass & Bio-Waste Supply Chain Sustainability for Bio-energy and Bio-fuel Production. Procedia. Environ. Sci. 31, 31–39.

Gilbe, C., Ohman, M., Lindstrom, E., Bostrom, D., Backman, R., Samuelsson, R., Burvall, J., 2008. Slagging Characteristics during Residential Combustion of Biomass Pellets. Energ. Fuel. 22 (5), 3536-3543.

Glaser, B., Parr, M., Braun, C., Kopolo, G., 2009. Biochar is Carbon Negative. Nat. Geosci. 2 (1), 2-2.

Gunaseelan, V.N., 1997. Anaerobic Digestion of Biomass for Methane Production: A Review. Biomass Bioenerg. 13 (1-2), 83-114.

Hagemann, N., Kammann, C.I., Schmidt, H-P., Kappler, A., Behrens, S., 2017. Nitrate Capture and Slow release in Biochar Amended Compost and Soil. PLoS One. 12 (2), e0171214.

Hale, S. E., Lehmann, J., Rutherford, D., Zimmerman, A. R., Bachmann, R. T., Shitumbanuma, V., O'Toole, A., Sundqvist, K. L., Arp, P. H., Cornelissen, G., 2012. Quantifying the Total and Bioavailable Polycyclic Aromatic Hydrocarbons and Dioxins in Biochars. Environ. Sci. Technol. 46 (5), 2830-2838.

Hamilton, J.E., Adams, J.M. Northrop, W.F., 2014. Particulate and Aromatic Hydrocarbon Emissions from a Small-Scale Biomass Gasifier−Generator System. Energ. Fuels. 28, 3255−3261.

Han, G., Lan, J., Chen, Q., Yu, C., Bie, S., 2017. Response of Soil Microbial Community to Application of Biochar in Cotton Soils with Different Continuous Cropping Years. Scientific Reports 7, Article number: 10184.

Hassan, H., Lim, J. K., Hameed, B. H., 2016. Recent Progress on Biomass Co-Pyrolysis Conversion into High-Quality Bio-Oil. Bioresour. Technol. 221, 645-655.

Hays, M.D., Fine, P.M., Geron, C.D., Kleeman, M.J., Gullett, B.K., 2005. Open Burning of Agricultural Biomass: Physical and Chemical Properties of Particle-Phase Emissions. Atmos. Environ. 39 (36), 6747-6764.

He, R., Ye, X.P., English, B.C., Satrio, J.A., 2009. Influence of Pyrolysis Condition on Switchgrass Bio-Oil Yield and Physicochemical Properties. Bioresour. Technol. 100 (21), 5305-5311.

Hetland, R.B., Refsnes, M., Myran, T., Johansen, B.V., Uthus, N., Schwarze, P.E., 2000. Mineral and/or Metal Content as Critical Determinants of Particle-Induced Release of IL-6 and IL-8 from A549 cells. J. Toxicol. Env. Heal. A. 60, 47-65.

Hobbs, P.V., Reid, J.S., Kotchenruther, R.A., Ferek, R.J., Weiss, R., 1997. Direct Radiative Forcing by Smoke from Biomass Burning. Science, 275, 1776–1778.

Hu, Y., Li, G., Yan, M., Ping, C., Ren, J., 2014. Investigation into the Distribution of Polycyclic Aromatic Hydrocarbons (PAHs) in Wastewater Sewage Sludge and its Resulting Pyrolysis Bio-Oils. Sci. Total. Environ. 473-474, 459-464.

Huang, H.B., Aisyah, L., Ashman, P.J., Leung, Y.C., Kwong, C.W., 2013. Chemical Looping Combustion of Biomass-Derived Syngas using Ceria-Supported Oxygen Carriers. Bioresour. Technol. 140, 385–391.

Huang, Y.F., Chiueh, P.T., Lo, S.L., 2016. A Review on Microwave Pyrolysis of Lignocellulosic Biomass. Sustain. Environ. Res. 26 (3), 103-109.

Hung, C-Y., Tsai, W-T., Chen, J-W., Lin, Y-Q., Chang, Y-M., 2017. Characterization of Biochar Prepared from Biogas Digestate, Waste. Manage. 66, 53-60.

IEA, 2006. IEA Bioenergy Annual Report. International Energy Agency, 1–124.

IPCC, 2014. IPCC Special Report on Climate Change 2014: Mitigation of Climate Change. Cambridge University Press.

Isahak, W.N.R.W.I., Hisham, M.W.M., Yarmo, M.A., Hin, T.Y.Y., 2012. A Review on Bio-Oil Production from Biomass by using Pyrolysis Method. Renew. Sust. Energ. Rev. 16 (8), 5910-5923.

Islam, M. N., Ani, F. N., 2000. Techno-Economics of Rice Husk Pyrolysis, Conversion with Catalytic Treatment to Produce Liquid Fuel. Bioresour. Technol. 73 (1), 67-75.

Janvijitsakul, K., Kuprianov, V.I., 2008. Major Gaseous and PAH emissions from a Fluidized-Bed Combustor Firing Rice Husk with High Combustion Efficiency. Fuel Process. Technol. 89 (8), 777-787.

Jenkins, B.M., 1991. On the Electric Power Potential from Paddy Straw in the Punjab and the Optimal Size of the Power Generation Station. Bioresour. Technol. 37 (1), 35-41.

Jenkins, B.M., Baxter, L.L., Miles Jr., T.R., Miles, T.R., 1998. Combustion Properties of Biomass. Fuel Process. Technol. 54, 17-46.

Jenkins, B.M., Jones, A.D., Turn, S.Q., Williams, R.B., 1996. Emission Factors for Polycyclic Aromatic Hydrocarbons from Biomass Burning. Environ. Sci. Technol. 30 (8), 2462–2469.

Jiang, D., Zhuang, D., Fu, J., Huang, Y., Wen, K., 2012. Bioenergy Potential from Crop Residues in China: Availability and Distribution. Renew. Sust. Energ. Rev. 16, 1377– 1382.

Jien, S-H., Wang, C-S., 2013. Effects of Biochar on Soil Properties and Erosion Potential in a Highly Weathered Soil. CATENA. 110, 225-233.

Jindo, K., Mizumoto, H., Sawada, Y., Sanchez-Monedero, M.A., Sonoki, T., 2014. Physical and Chemical Characterization of Biochars Derived from Different Agricultural Residues. Biogeosciences. 11, 6613-6621.

Johansson, L.S., Leckner, B., Gustavsson, L., Cooper, D., Tullin, C., Potter, A., 2004. Emission Characteristics of Modern and Old-Type Residential Boilers Fired with Wood Logs and Wood Pellets. Atmos. Environ. 38, 4183-4195.

Johansson, L.S., Tullin, C., Leckner, B., Sjovall, P., 2003. Particle Emissions from Biomass Combustion in Small Combustors. Biomass Bioenerg. 25, 435-446.

Jung, K. H., Yan, B., Chillrud, S.N., Perera, F.P., Whyatt, R., Camann, D., Kinney, P. L., Miller, R. L., 2010. Assessment of Benzo(a)pyrene-Equivalent Carcinogenicity

and Mutagenicity of Residential Indoor versus Outdoor Polycyclic Aromatic Hydrocarbons Exposing Young Children in New York City. Int. J. Environ. Res. Pu. 7, 1889-1900.

Kan, T., Strezov, V., Evans, T.J., 2016. Lignocellulosic Biomass Pyrolysis: A Review of Product Properties and Effects of Pyrolysis Parameters. Renew. Sust. Energ. Rev. 57, 1126-1140.

Karhu, K., Mattila, T., Bergström, I., Regina, K., 2011. Biochar Addition to Agricultural Soil Increased CH_4 Uptake and Water Holding Capacity – Results from a Short-Term Pilot Field Study. Agric. Ecosyst. Environ. 140 (1-2), 309-313.

Kaufman, Y.J., Fraser, R.S., 1997. Confirmation of the Smoke Particles Effect on Clouds and Climate. Science, 277, 1636–1639.

Keith, L., 2015. The Source of U.S. EPA's Sixteen PAH Priority Pollutants. Polycylic Aromat. Compd. 35 (2-4), 147-160.

Kern, S., Halwachs, M., Kampichler, G., Pfeifer, C., Pröll, T., Hofbauer, H., 2012. Rotary Kiln Pyrolysis of Straw and Fermentation Residues in a 3 MW Pilot Plant – Influence of Pyrolysis Temperature on Pyrolysis Product Performance. J. Anal. Appl. Pyrol. 97, 1–10.

Khadilkar, A.B., Rozelle, P.L., Pisupati, S.V., 2015. A Study on Initiation of Ash Agglomeration in Fluidized Bed Gasification Systems. Fuel. 152, 48-57.

Khan, A.A., de Jong, W., Jansens, P.J., Spliethoff, H., 2009. Biomass Combustion in Fluidized Bed Boilers: Potential Problems and Remedies. Fuel Process. Technol. 90 (1), 21-50.

Kim Oanh, N.T., Albina, D.O., Ping, L., Wang, X., 2005. Emission of Particulate Matter and Polycyclic Aromatic Hydrocarbons from Select Cookstove–Fuel Systems in Asia. Biomass. Bioenerg. 28 (6), 579-590.

Kistler, M., Schmidl, C., Padouvas, E., Giebl, H., Lohninger, J., Ellinger, R., Bauer, H., Puxbaum, H., 2012. Odor, Gaseous and PM10 Emissions from Small Scale Combustion of Wood Types Indigenous to Central Europe. Atmos. Environ. 51, 86-93.

Kramlich, J.C., Malte, P.C., Grosshandler, W.L., 1981. The Reaction of Fuel Sulfur in Hydrocarbon Combustion. Eighteenth Symposium (International) on Combustion. The Combustion Institute. Pittsburgh, PA., 151-161.

Kumar, A., Kumar, N., Baredar, P., Shukla, A., 2015. A Review on Biomass Energy Resources, Potential, Conversion and Policy in India. Renew. Sust. Energ. Rev. 45, 530–539.

Kwong, P.C.W., Chao, C.Y.H., Wang, J.H., Cheung, C.W., Kendall, G., 2007. Co-Combustion Performance of Coal with Rice husks and Bamboo. Atmos. Environ. 41 (35), 7462-7472.

Ledesma, E. B., Marsh, N. D., Sandrowitz, A. K., Wornat, M. J., 2002. Global Kinetic Rate Parameters for the Formation of Polycyclic Aromatic Hydrocarbons from the Pyrolysis of Catechol, a Model Compound Representative of Solid Fuel Moieties. Energ. Fuels. 16 (6), 1331–1336.

Lehmann, J., 2007. A Handful of Carbon. Nature. 447, 143–144.

Lehmann, J., Czimczik, C., Laird, D., Sohi, S., 2009. Stability of biochar in soil. In Biochar for Environmental Management: Science and Technology; Lehmann, J., Joseph, S., Eds.; Earthscan: London, UK, 183-206.

Lehto, J., Oasmaa, A., Solantausta, Y., Kytö, M., Chiaramonti, D., 2014. Review of Fuel Oil Quality and Combustion of Fast Pyrolysis Bio-Oils from Lignocellulosic Biomass. Appl. Energ. 116, 178-190.

Li, B., Lv, W., Zhang, Q., Tiejun, M., Ma, L., 2014. Pyrolysis and Catalytic Upgrading of Pine Wood in a Combination of Auger Reactor and Fixed Bed. Fuel. 129, 61-67.

Li, Q., Jiang, J., Zhang, Q., Zhou, W., Cai, S., Duan, L., Ge, S., Hao, J., 2016. Influences of Coal Size, Volatile Matter Content, and Additive on Primary Particulate Matter Emissions from Household Stove Combustion. Fuel. 182, 780–787.

Liang, C., Gascó, G., Fu, S., Méndez, A., Paz-Ferreiro, J., 2016. Biochar from Pruning Residues as a Soil Amendment: Effects of Pyrolysis Temperature and Particle Size. Soil. Tillage. Res. 164, 3-10.

Lima, A. L. C., Farrington, J. W., Reddy, C. M., 2005. Combustion-Derived Polycyclic Aromatic Hydrocarbons in the Environment—A Review. Environ. Forensics. 6, 109–131.

Linak, W.P., Miller, C.A., Wendt, J.O.L., 2000a. Comparison of Particle Size Distributions and Elemental Partitioning from the Combustion of Pulverized Coal and Residual Fuel Oil, Comparison of Particle Size Distributions and Elemental Partitioning from the Combustion of Pulverized Coal and Residual Fuel Oil. J. Air. Waste. Manage. 50 (8), 1532-1544.

Linak, W.P., Miller, C.A., Wendt, J.O.L., 2000b. Fine Particle Emissions from Residual Fuel Oil Combustion: Characterization and Mechanisms of Formation. Proc. Combust. Inst. 28, 2651–2658.

Liu, S.C., Tsai, W.T., 2016. Thermochemical Characteristics of Dairy Manure and its Derived Biochars from a Fixed-Bed Pyrolysis. Int. J. Green Energ. 13 (10), 963-968.

Löffler, G., Sieber, R., Harasek, M., Hofbauer, H., Hauss, R.,Landauf, J., 2005. NOx Formation in Natural Gas Combustion - Evaluation of Simplified Reaction Schemes for CFD Calculations. Ind. Eng. Chem. Res. 44 (17), 6622–6633.

Luo, Z., Wang, S., Liao, Y., Zhou, J., Gu, Y., Cen, K., 2004. Research on Biomass Pyrolysis for Liquid Fuel. Biomass. Bioenerg. 26 (5), 455-462.

Lyu, H., He, Y., Tang, J., Giesy, G. P., 2016. Effect of Pyrolysis Temperature on Potential Toxicity of Biochar if Applied to the Environment. Environ. Pollut. 218, 1-7.

Ma, T., Fan, C., Hao, L., Li, S., Song, W., Lin, W., 2016. Biomass-Ash-Induced Agglomeration in a Fluidized Bed. Part 1: Experimental Study on the Effects of a Gas Atmosphere. Energ. Fuel. 30, 6395-6404.

Major, J., Rondon, M., Molina, D., Riha, S.J., Lehmann, J., 2010. Maize Yield and Nutrition during 4 years after Biochar Application to a Colombian Savanna Oxisol. Plant. Soil. 333, 117-128.

Mantananont, N., Patumsawad, S., 2016. Particulate Matter and Gaseous Emission Rate from Combustion of Thai lignite and Agricultural Residues in a Fixed-Bed Combustor. Energ. Source. Part A. 38 (4), 478-484.

Manya, J.J., 2012. Pyrolysis for Biochar Purposes: A Review to Establish Current Knowledge Gaps and Research Needs. Environ. Sci. Technol. 46, 7939–7954.

Marshall, J. A., Morton, B. J., Muhlack, R., Chittleborough, D., Kwong, C. W., 2017. Recovery of Phosphate from Calcium-Containing Aqueous Solution Resulting from Biochar-Induced Calcium Phosphate Precipitation. J. Clean. Prod. 165, 27-35.

Martin, J.A., Boateng, A.A., 2014. Combustion Performance of Pyrolysis Oil/Ethanol Blends in a Residential-Scale Oil-Fired Boiler. Fuel. 133, 34−44.

Mason, S.A., Field, R.J., Yokelson, R.J., Kochivar, M.A., Tinsley, M.R., Ward, D.E., Hao, W.M., 2001. Complex Effects Arising in Smoke Plume Simulations due to Inclusion of Direct Emissions of Oxygenated Organic Species from Biomass Combustion. J. Geophys. Res. 106 (12), 12527–12539.

Mastral, A. M., Callen, M., Murillo, R., 1996. Assessment of PAH Emissions as a Function of Coal Combustion Cariables. Fuel. 75 (13), 1533-1536.

McGrath, T. E., Chan, W. G., Hajaligol, M. R., 2003. Low Temperature Mechanism for the Formation of Polycyclic Aromatic Hydrocarbons from the Pyrolysis of Cellulose. J. Anal. Appl. Pyrolysis. 66 (1-2), 51–70.

McKendry, P., 2002. Energy Production from Biomass, (Part 3): Gasification Technologies. Bioresour. Technol. 83 (1), 55–63.

Meng, A., Zhang, Y., Zhuo, J., Li, Q., Qin, L., 2015. Investigation on Pyrolysis and Carbonization of Eupatorium Adenophorum Spreng and Tobacco Stem. J. Energ. Inst. 88, 480–489.

Miles, T.R., Miles Jr, T.R., Baxter, L.L., Bryers, R.W., Jenkins, B.M., Oden, L.L., 1996. Boiler Deposits from Firing Biomass Fuels. Biomass. Bioenerg. 10 (2–3), 125-138.

Mitchell, E.J.S., Lea-Langton, A.R., Jones, J.M., Williams, A., Layden, P., Johnson, R., 2016. The Impact of Fuel Properties on the Emissions from the Combustion of Biomass and Other Solid Fuels in a Fixed Bed Domestic Stove. Fuel Process. Technol., 142, 115–123.

Mohammadi, A., Cowie, A., Mai, T.L.A., de la Rosa, R.A., Kristiansen, P., Brandao, M., Joseph, S., 2016. Biochar Use for Climate-Change Mitigation in Rice Cropping Systems. J. Clean Prod. 116, 61-70.

Mohan, D., Pittman, C.U., Steele, P.H., 2006. Pyrolysis of Wood/Biomass for Bio-Oil: A Critical Review. Energ. Fuel. 20, 848-889.

Moon, J.H., Lee, J.W., Lee, U.D., 2011. Economic Analysis of Biomass Power Generation Schemes under Renewable Energy Initiative with Renewable Portfolio Standards (RPS) in Korea. Bioresour. Technol. 102 (20), 9550-9557.

Morf, P., Hasler, P., Nussbaumer, T., 2002. Mechanism and Kinetics of Homogeneous Secondary Reactions of Tar from Continuous Pyrolysis of Wood Chips. Fuel. 81, 843–853.

Moron, W., Rybak, W., 2015. NOx and SO2 Emissions of Coals, Biomass and their Blends under Different Oxy-Fuel Atmospheres. Atmos. Environ. 116, 65-71.

Mortensen, P.M., Grunwaldt, J.D., Jensen, P.A., Knudsen, K.G., Jensen, A.D., 2011. A Review of Catalytic Upgrading of Bio-oil to Engine Fuels. Appl. Catal. A-Gen. 407, 1-19.

Munir, S., Nimmo, W., Gibbs, B.M., 2011. The Effect of Air Staged, Co-Combustion of Pulverised Coal and Biomass Blends on NOx Emissions and Combustion Efficiency. Fuel. 90 (1), 126–135.

Naqvi, S.R., Uemura, Y., Yusup, S.B., 2014. Catalytic Pyrolysis of Paddy Husk in a Drop Type Pyrolyzer for Bio-Oil Production: The Role of Temperature and Catalyst. J. Anal. Appl. Pyrol. 106, 57-62.

Nasser, R.A., Salem, M.Z.M., Al-Mefarrej, H.A., Abdel-Aaal, M.A., Soliman, S.S., 2014. Fuel Characteristics of Vine Prunings (Vitis Vinifera L.) as a Potential Source for Energy Production. Bioresources. 9 (1), 482 – 496.

National Research Council (NRC), 2002. Biosolids Applied to Land: Advancing Standards and Practices. Committee on Toxicants Pathogens. National Academy Press.

Ng, E.P., Lim, G.K., Khoo, G.L., Tan, K.H., Ooi, B.S., Adam, F., Ling, T.C., Wong, K.L., 2015. Synthesis of Colloidal Stable Linde Type J (LTJ) Zeolite Nanocrystals from Rice Husk Silica and their Catalytic Performance in Knoevenagel Reaction. Mater. Chem. Phys. 155, 30-35.

Nielsen, I.E., Eriksson, A.C., Lindgren, R., Martinsson, J., Nystrom, R., Nordin, E.Z., Sadiktsis, I., Boman, C., Nojgaard, J.K., Pagels, J., 2017. Time-Resolved Analysis of Particle Emissions from Residential Biomass Combustion – Emissions of Refractory Black Carbon, PAHs and Organic Tracers. Atmos. Environ. 165, 179-190.

Ning, S., Hung, M., Chang, Y., Wan, H., Lee, H., Shih, R., 2013. Benefit Assessment of Cost, Energy, and Environment for Biomass Pyrolysis Oil. J. Clean Prod. 59, 141-149.

Nisbet, I. C. T., LaGoy, P. K., 1992. Toxic Equivalency Factors (TEFs) for Polycyclic Aromatic Hydrocarbons (PAHs). Regul. Toxicol. Pharm. 16 (3), 290-300.

Nussbaumer, T., 2003. Combustion and Co-Combustion of Biomass: Fundamentals, Technologies, and Primary Measures for Emission Reduction. Energ. Fuels. 17, 1510-1521.

Nussbaumer, T., Czasch, C., Klippel, N., Johansson, L., Tullin, C., 2008. Particulate Emissions from Biomass Combustion in IEA Countries: Survey on Measurements and Emission Factors. International Energy Agency (IEA) Bioenergy Task 32 and Swiss Federal Office of Energy (SFOE): Zurich.

Obernberger, I., 1998. Decentralized Biomass Combustion: State of the Art and Future Development. Biomass. Bioenerg. 14 (1), 33-56.

Obia, A., Cornelissen, G., Mulder, J., Dörsch, P., 2015. Effect of Soil pH Increase by Biochar on NO, N_2O and N_2 Production during Denitrification in Acid Soils. PLoS One. 10 (9), e0138781.

Okasha, F., 2007. Staged Combustion of Rice Straw in a Fluidized Bed. Exp. Therm. Fluid. Sci. 32 (1), 52-59.

Olave, R.J., Forbes, E.J.A., Johnston, C.R., Relf, J., 2017. Particulate and Gaseous Emissions from Different Wood Fuels during Combustion in a Small-Scale Biomass Heating System. Atmos. Environ. 157, 49-58.

Olson, D.B., Pickens, J.C., Gill, R.J., 1985. The Effects of Molecular Structure on Soot Formation II. Diffusion Flames. Combust. Flame. 62, 43-60.

Pedersen, P. S, Ingwersen, J., Nielsen, T., Larsen, E., 1980. Effects of Fuel, Lubricant, and Engine Operating Parameters on the Emission of Polycyclic Aromatic Hydrocarbons. Environ. Sci. Technol. 14 (1), 71-79.

Prather, M., Derwent, R., Ehhalt, D., Fraser, P., Sanhueza, E., Zhou, X., 1994. Other Trace Gases and Atmospheric Chemistry. Climate Change 1994: Radiative Forcing of Climate Change and an Evaluation of the IPCC IS92 Emission Scenarios, edited by J. T. Houghton et al., Cambridge Univ. Press, New York, 72-126.

Pratiwi, E. P. A., Shinogi, Y., 2016. Rice Husk Biochar Application to Paddy Soil and its Effects on Soil Physical Properties, Plant Growth, and Methane Emission. Paddy. Water. Environ. 14 (4), 521-532.

Quilliam, R. S., Rangecroft, S., Emmett, B. A., Jones, D. L., Is Biochar a Source or Sink for Polycyclic Aromatic Hydrocarbon (PAH) Compounds in Agricultural Soils? GCB Bioenerg. 5 (2), 1-7.

Reddy, M.S., Venkataraman, C., 2002. Inventory of Aerosol and Sulphur Dioxide Emissions from India. Part II - Biomass Combustion. Atmos. Environ. 36, 699–712.

Reza, M.T., Andert, J., Wirth, B., Busch, D., Pielert, J., Lynam, J.G., Mumme, J., 2014. Hydrothermal Carbonization of Biomass for Energy and Crop Production. Appl. Bioenerg. 1, 11–29.

Richter, H., Howard, J. B., 2000. Formation of Polycyclic Aromatic Hydrocarbons and their Growth to Soot—A Review of Chemical Reaction Pathways. Prog. Energy Combust. Sci. 26, 565–608.

Roberts, K.G., Gloy, B.A., Joseph, S., Scott, N.R., Lehmann, J., 2010. Life Cycle Assessment of Biochar Systems: Estimating the Energetic, Economic, and Climate Change Potential. Environ. Sci. Technol. 44 (2), 827-833.

Ronsse, F., Hecke, S.V., Dickinson, D., Prins, W., 2013. Production and Characterization of Slow Pyrolysis Biochar: Influence of Feedstock Type and Pyrolysis Conditions. 5 (2), 104–115.

Russell, S.H., Gomez, J.L.T., Meredith, W., Langston, P., Snape, C.E., 2017. Increased Charcoal Yield and Production of Lighter Oils from the Slow Pyrolysis of Biomass. J. Anal. Appl. Pyrol. 124, 536-541.

Salvi, S., 2007. Health Effects of Ambient Air Pollution in Children. Paediatr. Respir. Rev. 8 (4), 275–280.

Sanchis, E., Ferrer, M., Calvet, S., Coscolla, C., Yusa, V., Cambra-Lopez, M., 2014. Gaseous and Particulate Emission Profiles during Controlled Rice Straw Burning. Atmos. Environ. 98, 25-31.

Sanginés, P., Dominguéz, M.P., Sánchez, F., San Minguel, G., 2015. Slow Pyrolysis of Olive Stones in a Rotary Kiln: Chemical and Energy Characterization of Solid, Gas, and Condensable Products. J. Renew. Sust. Energ. 7, 1–13.

Sass, R.L., Fisher, F.M., Harcombe, P.A., Turner, F.T., 1990. Methane Production and Emission in a Texas Rice Field. Global. Biogeochem. Cy. 4 (1), 47-68.

Schmidl, C., Luisser, M., Padouvas, E., Lasselsberger, L., Rzaca, M., Cruz, C.R.S., Handler, M., Peng, G., Bauer, H., 2011. Particulate and Gaseous Emissions from Manually and Automatically Fired Small Scale Combustion Systems. Atmos. Environ. 45, 7443-7454.

Shen, G., Preston, W., Ebersviller, S.M., Williams, C., Faircloth, J.W., Jetter, J.J., Hays, M.D., 2017. Polycyclic Aromatic Hydrocarbons in Fine Particulate Matter Emitted from Burning Kerosene, Liquid Petroleum Gas, and Wood Fuels in Household Cookstoves. Energ. Fuel. 31, 3081−3090.

Shen, G., Tao, S., Chen, Y., Zhang, Y., Wei, S., Xue, M., Wang, B., Wang, R., Lv, Y., Li, W., Shen, H., Huang, Y., Chen, H., 2013a. Emission Characteristics for Polycyclic Aromatic Hydrocarbons from Solid Fuels Burned in Domestic Stoves in Rural China. Environ. Sci. Technol. 47 (24), 14485–14494.

Shen, G., Tao, S., Wei, S., Zhang, Y., Wang, R., Wang, B., Li, W., Shen, H., Huang, Y., Chen, Y., Chen, H., Yang, Y., Wang, W., Wei, W., Wang, X., Liu, W., Wang, X., Masse Simonich, S.L., 2012. Reductions in Emissions of Carbonaceous Particulate Matter and Polycyclic Aromatic Hydrocarbons from Combustion of Biomass Pellets in Comparison with Raw Fuel Burning. Environ. Sci. Technol. 46 (11), 6409-6416.

Shen, G., Wang, W., Yang, Y., Ding, J., Xue, M., Min, Y., Zhu, C., Shen, H., Li, W., Wang, B., Wang, R., Wang, X., Tao, S., Russell, A.G., 2011. Emissions of PAHs from Indoor Crop Residue Burning in a Typical Rural Stove: Emission Factors, Size Distributions, and Gas-Particle Partitioning. | Environ. Sci. Technol. 2011, 45, 1206–1212.

Shen, G., Xue, M., Wei, S., Chen, Y., Zhao, W., Li, B., Wu, H., Tao, S., 2013b. Influence of Fuel Moisture, Charge Size, Feeding Rate and Air Ventilation Conditions on the Emissions of PM, OC, EC, Parent PAHs, and their Derivatives from Residential Wood Combustion. J. Environ. Sci. 25 (9), 1808-1816.

Shen, H.Z., Huang, Y., Wang, R., Zhu, D., Li, W., Shen, G.F., Wang, B., Zhang, Y., Chen, Y., Lu, Y., Chen, H., Li, T., Sun, K., Li, B., Liu, W., Liu, J., Tao, S., 2013c. Global Atmospheric Emissions of Polycyclic Aromatic Hydrocarbons from 1960 to 2008 and Future Predictions. Environ. Sci. Technol. 47, 6415–6424.

Shihiadeh, A., Hochgreb, S., 2002. Impact of Biomass Pyrolysis Oil Process Conditions on Ignition Delay in Compression Ignition Engines. Energ. Fuel. 16, 552-561.

Shirai, H., Ikeda, M., Aramaki, H., 2013. Characteristics of Hydrogen Sulphide Formation in Pulverized Coal Combustion. Fuel. 114, 114-119.

Singh, B., Singh, B. P., Cowie, A. L., 2010. Characterisation and Evaluation of Biochars for their Application as a Soil Amendment. Aust. J. Soil Res. 48 (6−7), 516−525.

Singh, D., Subramanian, K.A., Juneja, M., Singh, K., Singh, S., Badola, R., Singh, N., 2016. Investigating the Effect of Fuel Cetane Number, Oxygen Content, Fuel Density, and Engine Operating Variables on NOx Emissions of a Heavy Duty Diesel Engine. Environ. Prog. Sustain. 36, 214–221.

Singh, S., Prakash, V., 2007. The Effect of Temperature on PAHs Emission from Incineration of Acrylic Waste. Environ. Monit. Assess. 127 (1-3), 73-77.

Sirisomboon, K., Kuprianov, V.I., 2017. Effects of Fuel Staging on the NO Emission Reduction during Biomass–Biomass Co-Combustion in a Fluidized-Bed Combustor. Energ. Fuel. 31 (1), 659–671.

Smith, K.R., Uma, R., Kishore, V.V.N., Lata, K., Joshi, V., Zhang, J., Rasmussen, R.A., Khalil, M.A.K., 2000. Greenhouse Gases from Small-Scale Combustion Devices in Developing Countries Phase IIa: Household Stoves in India; EPA-600/R-00-052. U.S. Environmental Protection Agency, Research Triangle Park, NC, 27711.

Song, X.F., Ji, X.Y., Bie, H.P., Liu, Q.Q., Bie, R.S., 2015. Characteristics of Gas and Char Generation Study from Reed Black Liquor Particles (RBLP) Pyrolysis in Fluidized Bed. Fuel. 159, 89–97.

Sparrevik, M., Adam, C., Martinsen, V., Jubaedah, Cornelissen, G., 2015. Emissions of Gases and Particles from Charcoal/Biochar Production in Rural Areas using Medium-Sized Traditional and Improved “Retort” Kilns. Biomass. Bioenerg. 72, 65-73.

Spokas, K.A., Cantrell, K.B., Novak, J.M., Archer, D.W., Ippolito, J.A., Collins, H.P., Boateng, A.A., Lima, I.M., Lamb, M.C., McAloon, A.J., Lentz, R.D., Nichols, K.A., 2012. Biochar: A Synthesis of its Agronomic Impact Beyond Carbon Sequestration. J. Environ. Qual. 41, 973–989.

Sun, Y., Liu, Q., Wang, H., Zhang, Z., Wang, X., 2017. Role of Steel Slags on Biomass/Carbon Dioxide Gasification Integrated with Recovery of High Temperature Heat. Bioresour. Technol. 223, 1–9.

Susastriawan, A.A.P., Saptoadi, H., Purnomo, 2017. Small-Scale Downdraft Gasifiers for Biomass gasification: A Review. Renew. Sust. Energ. Rev. 76, 989-1003.

Taherymoosavi, S., Verheyen, V., Munroe, P., Joseph, S., Reynolds, A., 2017. Characterization of Organic Compounds in Biochars Derived from Municipal Solid Waste. Waste. Manage. 67, 131-142.

Tran, K.Q., Luo, X., Seisenbaeva, G., Jirjis, R., 2013. Stump Torrefaction for Bioenergy Application. Appl. Energ. 112, 539-546.

Tsai, W.T., Lee, M.K., Chang, Y.M., 2007. Fast Pyrolysis of Rice Husk: Product Yields and Compositions. Bioresour. Technol. 98 (1), 22-28.

Tzanetakis, T., Farra, N., Moloodi, S., Lamont, W., McGrath, A., Thomson, M.J., 2010. Spray Combustion Characteristics and Gaseous Emissions of a Wood Derived Fast Pyrolysis Liquid-Ethanol Blend in a Pilot Stabilized Swirl Burner. Energ. Fuels. 24, 5331−5348.

Umbria, A., Galan, M., Munoz, M.J., Martin, R., 2004. Characterisation of Atmospheric Particles: Analysis of Particles in the Campo de Gibraltar. Atmosfera. 17 (4), 191-206.

USEPA, Method 5. 2000. Determination of Particulate Matter Emissions from Stationary Sources. US Environmental Protection Agency, Washington DC.

Valix, M., Katyal, S., Cheung, W.H., 2017. Combustion of Thermochemically Torrefied Sugar Cane Bagasse. Bioresour. Technol. 223, 202-209.

van der Stelt, M.J.C., Gerhauser, H., Kiel, J.H.A., Ptasinski, K.J., 2011. Biomass Upgrading by Torrefaction for the Production of Biofuels: A Review. Biomass. Bioenerg. 35, 3748-3762.

Vassilev, S.V., Baxter, D., Andersen, L.K., Vassileva, C.G., 2010. An Overview of the Chemical Composition of Biomass. Fuel. 89, 913–933.

Verma, M., Godbout, S., Brar, S.K., Solomatnikova, O., Lemay, S.P., Larouche, J.P., 2012. Biofuels Production from Biomass by Thermochemical Conversion Technologies. Int. J. Chem. Eng. http://dx.doi.org/10.1155/2012/542426.

Wang, H., 2011. Formation of Nascent Soot and Other Condensed-Phase Materials in Flames. Proc. Combust. Inst. 33 (1), 41–67.

Wang, X., Chen, H., Luo, K., Shao, J., Yang, H., 2008. The Influence of Microwave Drying on Biomass Pyrolysis. Energ. Fuel. 22, 67–74.

Wang, X., Ren, Q., Li, W., Li, H., Li, S., Lu, Q., 2017. Nitrogenous Gas Emissions from Coal/Biomass Co-combustion under a High Oxygen Concentration in a Circulating Fluidized Bed. Energ. Fuel. 31, 3234−3242.

Wang, Z., Delaune, R.D., Lindau, C.W., Patrick Jr, W.H., 1992. Methane Production from Anaerobic Soil Amended with Rice Straw and Nitrogen Fertilizers. Fert. Res. 33 (2), 115-121.

Wang, Z., Zheng, H., Luo, Y., Deng, X., Herbert, S., Xing, B., 2013. Characterization and Influence of Biochars on Nitrous Oxide Emission from Agricultural Soil. Environ. Pollut. 174, 289-296.

Westerholm, R. N., Alsberg, T. E., Frommelin, A. B., Strandell, M. E., 1988. Effect of Fuel Polycyclic Aromatic Hydrocarbon Content on the Emissions of Polycyclic Aromatic Hydrocarbons and other Mutagenic Substances from a Gasoline-Fueled Automobile. Environ. Sci. Technol. 22 (8), 925-930.

Williams, P.T., Nugranad, N., 2000. Comparison of Products from the Pyrolysis and Catalytic Pyrolysis of Rice Husks. Energy. 25 (6), 493-513.

Wilson, W.E., Suh, H.H., 1997. Fine Particles and Coarse Particles: Concentration Relationships Relevant to Epidemiologic Studies. J. Air. Waste Manage. 47 (12), 1238-1249.

Woolf, D., Amonette, J.E., Street-Perrott, F.A., Lehmann, J., Joseph, S., 2010. Sustainable Biochar to Mitigate Global Climate Change. Nat. Commun. 1 (5), 56.

Xin, Y., Cao, H., Yuan, Q., Wang, D., 2017. Two-Step Gasification of Cattle Manure for Hydrogen-Rich Gas Production: Effect of Biochar Preparation Temperature and Gasification Temperature. Waste. Manage. 68, 618-625.

Xu, R., Ferrante, L., Briens, C., Berruti, F., 2009. Flash Pyrolysis of Grape Residues into Biofuel in a Bubbling Fluid Bed. J. Anal. Appl. Pyrol. 86 (1), 58-65.

Yagi, K., Minami, K., 1989. Effect of Organic Matter Application on Methane Emission from Some Japanese Paddy Fields. Soil Sci. Plant. Nutr. 36 (4), 599-610.

Yamato, M., Okimori, Y., Wibowo, I.F., Anshori, S., Ogawa, M., 2006. Effects of the Application of Charred Bark of Acacia Mangiumon the Yield of Maize, Cowpea and

Peanut, and Soil Chemical Properties in South Sumatra, Indonesia. Soil. Sci. Plant. Nutr. 52, 489-495.

Yan, Q.Y., Zhang, Q., Yang, L., Wang, X., 2016. Overall Review of Feed-In Tariff and Renewable Portfolio Standard Policy: A Perspective of China. IOP Conf. Ser. Earth Environ. Sci. 40, 012076.

Yang, G., Sun, Y., Zhang, J., Wen, C., 2016. Fast Carbonization using Fluidized Bed for Biochar Production from Reed Black Liquor: Optimization for H_2S Removal. Environ. Technol. 37 (19), 2447-2456.

Yang, H., Yan, R., Chen, H., Lee, D.H., Zheng, C., 2007. Characteristics of Hemicellulose, Cellulose and Lignin Pyrolysis. Fuel. 86 (12–13), 1781–1788.

Yin, F., Tremain, P., Yu, J., Doroodchi, E., Moghtaderi, B., 2017. Investigations on the Synergistic Effects of Oxygen and CaO for Biotars Cracking during Biomass Gasification. Energ. Fuel. 31, 587–598.

Yue, Y., Lin, Q., Irfan, M., Chen, Q., Zhao, X., 2016. Characteristics and Potential Values of Bio-Oil, Syngas, and Biochar Derived from Salsola Collina Pall. in a Fixed Bed Slow Pyrolysis System. Bioresour. Technol. 220, 378-383.

Zhang, H., Ding, X., Chen, X., Ma, Y., Wang, Z., Zhao, X., 2015. A New Method of Utilizing Rice Husk: Consecutively Preparing D-xylose, Organosolv Lignin, Ethanol and Amorphous Superfine Silica. J. Hazard Mater. 291, 65-73.

Zhang, H., Hu, D., Chen, J., Ye, X., Wang, S.X., Hao, J.M., Wang, L., Zhang, R., An, Z., 2011. Particle Size Distribution and Polycyclic Aromatic Hydrocarbons Emissions from Agricultural Crop Residue Burning. Environ. Sci. Technol. 45, 5477–5482.

Zhang, J., Morawska, L., 2002. Combustion Sources of Particles: 2. Emission Factors and Measurement Methods. Chemosphere. 49 (9), 1059-1074.

Zhang, J., Smith, K.R., 2007. Household Air Pollution from Coal and Biomass Fuels in China: Measurements, Health Impacts, and Interventions. Environ. Health. Perspect. 115 (6), 848-855.

Zhang, J., Smith, K.R., Ma, Y., Ye, S., Jiang, F., Qi, W., Liu, P., Khalil, M.A.K., Rasmussen, R.A., Thornelo, S.A., 2000. Greenhouse Gases and Other Airborne

Pollutants from Household Stoves in China: A Database for Emission Factors. Atmos. Environ. 34, 4537-4549.

Zhang, W., Lu, Z., Xu, Y., Wang, C., Gu, Y., Xu, H., Streets, D.G., 2018. Black Carbon Emissions from Biomass and Coal in Rural China. Atmos. Environ. 176, 158-170.

Zhang, Y., Tao, S., Shen, H., Ma, J., 2009. Inhalation Exposure to Ambient Polycyclic Aromatic Hydrocarbons and Lung Cancer Risk of Chinese Population. Proc. Natl. Acad. Sci. U S A. 106, 21063–21067.

Tables

Table 1.1 - Proximate and ultimate analysis of various agricultural by-products. Data adapted from Vassilev et al. (2010).

Ultimate Analysis	**Units**	**Wheat Straw**	**Almond Shell**	**Olive Husk**	**Coconut Shell**	**Rice Husk**	**Pine Sawdust**
C*	*wt. %*	49.4	50.3	50.0	51.1	49.3	51.0
H*	*wt. %*	6.1	6.2	6.2	5.6	6.1	6.0
N*	*wt. %*	0.7	1.0	1.6	0.1	0.8	0.1
S*	*wt. %*	0.2	0.05	0.05	0.1	0.1	0.01
O**	*wt. %*	43.6	42.5	42.1	43.1	43.7	42.9
Proximate Analysis							
Moisture	*wt. %*	10.1	7.2	6.8	3.1	10.6	15.3
VM	*wt. %*	67.2	69.5	73.7	70.5	56.1	70.4
Ash	*wt. %*	6.4	3.1	2.1	4.4	16.1	0.1
FC	*wt. %*	16.3	20.2	17.4	22.0	17.2	14.2

* d.a.f, ** Calculated by difference;

Table 1.2 - Annual estimate of straw residues in China in 2009. Data adapted from Jiang et al. (2012).

Crop	***Yield (Mte)***	***By-Product Yields (Mte)***
Rice	195.1	195.1
Wheat	115.1	126.6
Maize	163.7	327.5
Beans	19.3	30.0
Tubers	30.0	30.0
Oil-Bearing Crops	31.5	63.1
Cotton	6.4	19.1
Fiber Crops	0.4	0.6
Sugar Crops	121.7	12.2
Total	**530.8**	**806.9**

Table 1.3 - Emission factors for emitted pollutants from the utilization of various agricultural by-products in direct combustion (DC), cook stoves (CS), and open burning (OB).

Study	*Feedstock*	*Units*	*PM_{10}*	*$PM_{2.5}$*	*PAH*	*NO_x*	*SO_x*	*CO*
DC								
[1]	Coal/Rice Husk (50:50)	mg/MJ	1080	90[a]	0.06	-	-	-
[1]	Rice Husk	mg/MJ	1125	106[a]	-	-	-	-
[1]	Bamboo	mg/MJ	-	-	3			
[2]	Coal/Rice Husk (50:50)	mg/MJ	-	-	-	41	306	86
[2]	Coal/Bamboo (50:50)	mg/MJ	-	-	-	42	286	92
[3]	Rice Husk	mg/MJ	-	-	0.003	-	-	-
[4]	Rice Husk	mg/MJ	22[b]			694	89	197
[5]	Coal/Olive Pips (76:24)	mg/MJ	-	-	-	90	-	-
[6]	Coal/Wheat Straw (70:30)	mg/MJ	-	-	-	15	-	-
[6]	Coal/Corn Straw (70:30)	mg/MJ	-	-	-	78	-	-
CS								
[7]	Rice Straw	mg/MJ	1187[b]	-	-	-	-	7751
[8]	Wood	mg/MJ	95	91	-	110	-	9845
[9]	Wood	mg/MJ	-	-	0.7	-	-	-
[10]	Rice Straw	mg/kg	-	-	43	-	-	-
[10]	Wheat Straw	mg/kg	-	-	66	-	-	-
[11]	Wood	mg/MJ	21	-	-	94	-	118
[11]	Sessile Oak	mg/MJ	222	-	-	131	-	3681
[12]	Rice Husk	mg/kg	5000[b]	-	140	-	-	-
[13]	Rice Straw	mg/kg	-	-	1.64	-	-	-
[13]	Corn Straw	mg/kg	-	-	0.93	-	-	-
[13]	Wheat Straw	mg/kg	-	-	0.72	-	-	-
[14]	Rice Straw	mg/kg	-	-	-	3430	180	
OB								
[15]	Rice Straw	mg/kg	-	4200	-	3110	-	102000
[16]	Savanna	mg/kg	-	7170	-	3900	480	63000
[16]	Tropical Forest	mg/kg	18500	9100	-	2550	400	93000
[16]	Temperate Forest	mg/kg	-	12700	-	2510	-	89000
[17]	Rice Straw	mg/kg	-	-	26.1	-	-	-

a – refers to $PM_{2.1}$; b – refers to TSP; [1] (Chao et al., 2008); [2] (Kwong et al., 2007); [3] (Janvijitsakul and Kuprianov, 2008); [4] (Chungsangunsit et al., 2004); [5] (Fahlstedt et al., 1997); [6] (Wang et al., 2017); [7] (Smith et al., 2000); [8] (Mitchell et al., 2016); [9] (Shen et al., 2017); [10] (Shen et al., 2011); [11] (Kistler et al., 2012); [12] (Kim Oanh et al., 2005); [13] (Zhang et al., 2011); [14] (Cao et al., 2008); [15] (Christian et al., 2003); [16] (Akagi et al., 2011); [17] (Jenkins et al, 1996).

Table 1.4 - Typical pyrolysis product yields (wt. %) from different modes of pyrolysis (IEA, 2006).

Mode	***Conditions***	***Biochar***	***Bio-oil***	***Pyrogas***
Fast Pyrolysis	Moderate temperature (≈ 500 °C) and short residence times (≈ 1 s).	12 %	75 %	13 %
Intermediate Pyrolysis	Moderate temperature (≈ 500 °C) and moderate vapor residence times (≈ 10 – 20 s)	20 %	50 %	30 %
Slow Pyrolysis	Low temperatures (≈ 400 °C) and long residence times (> 10 mins)	35 %	30 %	35 %

Table 2.1 - Proximate and ultimate analysis of rice husk and biochar each pyrolysis temperature (T_p).

	Rice Husk	***Rice Husk Derived Biochar***				
***T_p* (°C)**	**-**	**400**	**500**	**600**	**700**	**800**
Proximate Analysis (wt %)						
Moisture	9.2	-	-	-	-	-
Volatiles	51.3	-	-	-	-	-
Fixed C	18.4	-	-	-	-	-
Ultimate Analysis (wt % d.a.f)						
C	38.1	43.0	43.5	43.4	41.6	41.7
H	5.00	2.21	1.92	1.58	1.19	1.19
N	0.26	0.47	0.30	0.30	0.35	0.37
S	0.52	0.41	0.13	0.09	0.01	0.00
O[#]	56.1	53.9	54.2	54.6	56.9	56.7
HHV (*MJ/kg*)	15.4	17.0	17.1	17.0	15.7	15.9
Yield (%)	-	44.5	41.1	40.0	39.1	37.6
Ash (%)	21.5	47.3	50.3	53.8	54.0	55.7

[#] Calculated by difference.

Table 2.2 - Contribution of smallest and largest PM size fractions to total $PM_{2.1}$ yield with varying contributions of bio-oil to pyrolysis volatiles HHV at each volatile production temperature (T_v).

T_v (°C)	***Bio-oil Contribution to Pyrolysis Volatiles HHV (%)***	***Wt. % of $PM_{2.1}$ Yield Contributed by Different Particle Sizes***	
		0.1 – 0.43 µm (Sub-micron)	**1.1 – 2.1 µm (Super-micron)**
400	90.3	40.8	28.4
500	74.0	48.6	24.5
600	63.9	50.3	25.8
700	53.0	52.7	21.9
800	43.6	52.0	21.8

Table 3.1 - Some properties of the PAH species detected in this work.

PAH	***Structure (# of rings)***	***Molecular weight (g/mole)***	***Vapor pressure (mm Hg)***	***TEF****
Naphthalene	2	128.17	8.89E−02	0.001
2-Bromonapthalene	2	207.07	5.70E-03	-
Acenaphthylene	3	152.20	2.90E−02	0.001
Acenaphthene	3	154.21	3.75E−03	0.001
Fluorene	3	166.22	3.24E−03	0.001
Phenanthrene	3	178.23	6.80E−04	0.001
Anthracene	3	178.23	2.55E−05	0.01
Pyrene	4	202.26	4.25E−06	0.001
Fluoranthene	4	202.26	8.13E−06	0.001
Chrysene	4	228.29	7.80E−09	0.01
Benzo(a)anthracene	4	228.29	1.54E−07	0.1
Benzo(b)fluoranthene	5	252.32	9.59E−11	0.1
Benzo(a)pyrene	5	252.32	4.89E−09	1
Indeno(1,2,3-cd)pyrene	6	276.34	1.40E−10	0.1
Benzo(g,h,i)perylene	6	276.34	1.00E−10	0.01
Dibenz(a,h)anthracene	6	278.35	2.10E−11	1

* TEF refers to the carcinogenic toxicity of each PAH species relative to BaP (Nisbet and LaGoy, 1992).

Table 3.2 - Biochar-bound PAH concentrations and BaP - TEQ at each pyrolysis temperature (T_p).

	PAH Concentration ($\mu g_{PAH}/g_{biochar}$)				
T_p (°C)	***400***	***500***	***600***	***700***	***800***
Naphthalene	0.402 ± 0.082	2.226 ± 0.433	1.253 ± 0.397	3.603 ± 0.813	3.692 ± 0.820
2-Bromonapthalene	n.d.	n.d.	n.d.	n.d.	n.d.
Acenaphthylene	0.123 ± 0.011	0.336 ± 0.013	0.362 ± 0.133	1.208 ± 0.397	1.648 ± 0.149
Acenaphthene	0.048 ± 0.012	0.120 ± 0.033	0.217 ± 0.097	0.027 ± 0.004	0.063 ± 0.008
Fluorene	0.110 ± 0.022	0.151 ± 0.029	0.598 ± 0.239	0.026 ± 0.005	0.145 ±0.056
Phenanthrene	0.175 ± 0.022	0.309 ± 0.133	0.890 ± 0.244	0.445 ± 0.171	1.101 ± 0.290
Anthracene	0.057 ± 0.057	0.038 ± 0.006	0.625 ± 0.088	0.058 ± 0.025	0.913 ± 0.196
Pyrene	0.038 ± 0.019	0.021 ± 0.021	0.494 ± 0.161	0.406 ± 0.167	1.052 ± 0.261
Fluoranthene	0.031 ± 0.013	0.023 ± 0.023	0.548 ± 0.168	0.378 ± 0.158	1.138 ± 0.349
Chrysene	0.016 ± 0.016	0.006 ± 0.006	0.491 ± 0.145	0.025 ± 0.014	0.448 ± 0.207
Benzo(a)anthracene	0.006 ± 0.006	0.006 ± 0.006	0.477 ± 0.138	0.003 ± 0.003	0.315 ± 0.141
Benzo(b)fluoranthene	0.005 ± 0.005	0.005 ± 0.005	0.532 ± 0.142	0.002 ± 0.002	0.312 ± 0.142
Benzo(a)pyrene	0.003 ± 0.003	0.004 ± 0.002	0.431 ± 0.138	0.003 ± 0.003	0.253 ± 0.112
Indeno(1,2,3-cd)pyrene	0.002 ± 0.002	0.002 ± 0.002	0.294 ± 0.100	0.001 ± 0.001	0.087 ± 0.038
Benzo(g,h,i)perylene	0.003 ± 0.003	0.001 ± 0.001	0.498 ± 0.179	0.000 ± 0.000	0.096 ± 0.046
Dibenz(a,h)anthracene	0.002 ± 0.002	0.001 ± 0.001	0.118 ± 0.048	0.000 ± 0.000	0.024 ± 0.012
Total PAH	1.022 ± 0.212	3.250 ± 0.499	7.829 ± 2.380	6.185 ± 1.664	11.284 ± 0.877
BaP-TEQ ($\mu g_{PAH}/g_{biochar}$)	0.008 ± 0.002	0.010 ± 0.001	0.700 ± 0.213	0.011 ± 0.003	0.372 ± 0.029

(n.d. = not detected)

Table 3.3 - Bio-oil PAH concentrations at each pyrolysis temperature (T_p).

	PAH Concentration ($\mu g_{PAH}/ml_{bio\text{-}oil}$)				
T_p (°C)	***400***	***500***	***600***	***700***	***800***
Naphthalene	0.07 ± 0	0.85 ± 0.04	0.60 ± 0.08	33.90 ± 12.61	204.67 ± 3.84
2-Bromonapthalene	n.d.	n.d.	n.d.	n.d.	n.d.
Acenaphthylene	0.42 ± 0.01	0.42 ± 0.10	1.00 ± 0.13	20.20 ± 8.64	277.12 ± 4.34
Acenaphthene	0.23 ± 0.01	0.25 ± 0.03	0.67 ± 0.08	3.20 ± 1.38	26.38 ± 2.36
Fluorene	0.10 ± 0.02	0.18 ± 0	0.36 ± 0.01	8.00 ± 3.35	163.37 ± 10.67
Phenanthrene	0.06 ± 0.01	0.10 ± 0.01	0.52 ± 0.07	9.17 ± 3.82	183.27 ± 4.86
Anthracene	0.03 ± 0	0.09 ± 0.01	0.15 ± 0.02	2.86 ± 1.25	102.19 ± 9.35
Pyrene	n.d.	n.d.	0.07 ± 0.01	1.49 ± 0.67	44.00 ± 3.99
Fluoranthene	n.d.	n.d.	0.09 ± 0.01	1.59 ± 0.70	47.95 ± 4.59
Chrysene	n.d.	n.d.	0.03 ± 0.03	0.75 ± 0.33	18.58 ± 1.73
Benzo(a)anthracene	n.d.	n.d.	0.02 ± 0.02	0.61 ± 0.29	20.23 ± 2.37
Benzo(b)fluoranthene	n.d.	n.d.	n.d.	0.71 ± 0.35	7.52 ± 0.65
Benzo(a)pyrene	n.d.	n.d.	n.d.	0.38 ± 0.10	9.99 ± 1.38
Indeno(1,2,3-cd)pyrene	n.d.	n.d.	0.04 ± 0.02	0.15 ± 0.05	2.94 ± 0.38
Benzo(g,h,i)perylene	n.d.	n.d.	0.02 ± 0.02	0.06 ± 0.06	1.07 ± 0.13
Dibenz(a,h)anthracene	n.d.	n.d.	n.d.	0.16 ± 0.06	3.45 ± 0.40
2 - 3 Ring %	100 ± 0	100 ± 0	92.94 ± 1.57	92.94 ± 0.32	86.01 ± 0.76
4 Ring %	n.d.	n.d.	5.51 ± 1.27	5.32 ± 0.29	11.75 ± 0.60
5 - 6 Ring %	n.d.	n.d.	1.55 ± 0.30	1.73 ± 0.03	2.24 ± 0.16
Total PAH ($\mu g_{PAH}/ml_{bio\text{-}oil}$)	0.91 ± 0.35	1.87 ± 0.03	3.54 ± 0.17	83.17 ± 33.60	1112.68 ± 50.99

(n.d. = not detected)

Table 3.4 - Concentration of the 10 most predominant aromatic species present in the bio-oil produced at each pyrolysis temperature (T_p).

Compound	***Concentration (µg/ml$_{bio-oil}$)***
400 °C Bio-Oil	
phenol	384.19
2-methoxy-4-methylphenol	273.07
4-methylphenol	251.33
5-methyl-2-furancarboxaldehyde/3-methyl-2-cyclopenten-1-one	228.79
2-methoxyphenol	199.56
3-methyl-1,2-cyclopentanedione	190.43
4-ethylphenol	164.08
butyrolacetone	143.55
2-methylphenol	128.31
4-ethyl-2-methoxyphenol	117.84
500 °C Bio-Oil	
phenol	715.13
4-methylphenol	455.21
2-methoxy-4-methylphenol	329.50
2-methylphenol	212.22
5-methyl-2-furancarboxaldehyde/3-methyl-2-cyclopenten-1-one	193.94
4-ethylphenol	190.77
4-ethyl-2-methoxyphenol	188.82
butyrolacetone	188.30
3-methyl-1,2-cyclopentanedione	167.26
4-ethyl-1,3-benzenediol	134.33
600 °C Bio-Oil	
2-methoxyphenol	630.05
phenol	346.82
2-methoxy-4-methylphenol	253.71
butyrolacetone	247.05
5-methyl-2-furancarboxaldehyde/3-methyl-2-cyclopenten-1-one	186.23
2,6-dimethoxyphenol	184.25
vanillin	151.45
4-methylphenol	142.59
4-ethylphenol	104.33
4-ethyl-2-methoxyphenol	102.75
700 °C Bio-Oil	
phenol	798.51
4-methylphenol	495.58
2-methylphenol	242.96
4-ethylphenol	111.73
3,5-dimethylphenol	65.23
2-methylnaphthalene	42.31
2,3-dihydrobenzofuran	40.84
1-methylnapthalene	37.82
(ethenyloxy)benzene	35.40
800 °C Bio-Oil	
phenol	1248.67
4-methylphenol	440.22
acenaphthylene	277.12
1-methylnapthalene	247.68
naphthalene	204.67
2-methylnapthalene	197.09
phenanthrene	183.27
fluorine	163.37
biphenyl	157.89
dibenzofuran	124.20

Table 4.1 - Proximate analysis of the as received grape pruning (GP) and rice husk (RH). Ultimate analysis of the GP, RH, and biochar derived between 400 – 800 °C. The results presented for the rice husk are adapted from Chapter 2.

	Moisture	***VM***	***Fixed C***	***Ash***	***C***	***H***	***N***	***S***	***O[a]***
Rice Husk									
RH	9.20	51.3	18.4	21.5	38.1	5.00	0.26	0.52	56.1
RH_{400}	-	-	-	47.3	43.0	2.21	0.47	0.41	53.9
RH_{500}	-	-	-	50.3	43.5	1.92	0.30	0.13	54.2
RH_{600}	-	-	-	53.8	43.4	1.58	0.30	0.09	54.6
RH_{700}	-	-	-	54.0	41.6	1.19	0.35	0.01	56.9
RH_{800}	-	-	-	55.7	41.7	1.19	0.37	0.00	56.7
Grape Pruning									
GP	6.79	65.4	21.0	6.67	49.2	6.69	1.00	0.27	42.9
GP_{400}	-	-	-	18.5	68.6	4.56	1.50	0.18	25.2
GP_{500}	-	-	-	20.3	72.9	3.64	1.46	0.14	21.9
GP_{600}	-	-	-	23.8	79.2	2.68	1.43	0.10	16.6
GP_{700}	-	-	-	24.9	77.4	1.76	1.26	0.06	19.5
GP_{800}	-	-	-	29.9	81.1	1.16	1.44	0.03	16.3

[a] d.a.f, calculated by difference.

Table 4.2 - Composition of the pyrogas fraction of raw pyrolysis volatiles produced from the grape pruning (GP) and rice husk (RH) between 400 and 800 °C. The results presented for the rice husk are adapted from Chapter 2.

Species	**400 °C**	**500 °C**	**600 °C**	**700 °C**	**800 °C**
GP (vol %)					
H_2	0.4	3.4	10.3	14.6	14.4
CO	14.5	11.6	10.0	10.2	14.8
CO_2	33.1	29.0	21.5	15.8	11.2
CH_4	2.0	6.0	8.3	9.3	9.6
HHV (MJ/kg)	1.8	3.1	4.7	6.0	6.8
RH (vol %)					
H_2	0.6	2.1	5.4	9.3	9.6
CO	20.4	20.4	24.3	25.2	21.9
CO_2	26.8	17.7	12.3	9.4	9.0
CH_4	1.5	3.7	3.8	3.1	5.9
HHV (MJ/kg)	2.3	3.2	4.2	4.7	5.4

Table 5.1 – Yields of pyrolysis products and HHV of the raw pyrolysis volatiles produced from dried and AR rice husk at various pyrolysis temperatures (T_p = 400 – 800 °C). The data for the dried rice husk is adapted from Chapter 2.

	Pyrolysis Product Yield (wt. %)			***Raw Pyrolysis Volatile HHV (MJ/kg)***
T_p	*Biochar*	*Bio-oil*	*Pyrogas*	
400 °C (Dried)	44.5	36.6	18.8	14.2
500 °C (Dried)	41.2	22.4	36.4	14.2
600 °C (Dried)	40.1	22.3	37.6	14.4
700 °C (Dried)	39.0	15.9	45.1	15.2
800 °C (Dried)	37.6	16.0	46.4	15.1
400 °C (AR)	38.4	41.8	19.9	12.1
500 °C (AR)	33.1	35.8	31.2	12.5
600 °C (AR)	33.2	32.4	34.4	12.5
700 °C (AR)	29.6	28.6	41.7	13.3
800 °C (AR)	29.4	25.0	45.6	13.2

Table 5.2 – Contribution by weight (%) of $PM_{0.1\text{-}1.1}$, $PM_{0.1\text{-}2.1}$ and $PM_{2.1\text{-}10}$ to the total PM_{10} yield for combustion (T_c = 850 °C) of the raw pyrolysis volatiles produced at each volatile production temperature (T_v) for the dried and AR rice husk.

	Dried			**AR**		
	% Cont. to PM_{10} Yield					
T_v *(°C)*	$PM_{0.1\text{-}1.1}$	$PM_{0.1\text{-}2.1}$	$PM_{2.1\text{-}10}$	$PM_{0.1\text{-}1.1}$	$PM_{0.1\text{-}2.1}$	$PM_{2.1\text{-}10}$
400	22.9	32.0	68.0	7.8	27.4	72.6
500	18.3	24.2	75.8	7.9	20.2	79.8
600	18.4	24.7	75.3	7.9	18.5	81.5
700	11.5	14.7	85.3	5.6	7.2	92.8
800	10.8	13.8	86.2	5.7	5.7	94.3

Table 5.3 – PM-bound PAH concentrations generated from combustion (T_c = 850 °C) of the raw pyrolysis volatiles at each volatile production temperature (T_V) for the dried rice husk.

	PM-Bound PAH Concentration ($\mu g_{PAH}/g_{PM}$)				
T_V (°C)	***400***	***500***	***600***	***700***	***800***
Dried					
Naphthalene	37.48	91.86	47.28	27.26	22.00
Acenaphthylene	30.21	57.40	34.70	51.46	44.95
Acenaphthene	34.14	90.38	45.79	27.26	22.00
Fluorene	10.05	14.71	6.60	15.67	13.52
Phenanthrene	59.34	128.46	92.33	97.40	89.23
Anthracene	38.76	44.15	52.07	51.41	48.46
Pyrene	51.74	63.79	48.75	60.17	56.94
Fluoranthene	63.48	115.22	68.04	75.99	71.09
Chrysene	23.51	48.01	58.86	76.99	71.95
Benzo(a)anthracene	16.49	25.96	43.50	59.48	54.30
Benzo(b)fluoranthene	3.99	36.51	80.38	85.28	91.75
Benzo(a)pyrene	12.78	25.98	62.33	70.78	77.15
Indeno(1,2,3-cd)pyrene	6.67	11.68	52.05	57.69	62.97
Benzo(g,h,i)perylene	11.50	14.58	69.39	124.46	106.92
Bibenz(a,h)anthracene	2.51	1.68	10.03	62.89	48.38
Total PAH Conc.	402.7 ± 208.9	770.4 ± 143.3	772.1 ± 173.0	944.2 ± 91.3	881.6 ± 108.2
% 2 - 3 Ring	52.1 ± 9.6	55.4 ± 14.3	36.1 ± 21.2	28.6 ± 8.9	27.2 ± 3.2
% 4 Ring	38.5 ± 1.3	32.8 ± 3.5	28.4 ± 3.1	28.9 ± 1.1	28.8 ± 5.1
% 5 - 6 Ring	9.3 ± 7.1	11.7 ± 8.7	35.5 ± 19.0	42.5 ± 7.3	43.9 ± 7.9

Table 5.4 – PM-bound PAH concentrations generated from combustion (T_c = 850 °C) of the raw pyrolysis volatiles at each volatile production temperature (T_V) for the AR rice husk.

	PM-Bound PAH Concentration ($\mu g_{PAH}/g_{PM}$)				
T_V (°C)	***400***	***500***	***600***	***700***	***800***
AR					
Naphthalene	179.68	182.38	193.76	154.91	171.53
Acenaphthylene	105.66	138.95	152.42	118.72	165.56
Acenaphthene	173.32	161.01	190.31	71.44	94.36
Fluorene	30.02	44.84	57.22	11.39	24.64
Phenanthrene	182.09	147.39	185.13	278.35	281.19
Anthracene	55.45	60.48	77.28	103.77	128.22
Pyrene	88.61	100.29	147.86	139.94	219.61
Fluoranthene	179.61	123.36	174.25	173.75	253.41
Chrysene	56.21	36.07	46.18	76.34	102.87
Benzo(a)anthracene	27.43	19.98	25.20	42.89	77.27
Benzo(b)fluoranthene	31.12	19.31	23.43	49.12	110.50
Benzo(a)pyrene	23.10	13.84	14.99	40.31	73.62
Indeno(1,2,3-cd)pyrene	3.21	3.08	2.02	33.36	58.16
Benzo(g,h,i)perylene	3.35	3.23	2.19	31.33	79.85
Dibenz(a,h)anthracene	0.30	0.28	0.24	1.45	12.06
Total PAH Conc.	1139.1 ± 94.0	1054.5 ± 125.0	1292.6 ± 203.1	1327.2 ± 166.5	1853.0 ± 140.2
% 2 - 3 Ring	63.8 ± 9.8	69.7 ± 1.8	66.2 ± 3.9	55.6 ± 3.7	46.7 ± 15.5
% 4 Ring	30.9 ± 6.8	26.5 ± 2.5	30.4 ± 4.1	32.6 ± 4.0	35.2 ± 2.4
% 5 - 6 Ring	5.4 ± 3.0	3.8 ± 0.7	3.3 ± 0.6	11.7 ± 7.0	18.0 ± 13.7

Table 6.1 - Summary of key benefits/drawbacks relating to emissions from pyrolysis-combustion process. Outcomes during operation for optimized biochar and energy production are presented.

	Optimized Biochar Production (T_v = 400 °C)	**Optimized Energy Production (T_v = 800 °C)**
Benefits	• Reduced PM-bound PAH toxicity. • Reduced char-bound PAH toxicity. • Reduced sulfurous gaseous pollutant yields. • Reduced nitrogeneous gaseous pollutant yields.	• Reduced PM yields
Drawbacks	• Increased PM yields	• Increased PM-bound PAH toxicity. • Increased char-bound PAH toxicity. • Increased sulfurous gaseous pollutant yields. • Increased nitrogeneous gaseous pollutant yields.

Figures

Fig. 1.1 - Illustration of the change in colour associated with the application of biochar to soils (Lehmann, 2007).

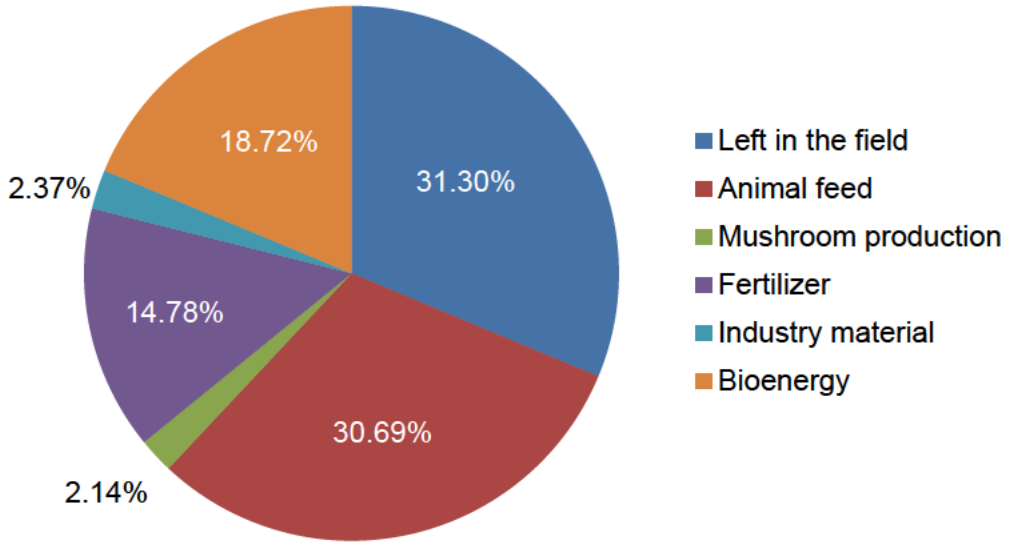

Fig. 1.2 - Utilization rates of agricultural by-products in China in 2012 (Jiang et al., 2012).

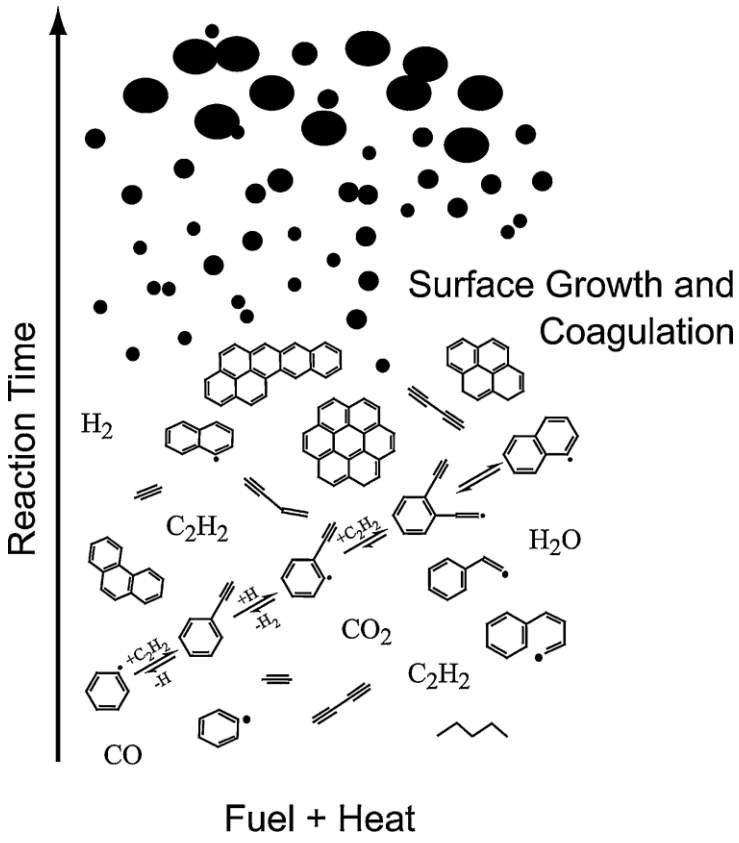

Fig. 1.3 - Schematic showing the formation of PAHs and soot particles during combustion (Lima et al., 2005).

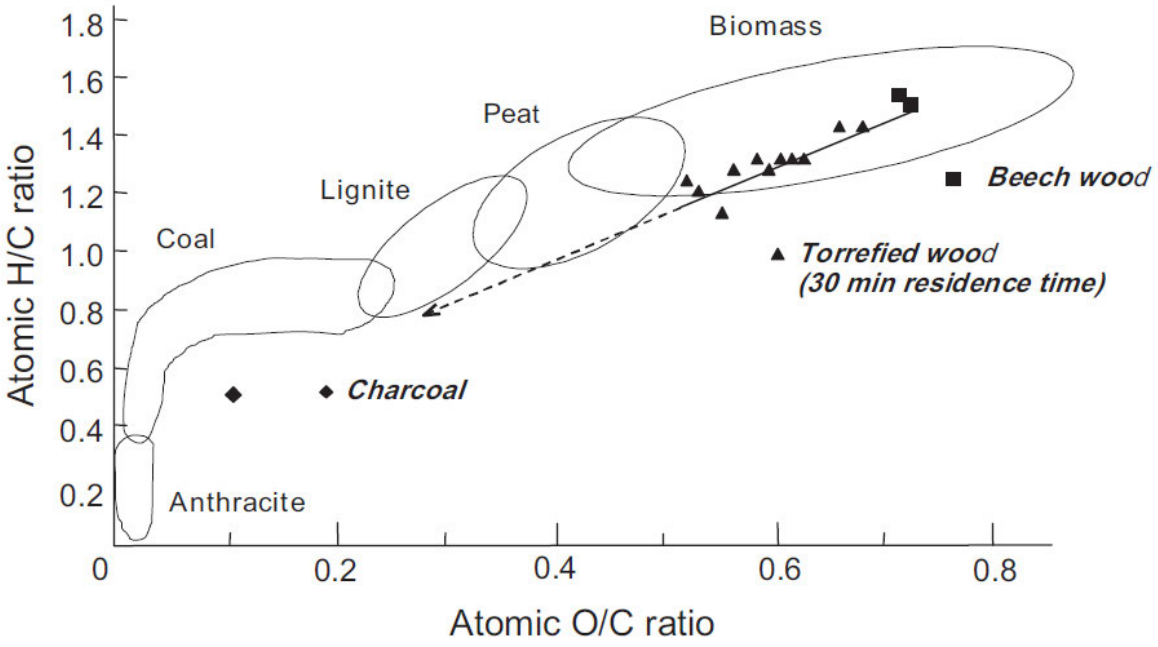

Fig. 1.4 - Van Krevelen diagram for untreated wood and torrefied wood in comparison to other common fuels (van der Stelt et al., 2011).

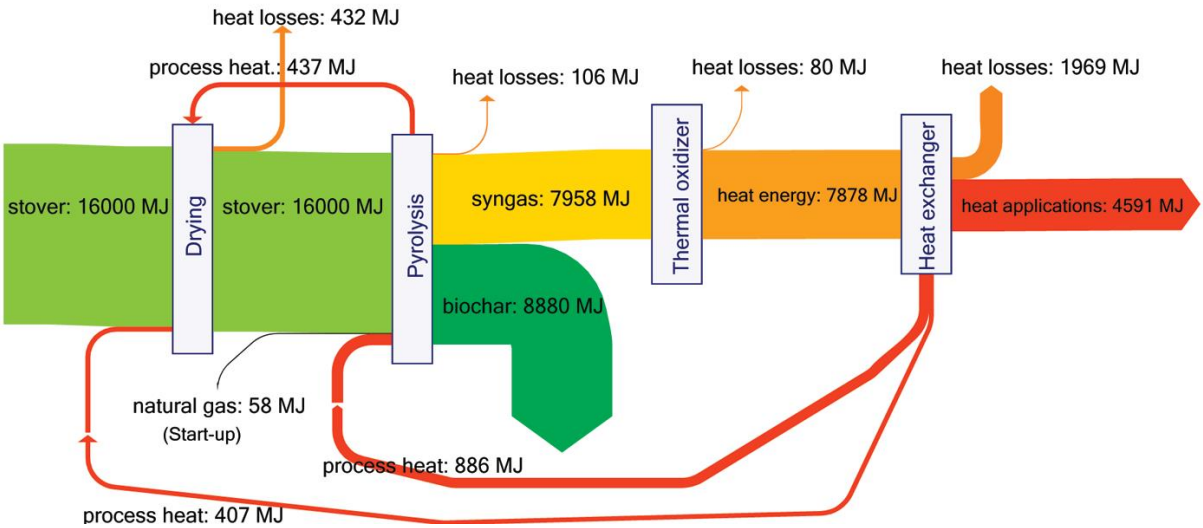

Fig. 1.5 - Energy flows (MJ/te dry feedstock) of a simulated pyrolysis-combustion system for biochar and bioenergy production using late stover (Roberts et al., 2010).

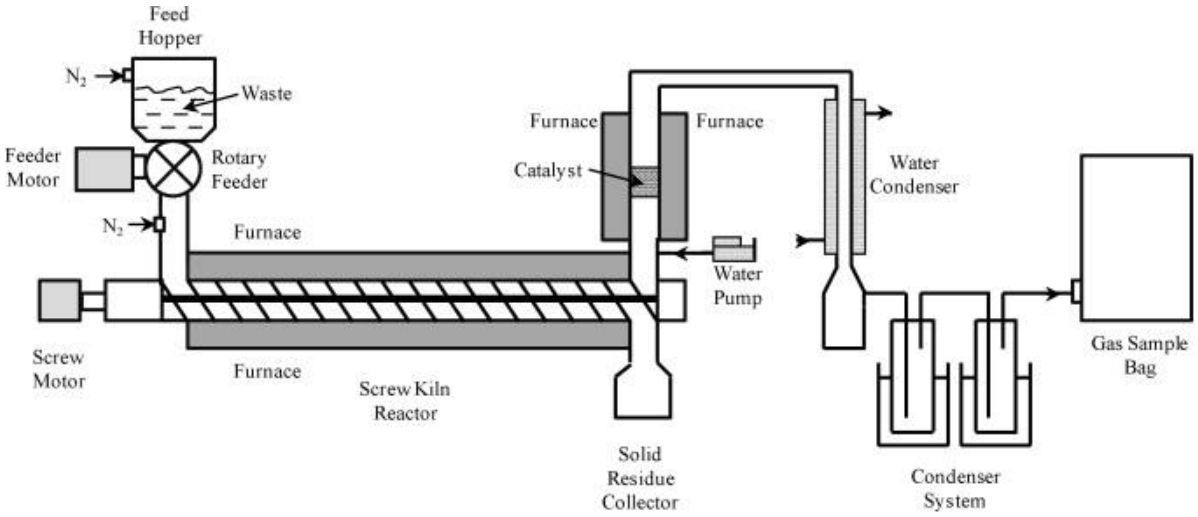

Fig. 1.6 - Schematic diagram of the continuous screw-kiln pyrolysis system (Efika et al., 2012).

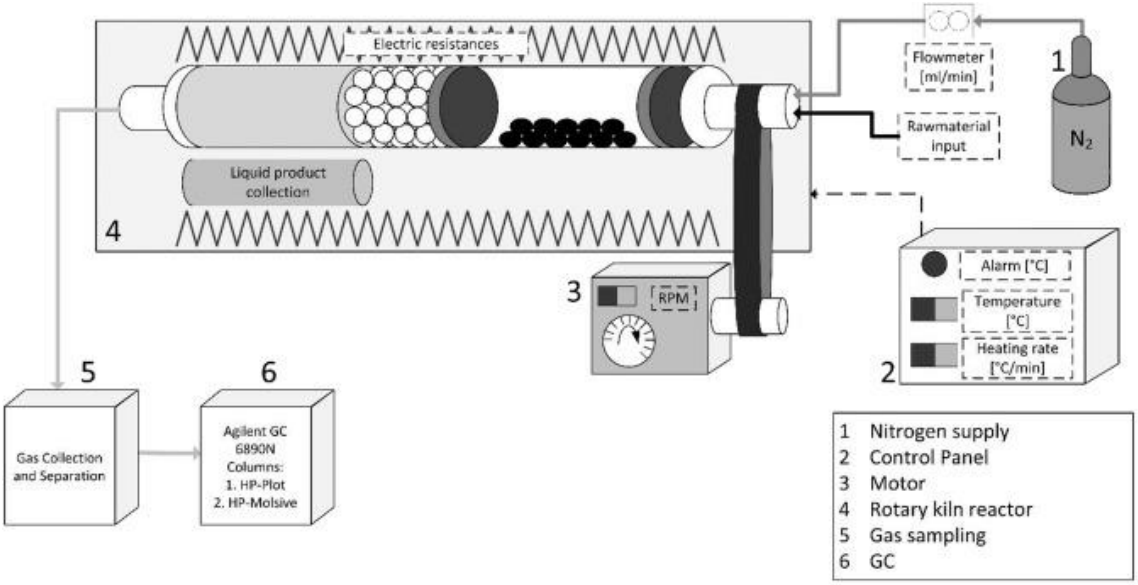

Fig. 1.7 - Rotary kiln (quartz) reactor for the production of char by waste tyre pyrolysis (Antoniou and Zabaniotou, 2015).

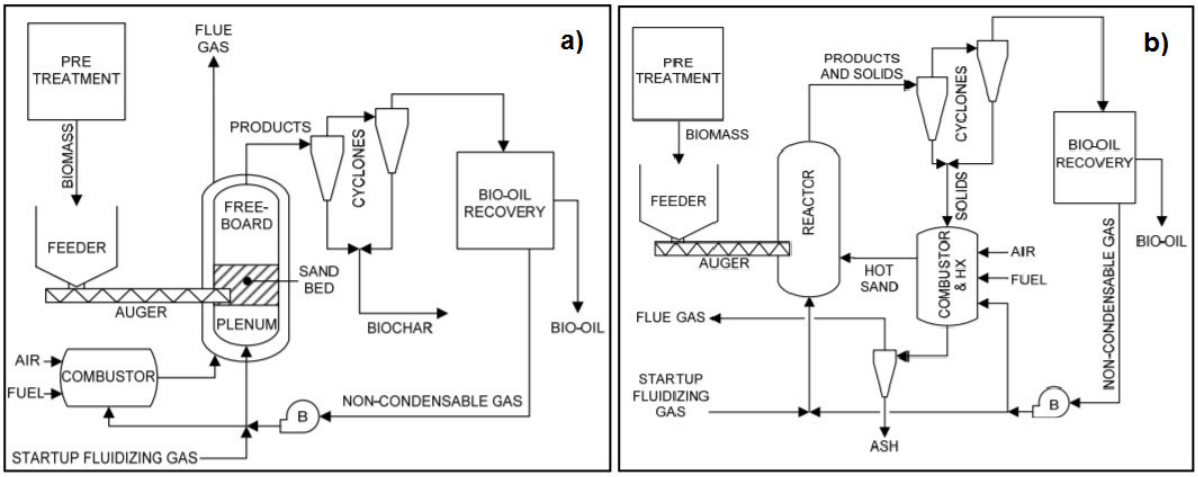

Fig. 1.8 - a) Bubbling fluidized bed reactor schematic and b) Circulating fluidized bed reactor schematic (Brown, 2009).

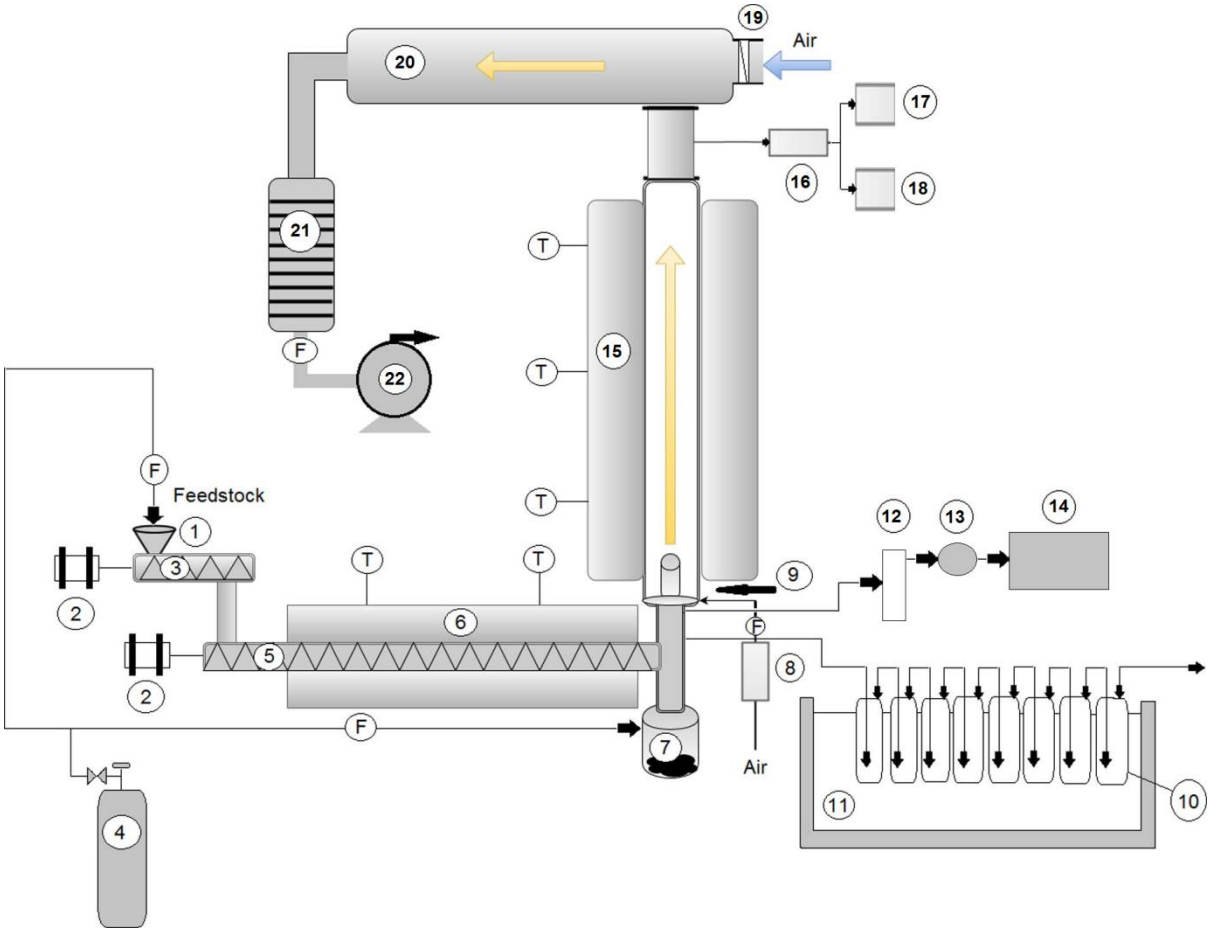

Fig. 2.1 - Schematic diagram of the pyrolysis-combustion and sampling systems (components: 1. Hopper; 2. Motor; 3. Feeding screw; 4. Nitrogen cylinder; 5. Main screw reactor; 6. Electric heaters; 7. Char collection vessel; 8. In-line HEPA filter for combustion air; 9. Burner; 10; Bio-oil collection vessel; 11. Ice/water mixture; 12. Gas collection bag; 13. Coalescing filter; 14. Gas chromatography/thermal conductivity detector (GC-TCD); 15. Combustion furnace; 16. Bio-oil/particulate filter; 17. CO_2 analyser; 18. CO/O_2 analyser; 19. HEPA filter; 20. Air dilution tunnel; 21. Cascade impactor; 22. Vacuum pump; T. temperature control; F. flowmeter).

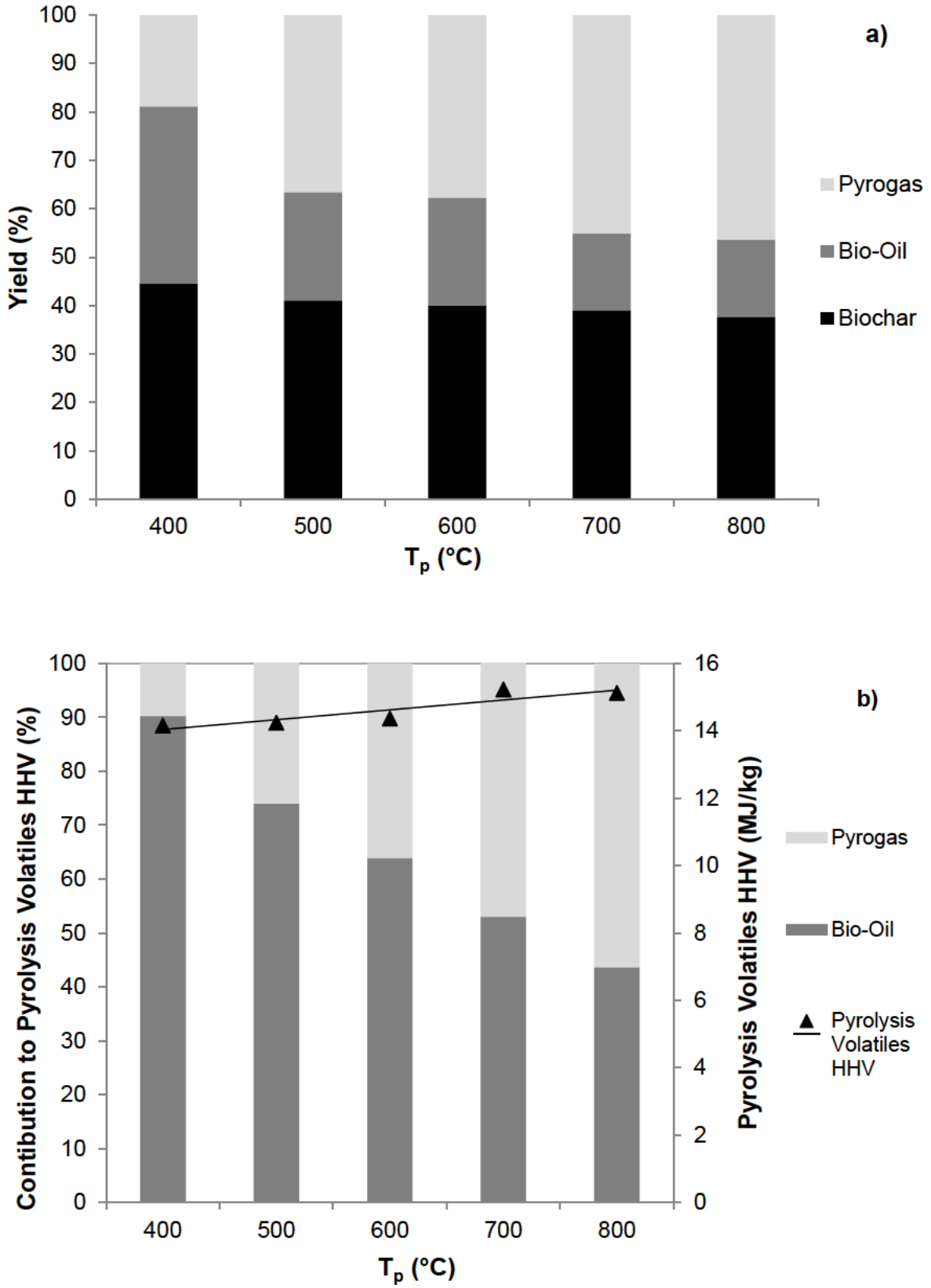

Fig. 2.2 - Relationship between the pyrolysis temperature and a) the yield of pyrolysis products, b) total raw pyrolysis volatiles HHV.

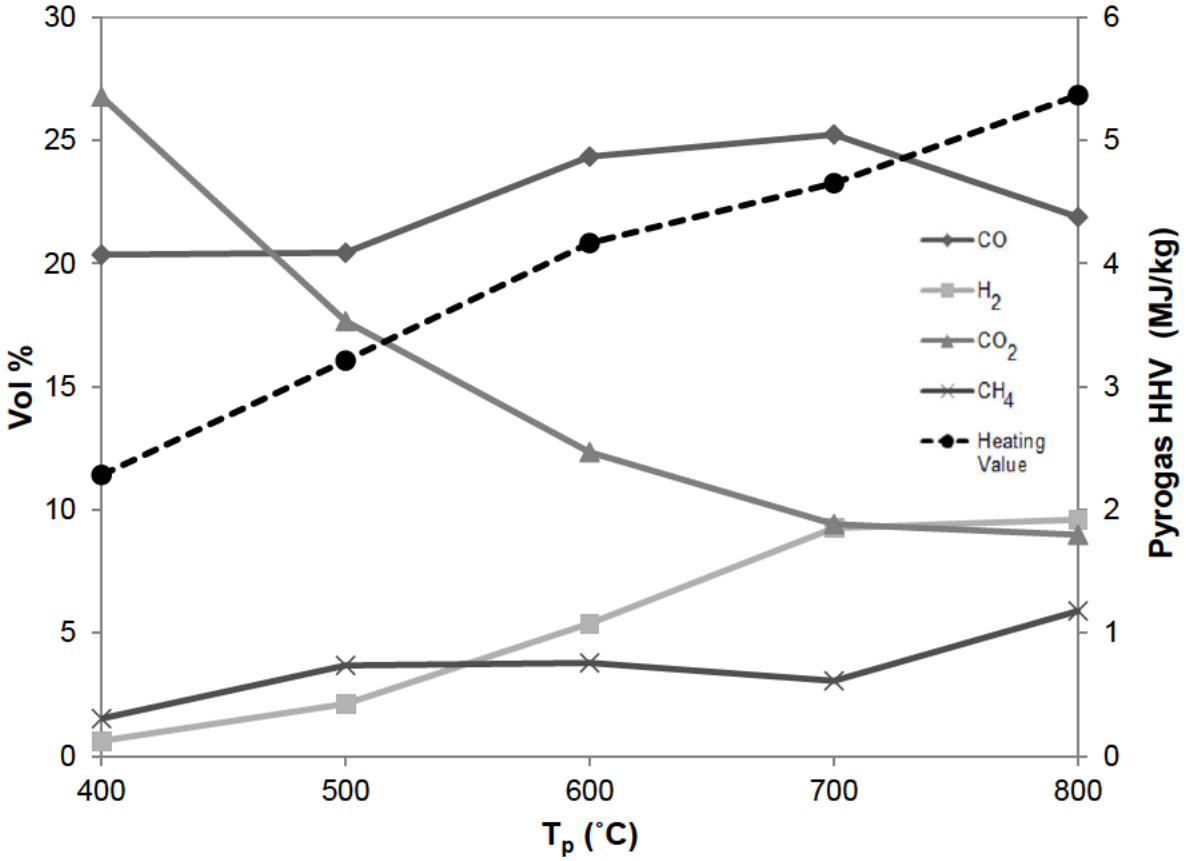

Fig. 2.3 - Composition of the non-condensable pyrogas fraction of the raw pyrolysis volatiles between 400 and 800 °C pyrolysis temperatures (corrected to 50 vol % nitrogen).

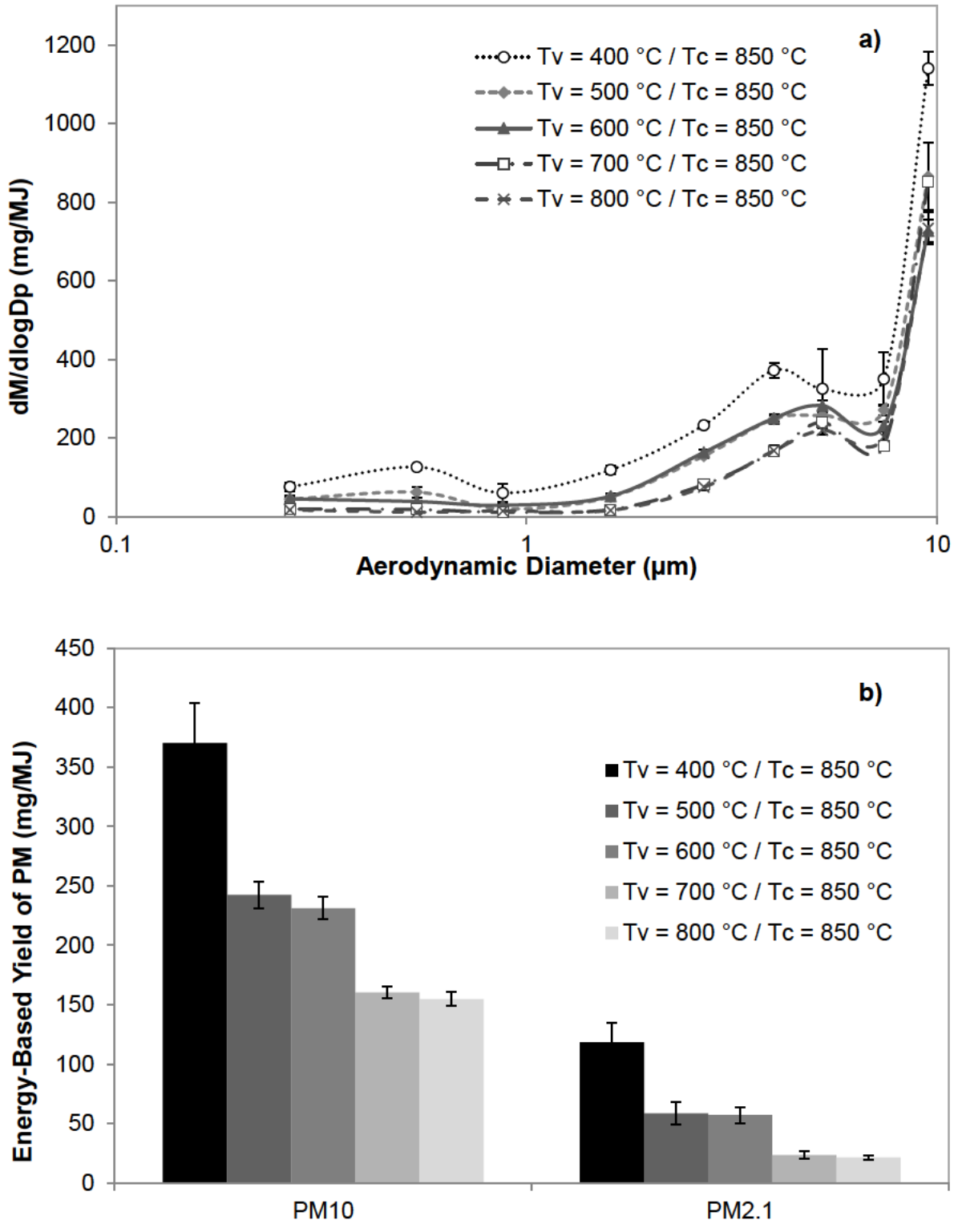

Fig 2.4 - a) Normalized mass-based particle-size distribution of PM from combustion of the raw pyrolysis volatiles and b) energy-based yields of PM_{10} and $PM_{2.1}$ from combustion of the raw pyrolysis volatiles. Raw pyrolysis volatiles were produced at various volatile production temperatures (T_V = 400 – 800 °C) and combusted at 850 °C.

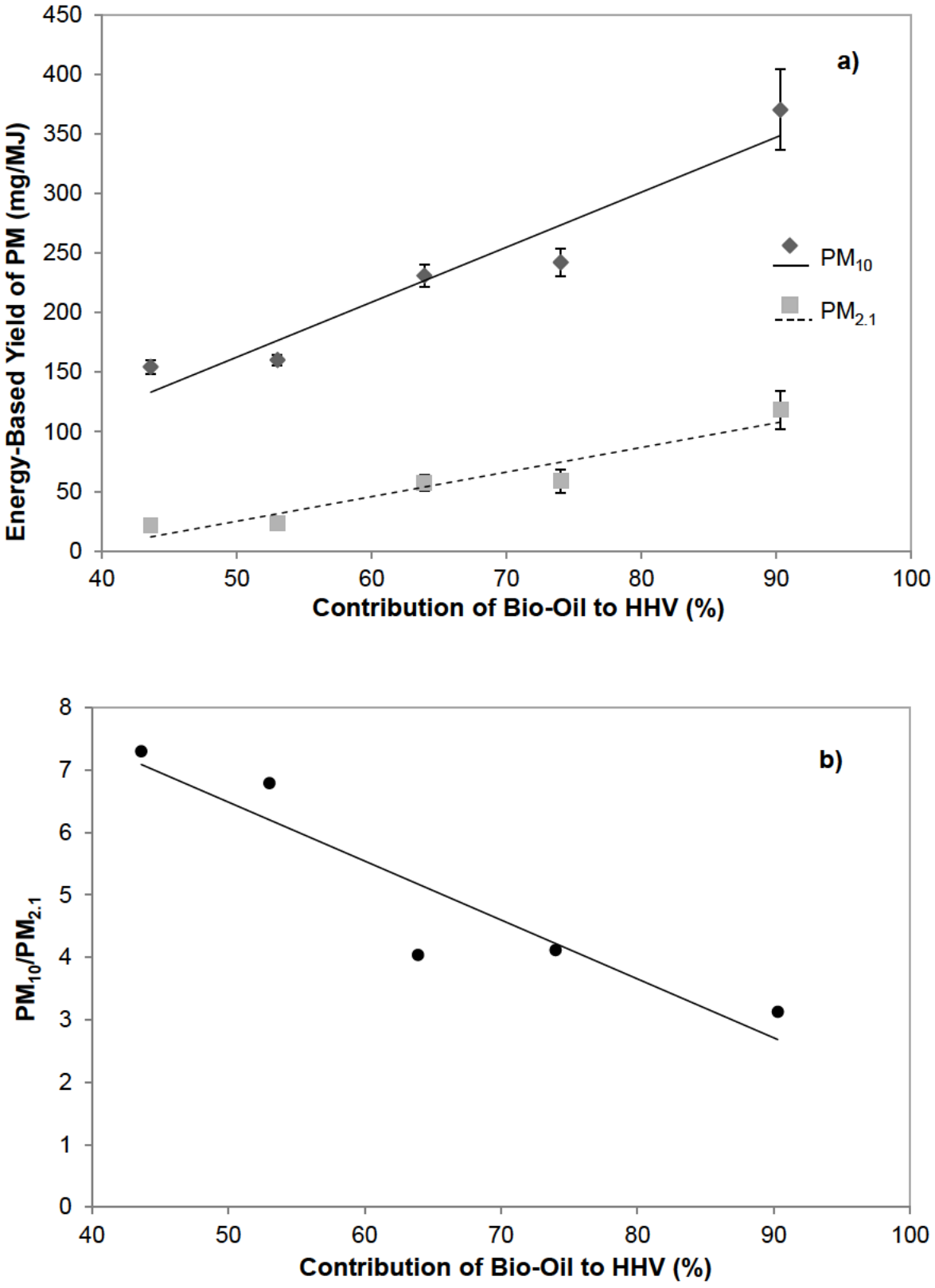

Fig. 2.5 – a) Relationship between the contribution (%) of bio-oil to the overall pyrolysis volatiles HHV and the PM_{10} and $PM_{2.1}$ emissions b) relationship between $PM_{10}/PM_{2.1}$ ratio of collected PM in the cascade impactor and the contribution of bio-oil the overall pyrolysis volatiles HHV.

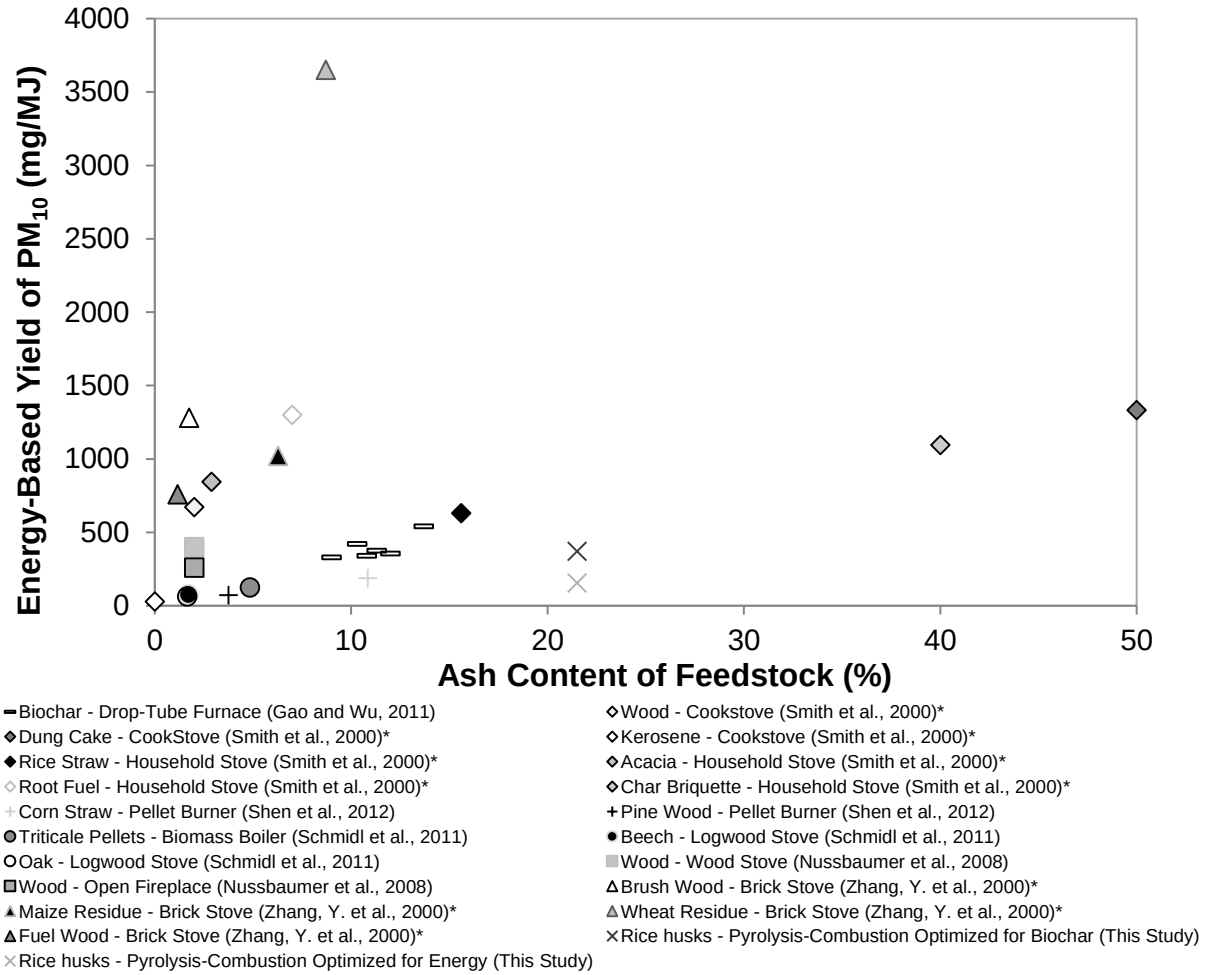

Fig. 2.6 - Relationship between ash content of feedstock and energy-based yield of PM_{10} (mg/MJ). The energy-based yields of PM_{10} for this process optimized for either biochar yield or energy generation are shown. *Refers to total suspended particles (TSP).

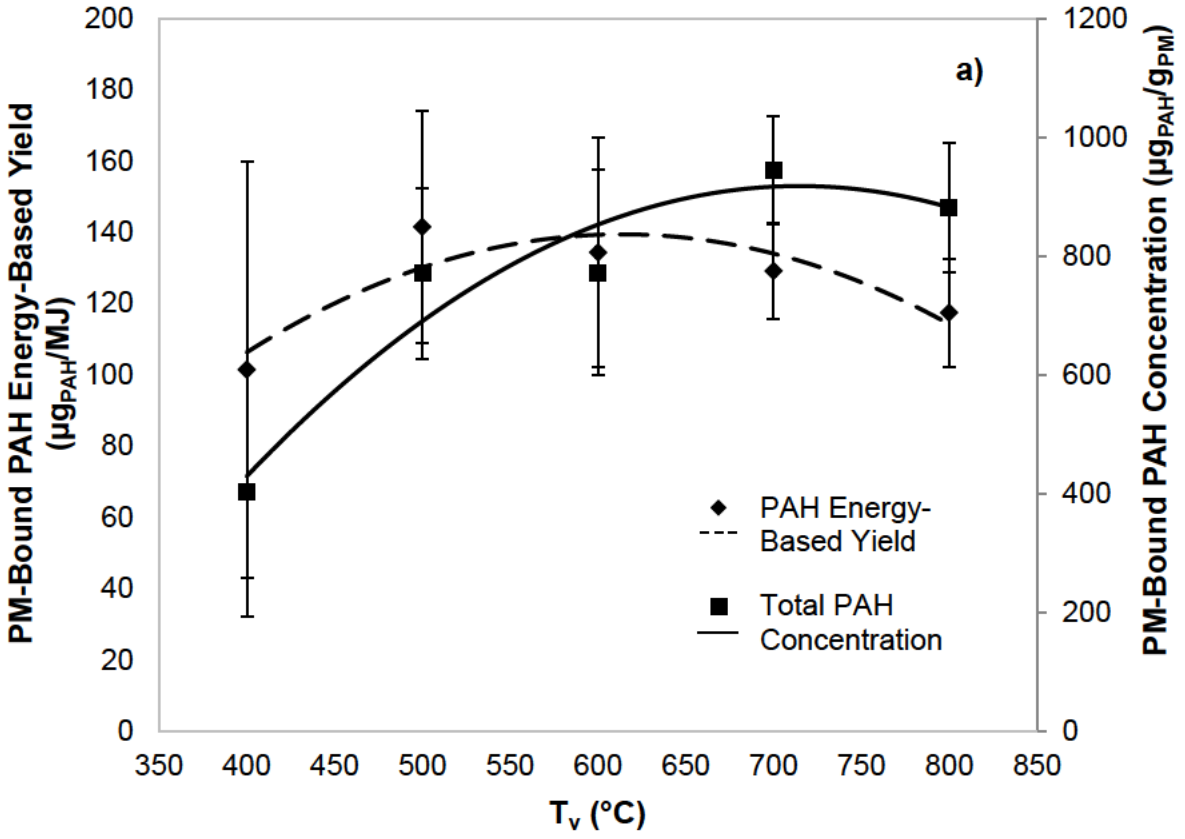
a)
PM-Bound PAH Energy-Based Yield (µg$_{PAH}$/MJ)
PM-Bound PAH Concentration (µg$_{PAH}$/g$_{PM}$)
T_v (°C)
PAH Energy-Based Yield
Total PAH Concentration
0
20
40
60
80
100
120
140
160
180
200
0
200
400
600
800
1000
1200
350
400
450
500
550
600
650
700
750
800
850

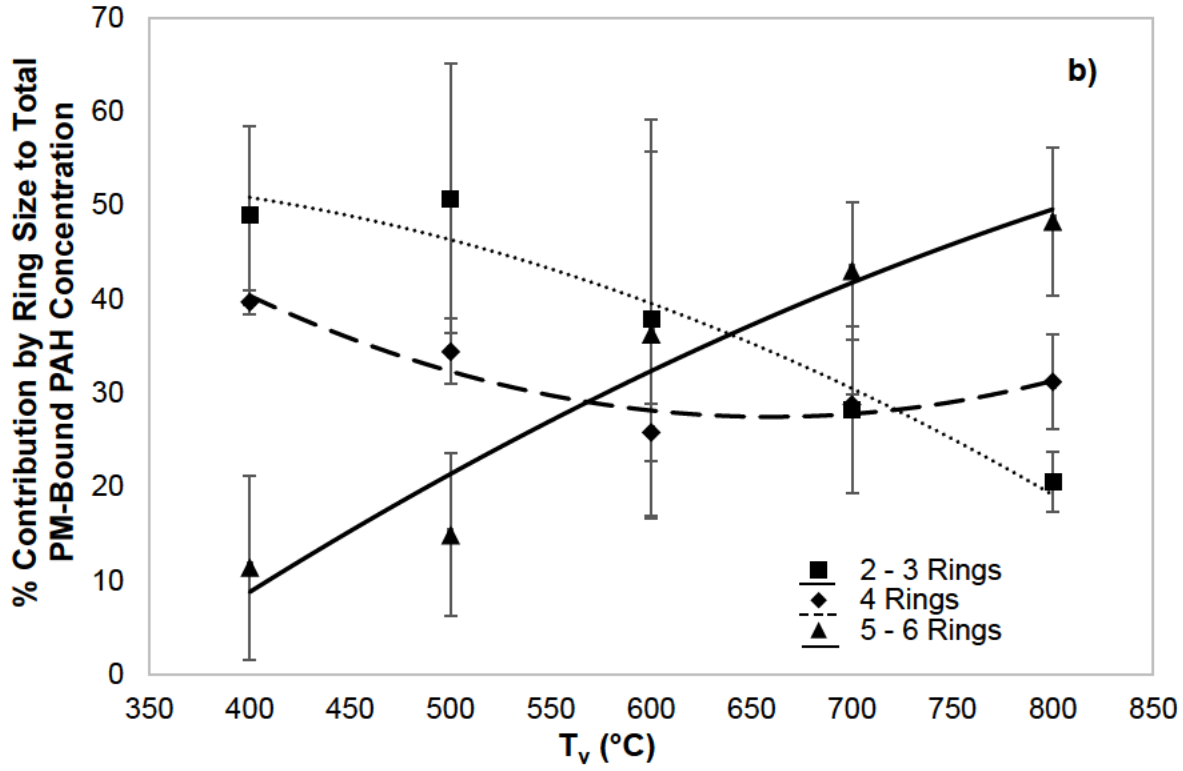

Fig. 3.1 - Influence of volatile production temperature (T_v) (400 – 800 °C) on a) PM-bound PAH energy-based yield ($\mu g_{PAH}/MJ$) and PM-bound PAH concentration ($\mu g_{PAH}/g_{PM}$), b) Contribution of 2 – 3, 4, and 5 – 6 ring PAHs to the total PM-bound PAH concentration. Combustion of the raw pyrolysis volatiles was carried out at 850 °C.

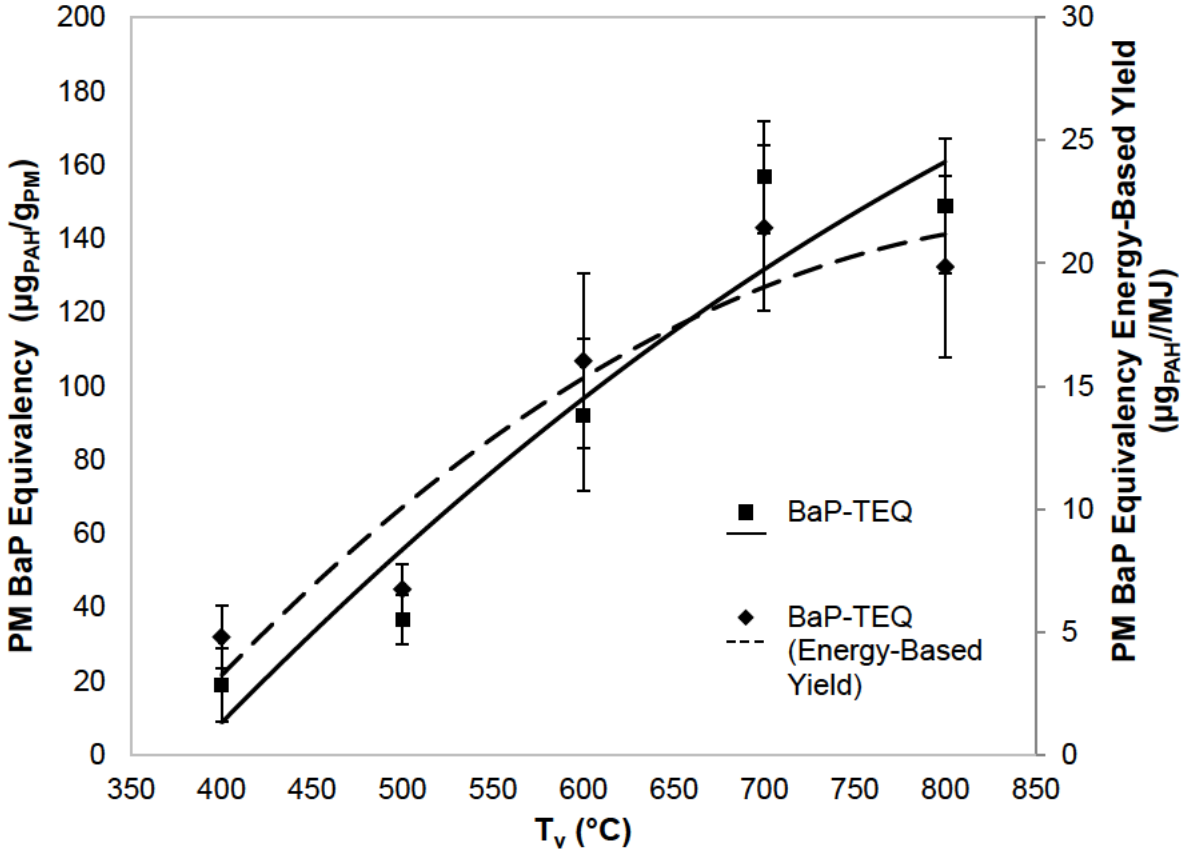

Fig. 3.2 - Influence of volatile production temperature (T_v) (400 – 800 °C) on the PM BaP equivalency (µg$_{PAH}$/g$_{PM}$) and PM BaP equivalent energy-based yield (µg$_{PAH}$/MJ). Combustion of the raw pyrolysis volatiles was carried out at 850 °C.

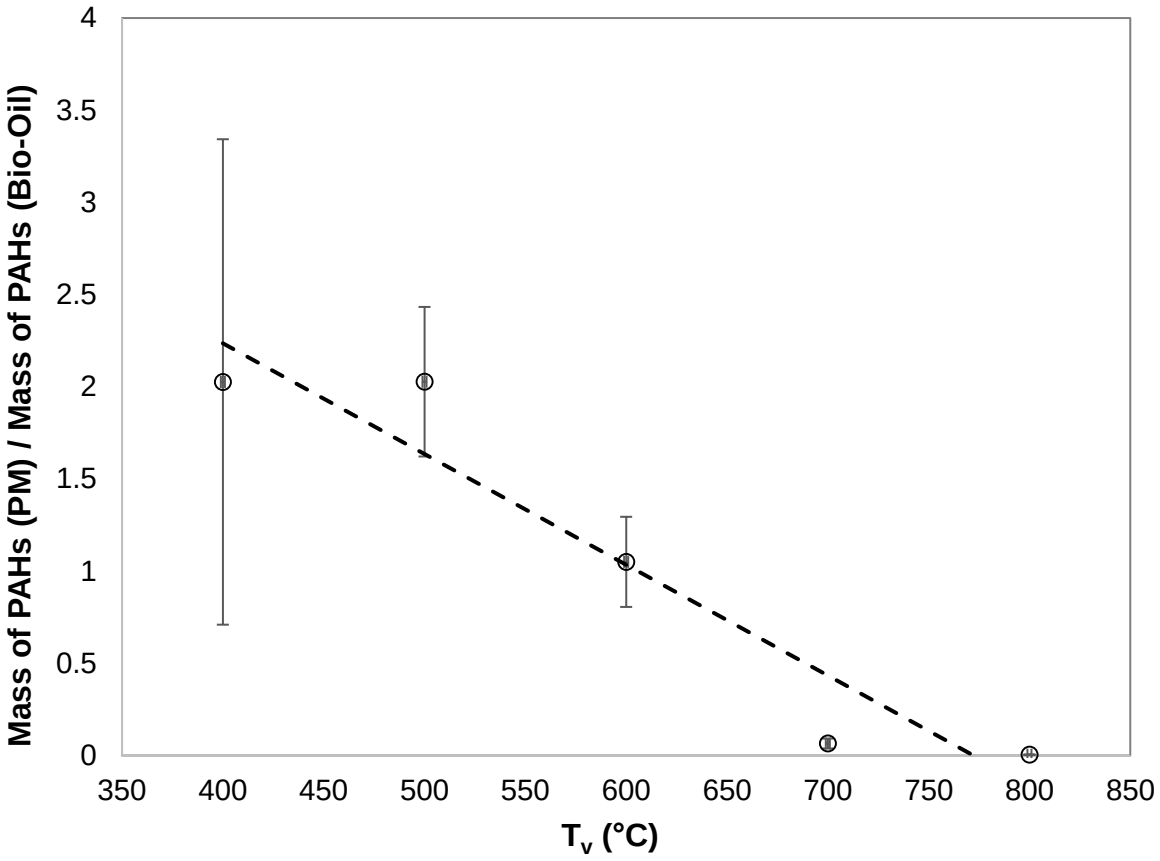

Fig. 3.3 - Influence of volatile production temperature (T_V) (400 – 800 °C) on the ratio of the mass of PM-bound PAHs to the mass of PAHs contained within the bio-oil. Combustion of the raw pyrolysis volatiles was carried out at 850 °C.

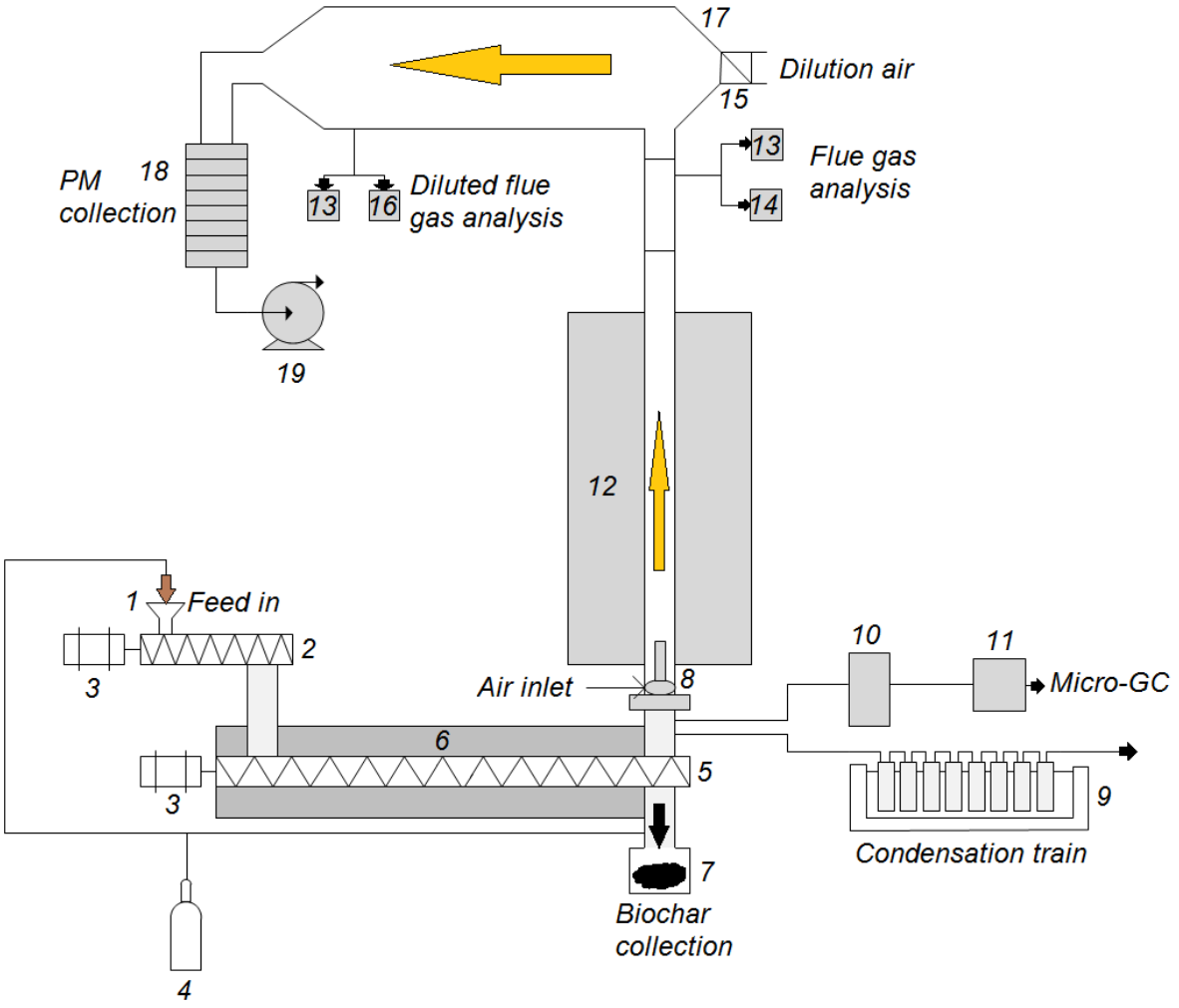

Fig. 4.1 - Schematic diagram of the pyrolysis-combustion and sampling systems (components: 1. Hopper; 2. Feeding screw; 3. Motor; 4. Nitrogen cylinder; 5. Main screw reactor; 6. Electric heaters; 7. Biochar collection vessel; 8. Burner; 9; Condensation train; 10. Gas collection bag; 11. Gas chromatograph/thermal conductivity detector (GC-TCD) with coalescing filter; 12. Combustion furnace; 13. CO_2 analyser; 14. CO/O_2 analyser; 15. HEPA filter; 16. H_2S, SO_2, NO, NO_2 analyser; 17. Air dilution tunnel; 18. Cascade impactor; 19. Vacuum pump).

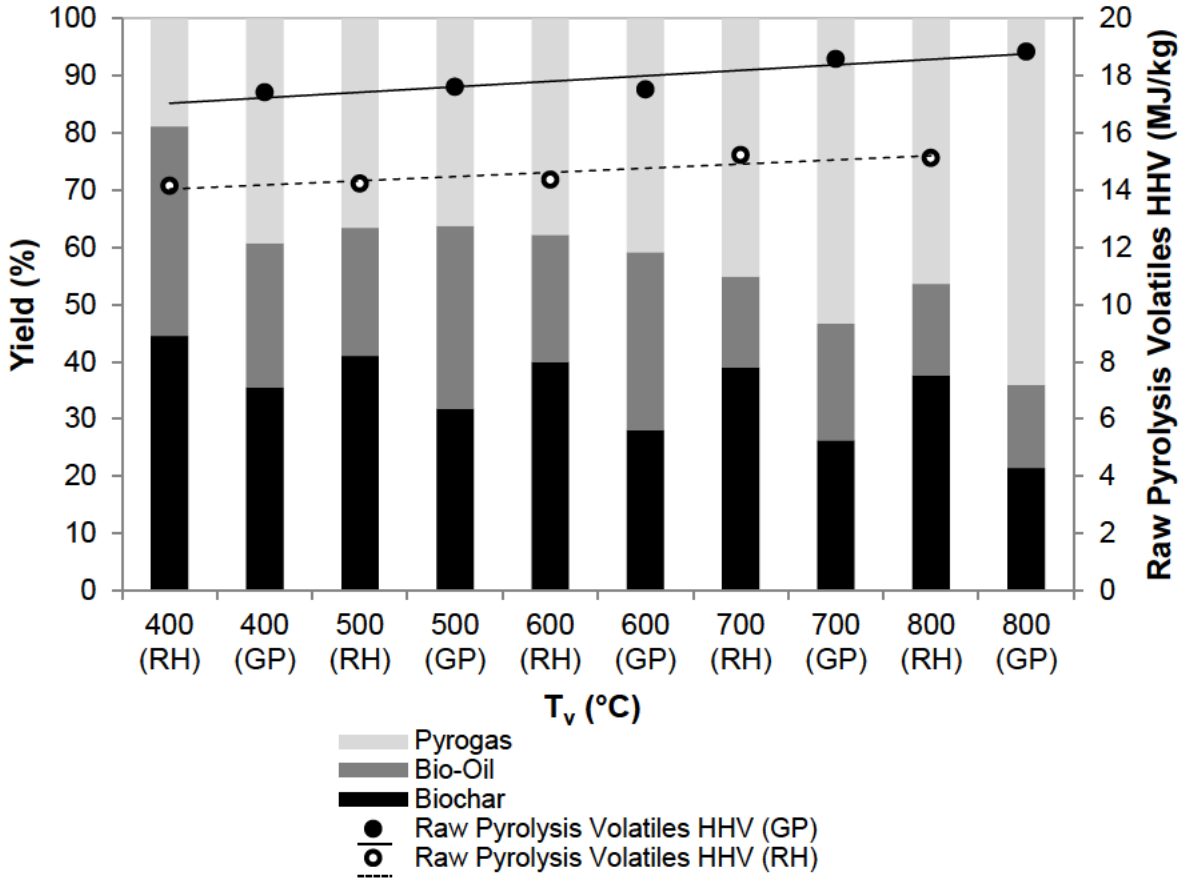

Fig. 4.2 - Yields of pyrolysis products and HHV of the raw pyrolysis volatiles for the rice husk (RH) and grape pruning (GP) at various volatile production temperatures (T_V) (400 – 800 °C). The data presented for rice husk is adapted from Chapter 2.

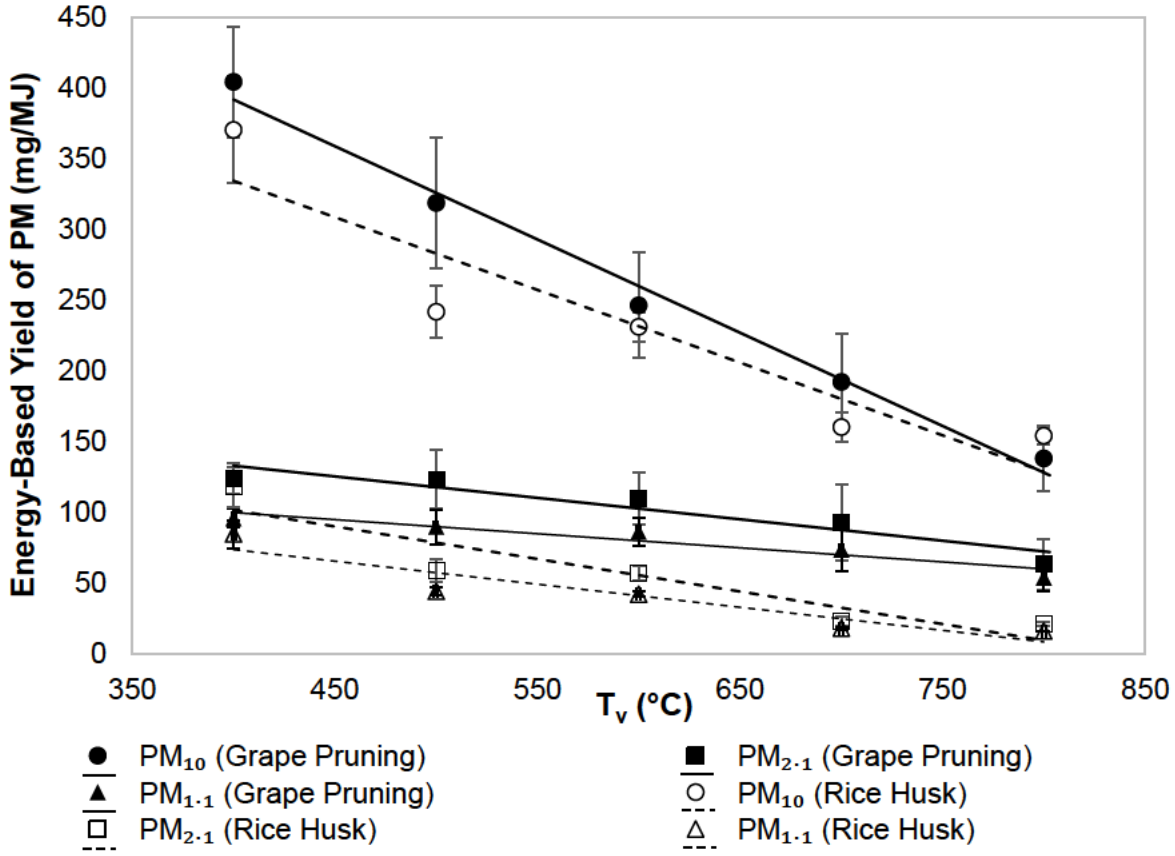

Fig. 4.3 - Energy-based yields of PM_{10}, $PM_{2.1}$, and $PM_{1.1}$ from combustion at 850 °C of the raw pyrolysis volatiles produced at various temperatures (400 – 800 °C) from the grape pruning and rice husk. The data presented for rice husk is adapted from Chapter 2.

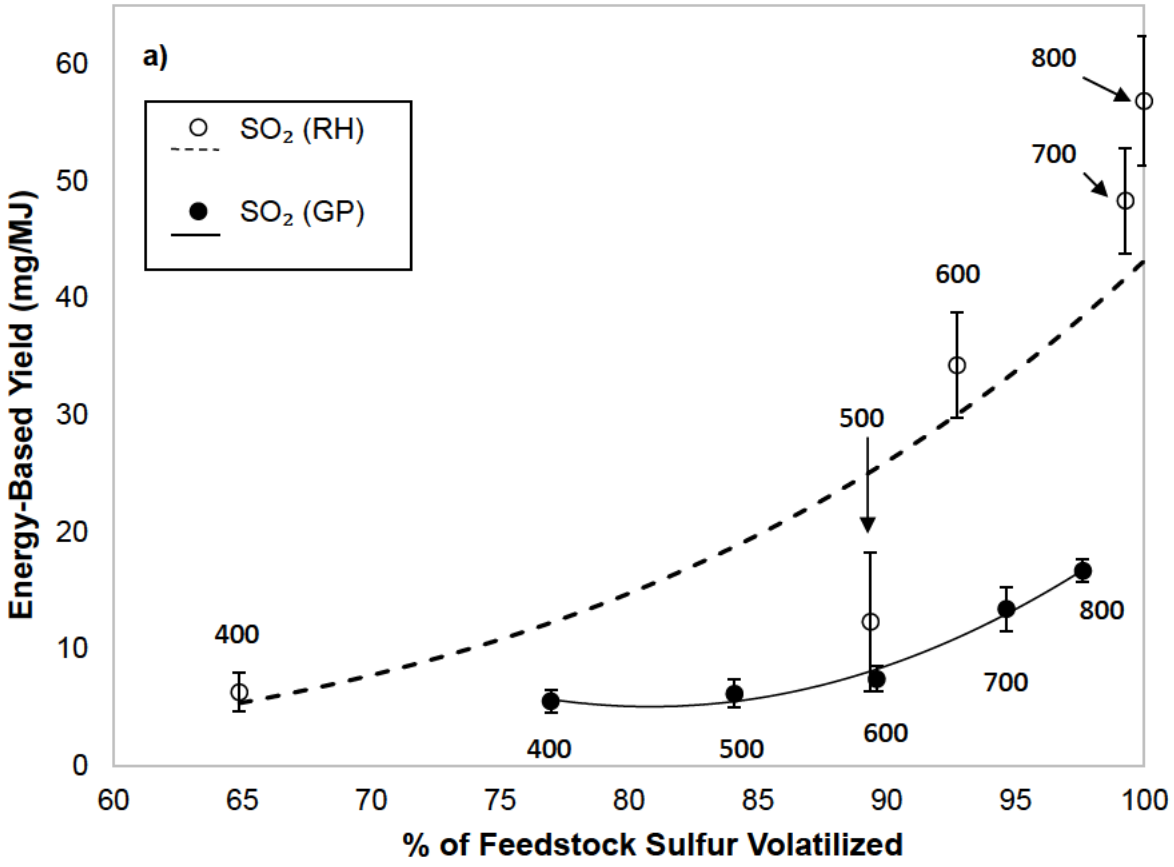
a)
SO2 (RH)
SO2 (GP)
Energy-Based Yield (mg/MJ)
% of Feedstock Sulfur Volatilized
0
10
20
30
40
50
60
60
65
70
75
80
85
90
95
100
400
500
600
700
800
400
500
600
700
800

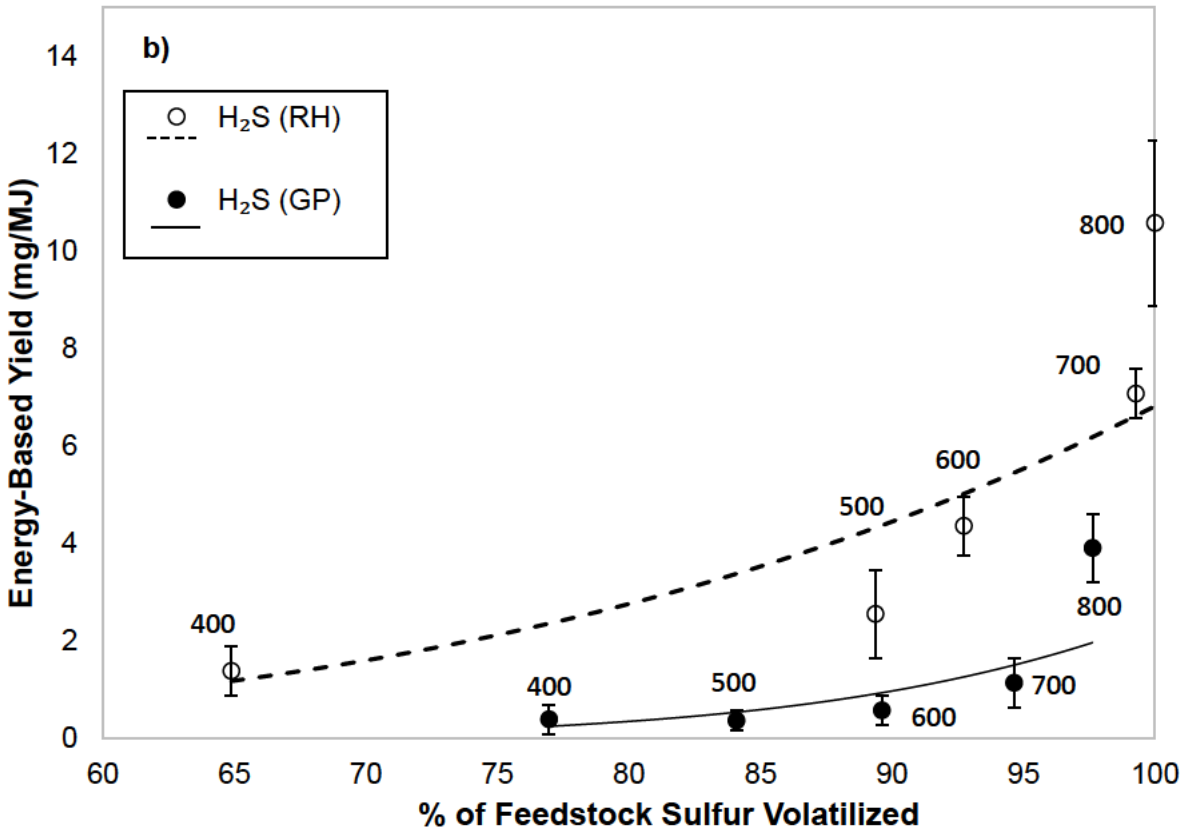

Fig. 4.4 - Energy-based yields of a) SO_2 and b) H_2S with differing degrees of fuel-bound sulfur volatilization between 400 – 800 °C utilizing grape pruning (GP) and rice husk (RH). The corresponding volatile production temperature of each point is indicated (°C). Combustion of the raw pyrolysis volatiles was carried out at 850 °C.

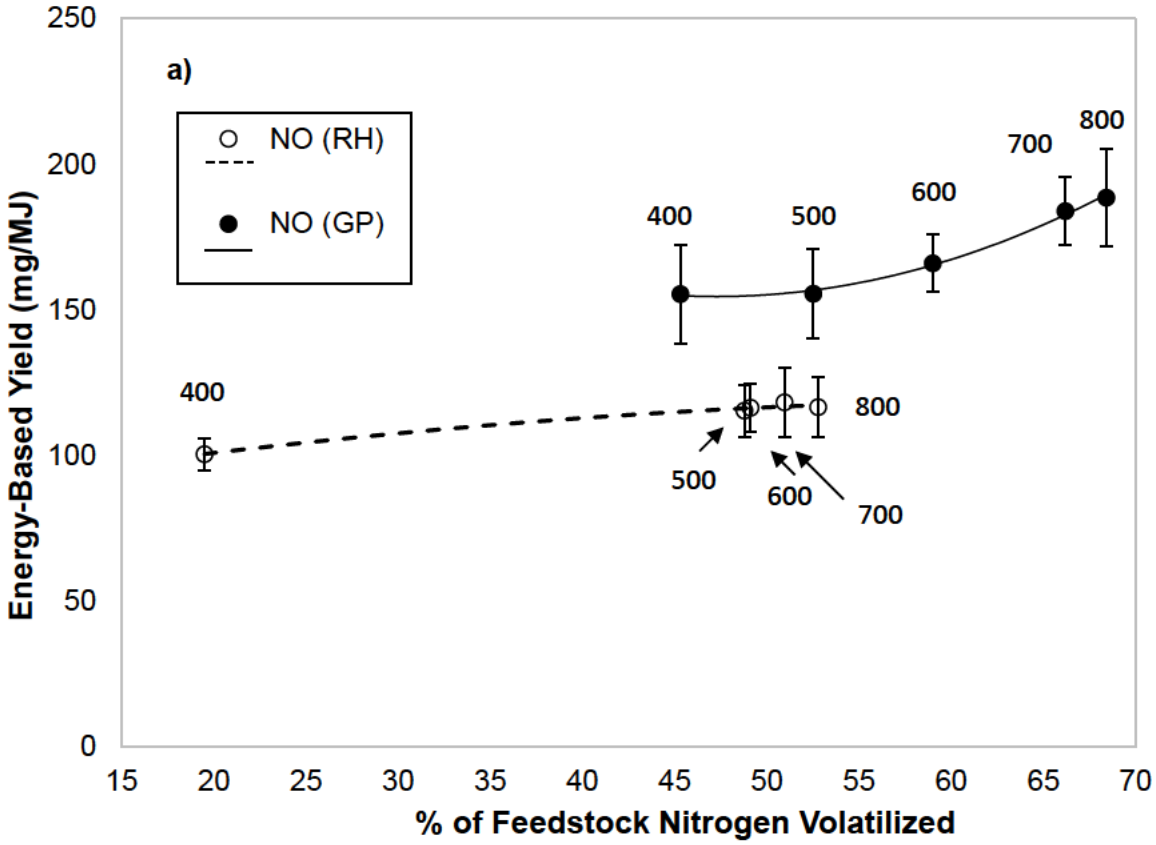
a)
NO (RH)
NO (GP)
400
500
600
700
800
400
800
500
600
700
Energy-Based Yield (mg/MJ)
% of Feedstock Nitrogen Volatilized
250
200
150
100
50
0
15
20
25
30
35
40
45
50
55
60
65
70

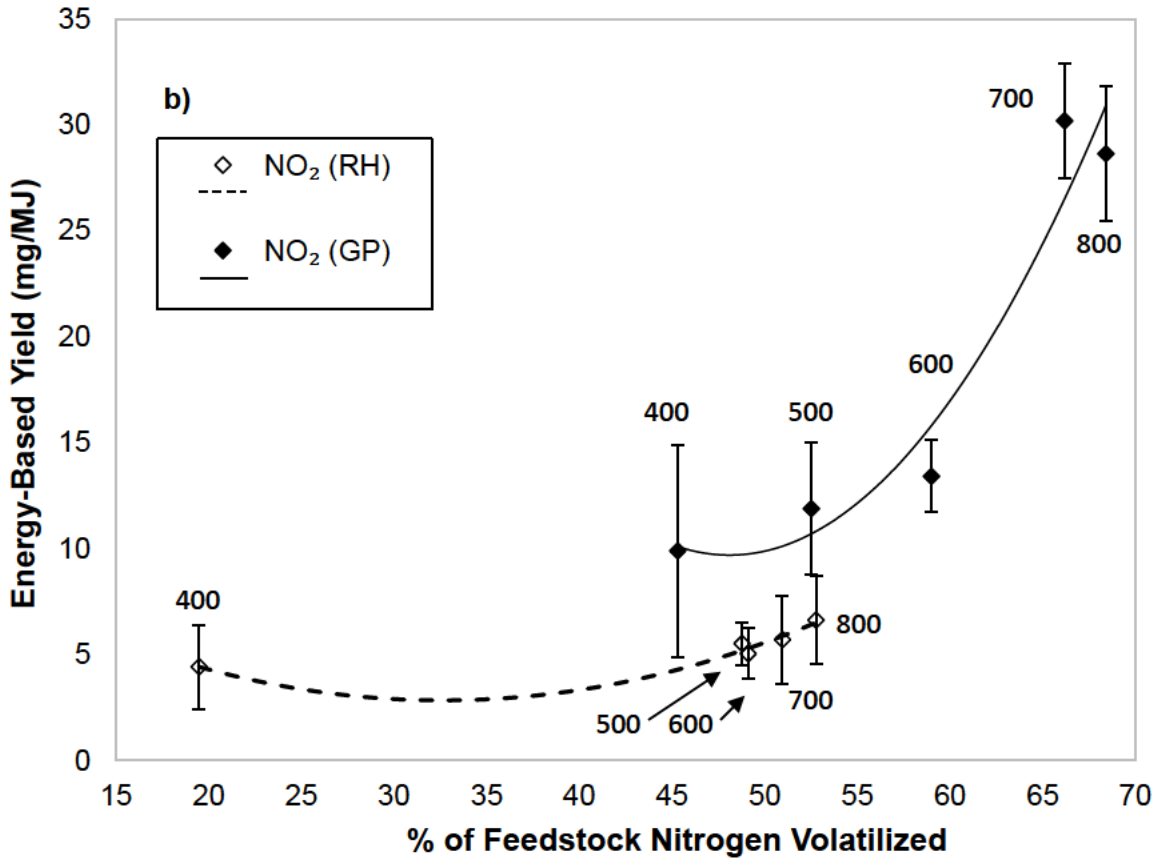

Fig. 4.5 - Energy-based yields of a) NO and b) NO_2 with differing degrees of fuel-bound nitrogen volatilization between 400 – 800 °C utilizing grape pruning (GP) and rice husk (RH). The corresponding volatile production temperature of each point is indicated (°C). Combustion of the raw pyrolysis volatiles was carried out at 850 °C.

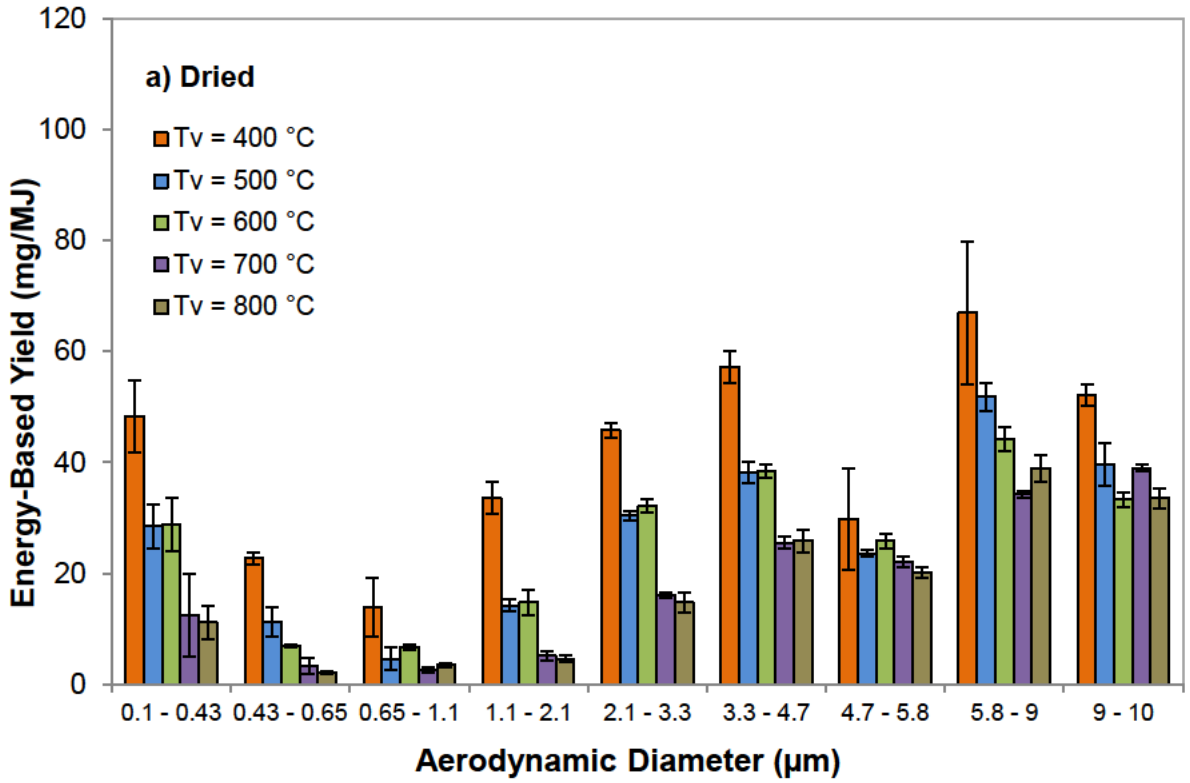
a) Dried
Tv = 400 °C
Tv = 500 °C
Tv = 600 °C
Tv = 700 °C
Tv = 800 °C
Energy-Based Yield (mg/MJ)
120
100
80
60
40
20
0
0.1 - 0.43
0.43 - 0.65
0.65 - 1.1
1.1 - 2.1
2.1 - 3.3
3.3 - 4.7
4.7 - 5.8
5.8 - 9
9 - 10
Aerodynamic Diameter (µm)

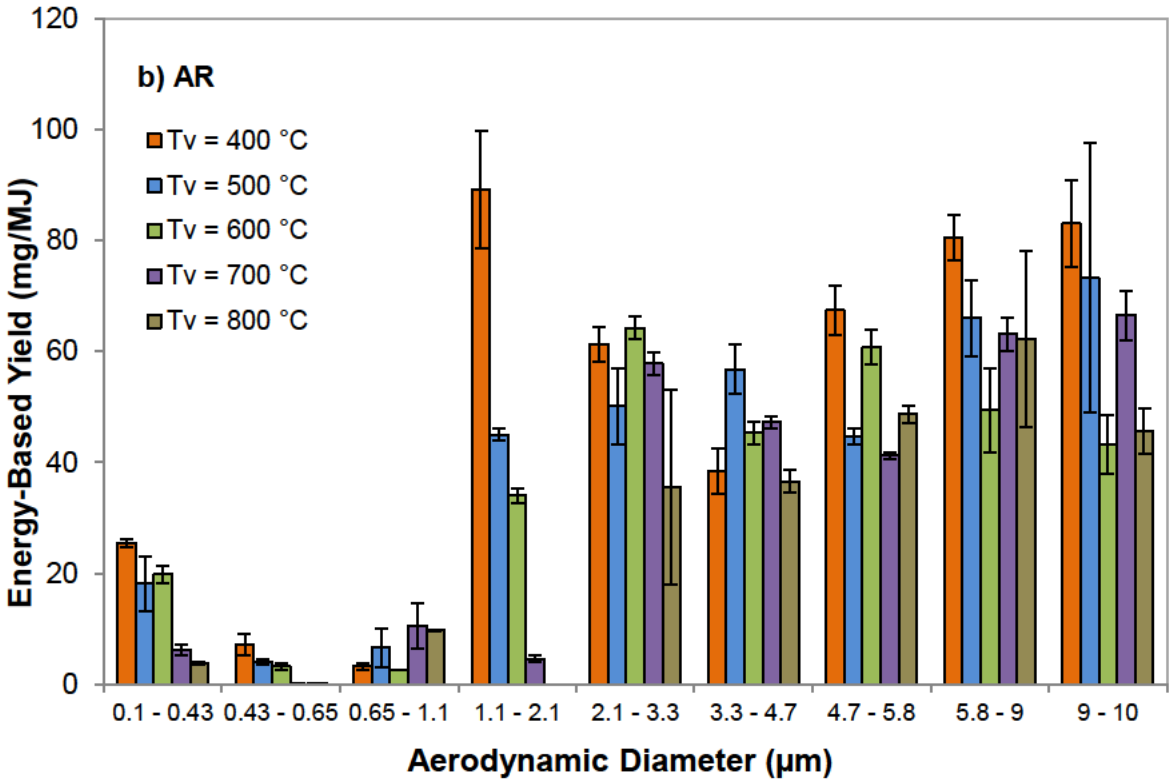

Fig. 5.1 - PM distribution from the combustion (T_c = 850 °C) of the raw pyrolysis volatiles produced at various volatile production temperatures (T_v = 400 – 800 °C) from a) dried rice husk and b) AR rice husk. The data for the dried rice husk is adapted from Chapter 2.

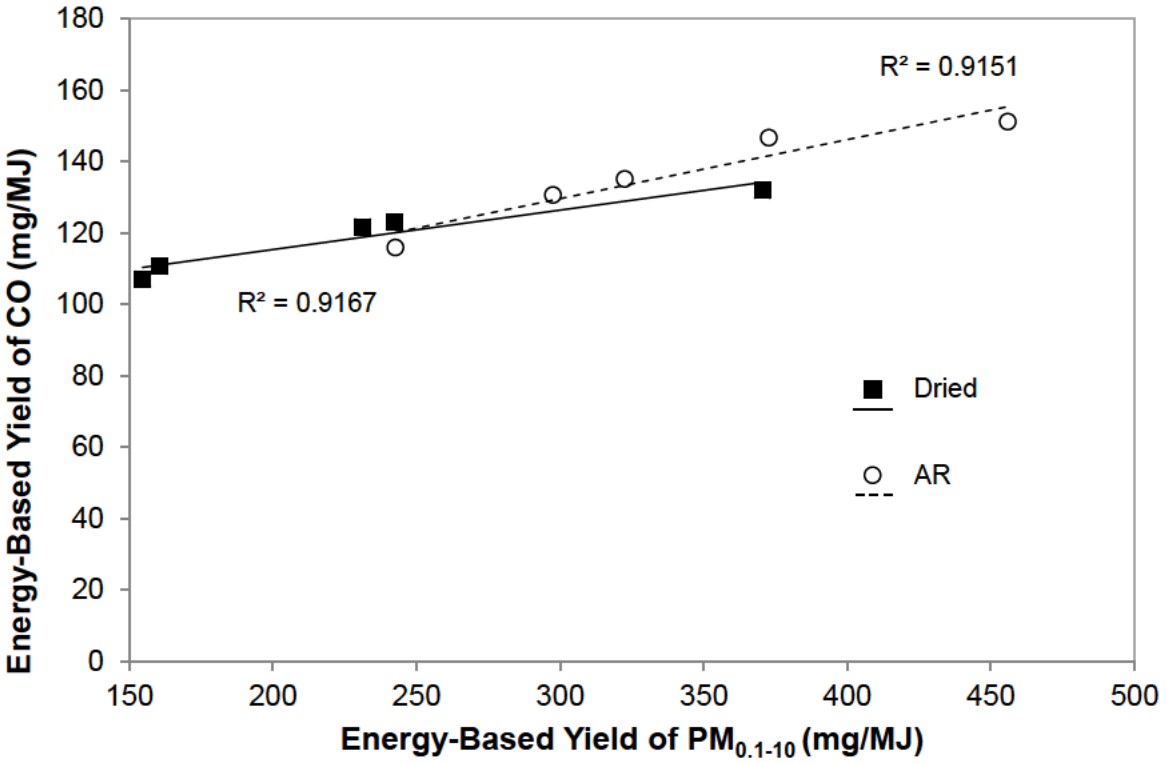

Fig. 5.2 - Relationship between energy-based yields of CO and PM_{10} during the combustion (T_c = 850 °C) of the raw pyrolysis volatiles using dried and AR rice husk.

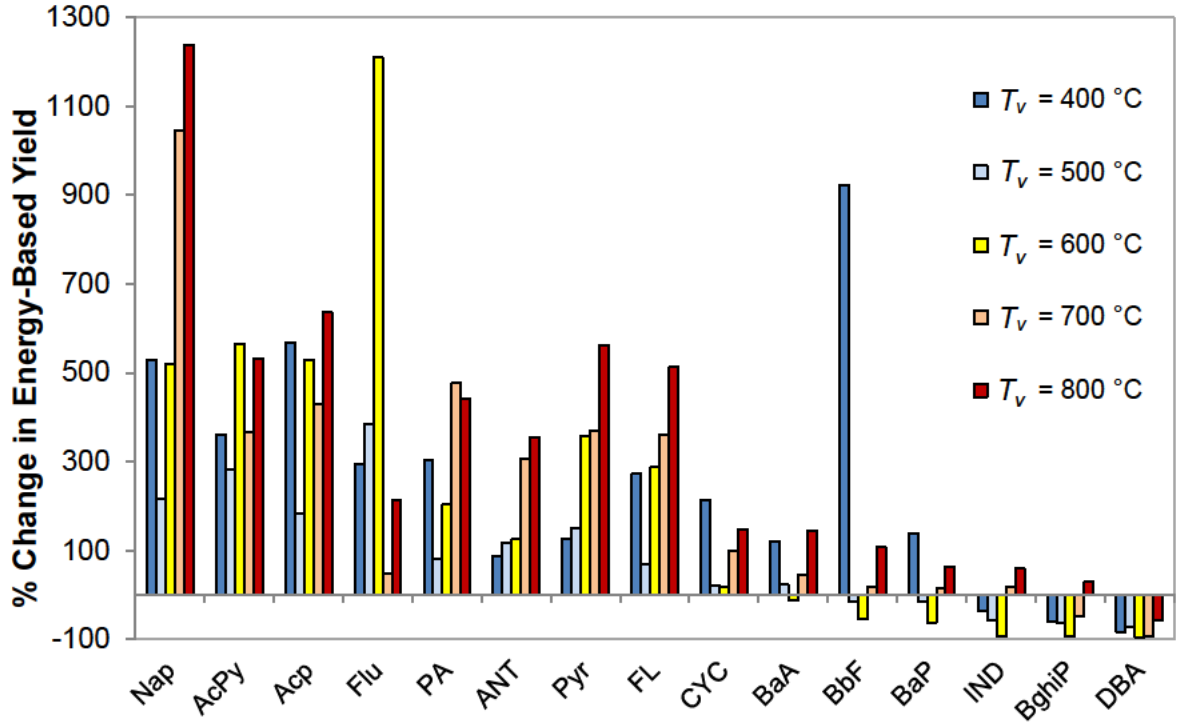

Fig. 5.3 - Percentage change in the energy-based yield of individual PM-bound PAH species between the AR and dried rice husk generated from combustion (T_c = 850 °C) of the raw pyrolysis volatiles produced at various volatile production temperatures (T_v = 400 – 800 °C). Positive and negative values indicate elevated and reduced PM-bound PAH concentrations for the AR husk respectively. NB: Nap = Napthalene, AcPy = Acenaphthylene, Acp = Acenaphthene, Flu = Fluorene, PA = Phenanthrene, ANT = Anthracene, Pyr = Pyrene, FL = Fluoranthene, CYC = Chrysene, BaA = Benzo(a)anthracene, BbF = Benzo(b)fluoranthene, BaP = Benzo(a)pyrene, IND = Indeno(1,2,3-cd)pyrene, BghiP = Benzo(g,h,i)perylene, DBA = Dibenz(a,h)anthracene.

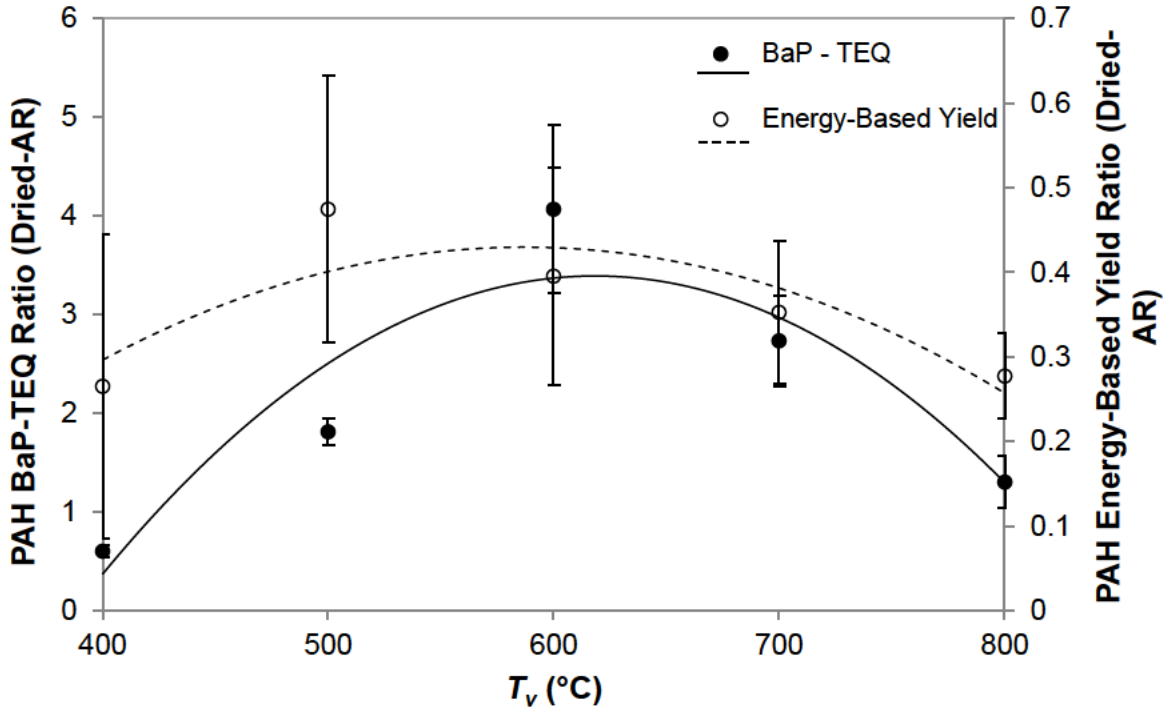

Fig. 5.4 - Ratio of energy-based yield and BaP – TEQ of PM-bound PAHs generated from combustion (T_c = 850 °C) of the raw pyrolysis volatiles produced from dried rice husk over AR rice husk ($dried_{husk}$-AR_{husk}) at various volatile production temperatures (T_v = 400 – 800 °C).

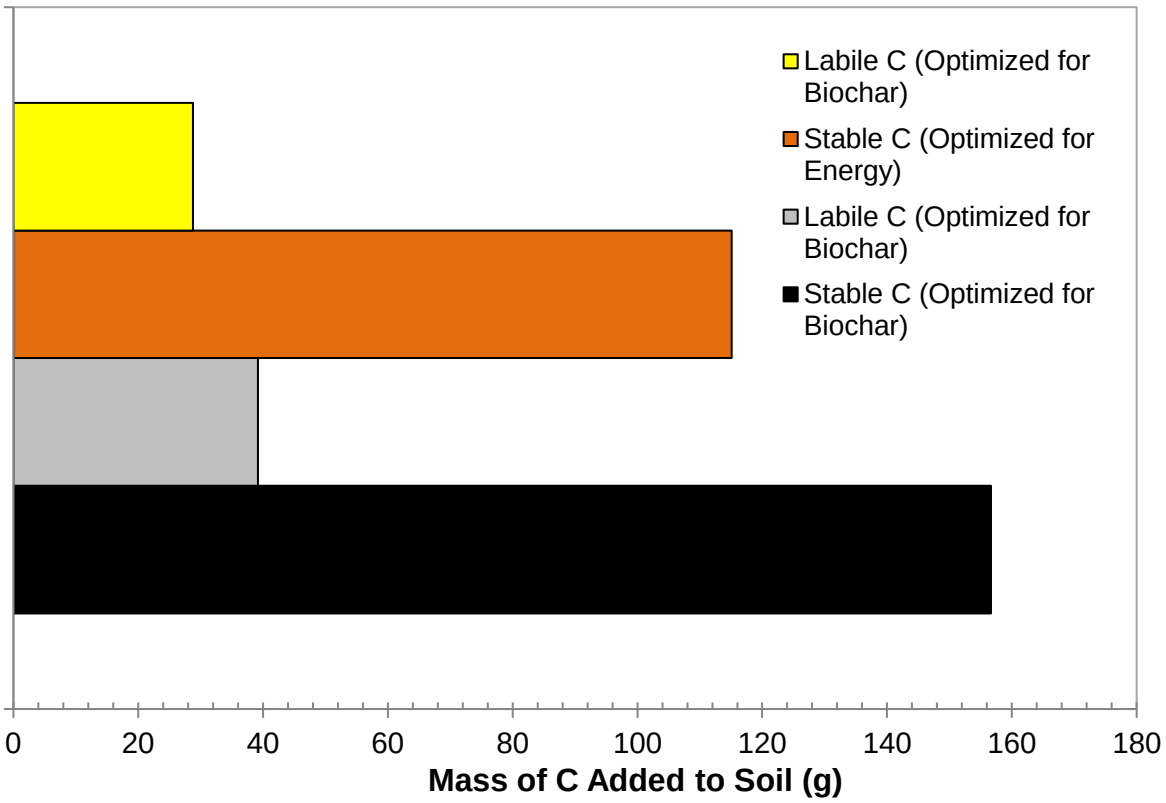

Fig. 6.1 - Mass (g) of stable and labile C added to the soil for the utilization of 1 kg of pre-dried rice husk in the pyrolysis-combustion process**.**